Understanding the Toxicity of Tire-Wear Particle Leachate on a Model Amphibian

Rachel S. Cheong

Department of Chemical Engineering, McGill University, Montreal, Quebec, Canada.

April 2023

A thesis submitted to McGill University in partial fulfillment of the requirements of the degree of Master of Science Chemical Engineering (Thesis)

Table of Contents

Abstract

Tire-wear particles (TWP) have been identified as a potentially toxic form of plastic in the environment as they contain a complex suite of chemical additives such as heavy metals and organic compounds which can leach into the aquatic environment. The ubiquity and increasing production of tires is raising concerns about the toxicity of this contaminant especially in freshwater bodies which can potentially accumulate as much as 90% of the micro-sized TWP released into this compartment. Nano-sized TWP are of particular concern as their small sizes may elicit cytotoxic effects. The exact mechanism of toxicity of this contaminant still requires further investigation, especially the possibility of specific toxicity pathways due to the nanoparticles and leached chemicals. To elucidate this mechanism of toxicity, a model amphibian, *Silurana tropicalis*, was exposed to three different fractions of a TWP leachate (fraction 1 = nanoparticles and leached chemicals; fraction 2 = leached chemicals; fraction 3 = nanoparticles) during its early developmental stages in 60-h and 9-day exposures. In the acute, 60-h exposure individuals were exposed to treatment concentrations ranging from 0 - 100% of the stock suspensions. Results of the acute exposure showed that fraction 3 caused a significant decrease in larval survival at all concentrations. The overall proportion of malformed tadpoles and tail malformations was significantly higher than the control and comparable among fractions, but fractions 1 and 2 exhibited more head, gut, and edema malformations compared to fraction 3. For the 9-day exposure, individuals were exposed to low treatment concentrations ranging from 0 - 10% of the stock suspensions. At all concentrations except 10% fraction 1, survival was significantly reduced after 9 days. Malformations, body length, tail length, and body width were not significantly affected at these lower concentrations, however, tadpoles in fraction 3 had significantly larger brains. Tadpoles in fractions 1 and 2 swam significantly less at the 10% treatment. These results reveal particle-specific and chemical-specific effects of TWP leachate which may have negative repercussions at the population level.

Résumé

Les particules d'usure des pneus ont été identifiées comme une forme de contamination plastique potentiellement toxique dans l'environnement car elles contiennent un mélange complexe d'additifs chimiques, tels que des métaux lourds et des composés organiques, qui peuvent s'infiltrer dans l'environnement aquatique. L'omniprésence et la production croissante de pneus suscitent des inquiétudes quant à la toxicité de ces particules, en particulier dans les écosystèmes d'eau douce, qui peuvent potentiellement accumuler jusqu'à 90 % des microparticules rejetées dans ces compartiments. Les particules d'usure des pneus de taille nanométrique sont particulièrement préoccupantes car leurs petites tailles peuvent provoquer des effets toxiques chez les organismes vivants. Les mécanismes exacts de la toxicité de ce contaminant nécessitent encore des recherches approfondies, en particulier la possibilité de voies de toxicité spécifiques propres aux nanoparticules et aux produits chimiques utilisés dans la synthèse des pneus. Pour élucider ces mécanismes de toxicité, un amphibien d'eau douce, *Silurana tropicalis*, a été exposé à trois fractions différentes d'un lixiviat de particules d'usure de pneus (fraction 1 = nanoparticules et composés chimiques dissous ; fraction 2 = composés chimiques dissous ; fraction 3 = nanoparticules) au cours de ses premiers stades de développement dans des expositions de 60 h et 9 jours. Dans la première exposition, dite aiguë, d'une durée de 60 h, les organismes ont été exposés à des concentrations de chaque fraction allant de 0 à 100 %. Les résultats ont montré que la fraction 3 provoquait une diminution significative de la survie des organismes à toutes les concentrations. La proportion globale de têtards malformés et de malformations de la queue était significativement plus élevée que le témoin et comparable entre les fractions, mais les fractions 1 et 2 présentaient plus de malformations de la tête, des intestins et des œdèmes par rapport à la fraction 3. Pour l'exposition de 9 jours, les individus ont été exposés à des concentrations plus faibles allant de 0 à 10 %. À toutes les concentrations sauf la fraction 1 à 10 %, la survie était significativement réduite après 9 jours. Les malformations, la longueur du corps, la longueur de la queue et la largeur du corps n'étaient pas

significativement affectées à ces concentrations plus faibles, cependant, les têtards de la fraction 3 avaient des cerveaux significativement plus gros. Les têtards des fractions 1 et 2 ont nagé significativement moins à la concentration de 10 %. Ces résultats révèlent des toxicités spécifiques aux particules et aux produits chimiques du lixiviat des particules d'usure des pneus qui peuvent avoir des répercussions négatives au niveau de la population.

Acknowledgements

I would first like to thank my thesis supervisor Nathalie Tufenkji for this research opportunity and for her continued support and guidance over the course of this master's project. Nathalie's optimism and problem-solving skills helped me through numerous logistical challenges. I would also like to thank my co-supervisor Stacey Robinson for her invaluable critical feedback and guidance during each phase of the project, especially during the data analysis phase. I am immensely grateful to my post-doctoral supervisor Eva Roubeau Dumont for her mentorship and guidance. I must express my profound gratitude to Valérie Langlois who so generously allowed me to conduct all my amphibian exposures at her lab - without her help, this project would not have been possible. Thank you, Paisley Thomson and Diana Castañeda-Cortés, for your guidance and direct involvement in the amphibian experiments - it was a pleasure working with you two! Special thanks to other members of the Langlois lab who volunteered their help, namely Kim Menard, Tuan To, Ève Larocque, Manon Karolkowski, Julie Robitaille, and Scott Hepditch. I would also like to express my gratitude to Laura Hernandez, Jun-Ray Macairan, Anthony Smith, Hoai-Nam Bui, Hans Larsson, Xiaoyu Gao, Jingyun Zheng, Anca Baesu, Subhasis Ghoshal and Stéphane Bayen for their vital contributions and for sharing their expertise. Thanks to other members of the Biocolloids and Surfaces Laboratory, Shawninder Chahal and Nicholas Lin who provided useful advice. Lastly, a special thanks to my family and Cheng Pan who have always been my biggest supporters.

This project was funded by McGill University through the McGill Engineering Undergraduate Student Masters Award (MEUSMA), the Natural Sciences and Engineering Research Council of Canada (NSERC) through its Pollution in Urban Environments Collaborative Research and Training Experience (PURE CREATE) program, the Canada Research Chairs program, Environment and Climate Change Canada (ECCC), the Increasing Knowledge on Plastic Pollution Initiative (IKPPI), Institut national de la recherche scientifique (INRS), the Integrated Quantitative Biology Initiative, and the Canadian Foundation of Innovation.

Contribution of Authors

Rachel Cheong, Eva Roubeau Dumont, Stacey Robinson, Nathalie Tufenkji and Valérie Langlois devised the experimental design. Rachel Cheong and Laura Hernandez generated the tire-wear particle leachate fractions. Laura Hernandez, Eva Roubeau Dumont, Xiaoyu Gao, Jingyun Zheng, Anca Baesu, Subhasis Ghoshal and Stéphane Bayen characterized the tire-wear particle leachate fractions and provided their expertise. Rachel Cheong, Paisley Thomson, and Diana Castañeda-Cortés performed the amphibian experiments. Anthony Smith, Hoai-Nam Bui, and Hans Larsson shared their expertise on X-Ray computed tomography (CT) and performed the CT scan acquisition; Rachel Cheong analyzed the CT scans. Rachel Cheong and Jun-Ray Macairan performed the CytoViva® image acquisition and analysis. Jun-Ray Macairan obtained the transmission electron microscopy images. Rachel Cheong performed the data analysis and statistical analyses under the direction of Stacey Robinson and Eva Roubeau Dumont. Hoai-Nam Bui, Xiaoyu Gao and Jingyun Zheng provided relevant information for the methodology. Rachel Cheong wrote the thesis, and co-authors reviewed all written work.

Author List and Affiliations

R. S. Cheong[1], E. Roubeau Dumont[1], P. E. Thomson[2], D. C. Castañeda-Cortés[2], L. M. Hernandez[1], X. Gao[3], J. Zheng[4], A. Baesu[4], J. R. Macairan[1], A. J. Smith[5], H-N. N. Bui[6], H. C. E. Larsson[6], S. Ghoshal[3], S. Bayen[4], V. S. Langlois[2], S. A. Robinson[7], N. Tufenkji[1]

[1] Department of Chemical Engineering, McGill University, Montreal, Quebec, Canada H3A 0C5

[2] Institut national de la recherche scientifique - Centre Eau Terre Environnement, Quebec City, Quebec, Canada, G1K 9A9

[3] Department of Civil Engineering, McGill University, Montreal, Quebec, Canada H3A 0C3

[4] Department of Food Science and Agricultural Chemistry, McGill University, Sainte Anne de Bellevue, Quebec, Canada H9X 3V9

[5] Department of Biology, McGill University, Montreal, Quebec, Canada H3A 1B1

[6] Redpath Museum, McGill University, Montreal, Quebec, Canada H3A 2K6

[7] Environment and Climate Change Canada, Ecotoxicology and Wildlife Health Division, Ottawa, Ontario, Canada K1A 0H3

Table of Figures

Supplementary Information Figures:

Table of Tables

Supplementary Information Tables:

Chapter 1: Introduction

1.1 Production, Use and Fate of Tires in the Environment

The production and use of plastics has increased exponentially over the last few decades (Kontrick, 2018) with global plastic production reaching 368 million tonnes in 2019 (Plastics-Europe, 2020). The use of plastics is pervasive, with applications in numerous industries such as packaging, building and construction, automotive, electric, electronic, agriculture, household, leisure and sports (Plastics-Europe, 2020). The most familiar forms of plastics include polyethylene (PE), polypropylene (PP), polyvinylchloride (PVC), polyethylene terephthalate (PET) and polystyrene (PS), however, another ubiquitous and stealthy source of plastics is tires which contributes 5-10% of the total global plastics in oceans (Kole, Löhr, Van Belleghem, & Ragas, 2017). Tires are classified as a type of thermoset plastic because tires are partially composed of a synthetic, organic polymer (Baensch-Baltruschat, Kocher, Stock, & Reifferscheid, 2020; Halle, Palmqvist, Kampmann, & Khan, 2020; Kole et al., 2017). Capolupo *et al.* compared the toxicity of several different kinds of plastic including car tire tread, PET, PP, PS and PVC, and found that the most toxic plastics originated from car tire tread and PVC due to the substantially higher number of additives present in these materials (Capolupo, Sørensen, Jayasena, Booth, & Fabbri, 2020).

With the incorporation of tires into numerous modes of transportation such as cars, buses, trucks, motorcycles, planes and off-road vehicles, the tire industry has burgeoned, experiencing exponential growth since the invention of pneumatic tires in the 1880's (Tire America, 2021). In 2019, 92.8 million vehicles (European Automobile Manufacturers Association, 2019) and 28.8 million tonnes of tire rubber (Malaysian Rubber Export Promotion Council, 2021) were produced worldwide.

With continual usage, tire tread is eventually worn down due to the friction between the surface of the tires and the road (Baensch-Baltruschat et al., 2020; Boucher & Friot, 2017). One study has estimated that approximately 3.4 million tonnes/year of tire-wear particles (TWP) are generated worldwide (Baensch-Baltruschat et al., 2020) with peak emissions in areas where there is high braking and acceleration (Knight, Parker-Jurd, Al-Sid-Cheikh, & Thompson, 2020). Furthermore, the number of microplastics (1 μm to 5 mm (Barbosa, Adeyemi, Bocato, Comas, & Campiglia, 2020; Klaine et al., 2012; Koelmans, Besseling, & Shim, 2015)) and nanoplastics (1 nm to 1 μm (Gigault et al., 2018)) released increases with greater frictional forces (Park, Kim, & Lee, 2018). Once in the environment, TWP may be further degraded via photodegradation or biodegradation (Baensch-Baltruschat et al., 2020). Detecting these nanoplastics is one of the biggest challenges in environmental risk assessment due to their small size and analytical difficulties (Cai et al., 2021).

The TWP can be transported via road run-off into different environmental compartments such as soil, atmosphere, and water (including rivers, freshwater bodies, and oceans). The fate of TWP in these environmental compartments depends on numerous factors such as the quantity of road run-off, the presence or absence of a road drainage system, and whether the drainage system is connected to a wastewater treatment plant and/or sewage system. The majority (> 90%) of TWP ends up in the soil and water, with a small fraction being emitted to the atmosphere (0.1-10% (Baensch-Baltruschat et al., 2020)). Unice *et al.* estimated that 18% of micrometer-sized TWP enter freshwater bodies via road run-off, of which only 2% reaches estuaries (Unice et al., 2019), and this highlights the tendency for TWP to accumulate in freshwater bodies (~90% accumulation). For surface waters, Wik and Dave reported predicted environmental concentrations (PECs) of TWP to be as high as 56 mg/L (A. Wik & G. Dave, 2009).

1.2 The Complex Nature of Tire Wear Debris

In addition to the inherent complexities associated with nanometer sized TWP, the particles themselves contain a cocktail of chemicals which vary with the tire's end-use application and brand (Wik & Dave, 2006). The basic material of tire tread is a mixture of natural rubber (polyisoprene) and synthetic rubbers (styrene butadiene rubber and/or butadiene rubber), supplemented by numerous additives such as fillers, preservatives, antioxidants, antiozonants, plasticizers, vulcanization agents, softeners, pigments, biocides, desiccants, processing aids and softeners (Baensch-Baltruschat et al., 2020; Boucher & Friot, 2017; Halle et al., 2020; Marwood et al., 2011).

Previous studies have identified organic compounds such as benzothiazole (Capolupo et al., 2020; Xu et al., 2019), polycyclic aromatic hydrocarbons (Marwood et al., 2011; Anna Wik & Göran Dave, 2009), volatile organic compounds (Pochron et al., 2017) and heavy metals like zinc, nickel, chromium, cadmium, lead, antimony, aluminum, titanium, iron and cobalt in TWP (Capolupo et al., 2020; Degaffe & Turner, 2011; Gualtieri, Andrioletti, Vismara, Milani, & Camatini, 2005; Ma et al., 2021; Marwood et al., 2011; Sommer et al., 2018; Xu et al., 2019). A recent study by Halle *et al.* positively identified 28 different organic compounds and metals present in TWP (Halle et al., 2021). Many of these additives are not chemically bound to the plastic polymer, therefore, these additives are able to leach from the particles once released into an aqueous environment (Capolupo et al., 2020). Moreover, degradation of leached compounds via weathering (increased temperature and mechanical stress) can further alter their chemical composition and toxicity (Kolomijeca et al., 2020). One study found that a derivative of the antioxidant N-(1,3-Dimethylbutyl)-N'-phenyl-p-phenylenediamine (6PPD) was responsible for the acute toxicity observed in coho salmon (Tian et al., 2020). The variety of additives and their

derivatives makes chemical analysis very difficult and presents a challenge for environmental risk assessment.

1.3 Toxicity of Tire Wear Debris

The toxicity of TWP is also a complex matter, stemming from both the particles and the leached chemicals. Table 1 summarizes the results of aquatic toxicity studies which have used TWP leachates and includes details regarding the leachate generation method, particle size, aquatic species used to test toxicity, exposure concentrations and durations, endpoints tested and results of toxicity tests.

Many of the early studies investigated the toxicity of the leachate with toxic effects ranging from mortality to teratogenicity for several different aquatic species. For example, Gualtieri *et al.* discovered that their leachate produced heavy teratogenic effects on *X. laevis* embryos at leachate concentrations derived from 50 and 100 g/L TWP (Gualtieri, Andrioletti, Vismara, et al., 2005). Mantecca *et al.* found that when exposed to organic extracts from TWP leachate, *X. laevis* tadpoles experienced severe developmental malformations such as irregular gut coiling and several different types of eye malformations (Mantecca et al., 2007). Marwood *et al.* found EC/LC50 values >10 g TWP/L for three different aquatic species (alga, daphnid and fish) and demonstrated that leachate prepared under elevated temperatures (44 ℃) was more toxic than that prepared at room temperature (22℃) (Marwood et al., 2011). Khan *et al.* showed that TWP leachate exerted chronic (21 days) toxicity on the freshwater amphipod, *Hyallela azteca*, as the species showed 93% mortality at TWP concentrations of 0.58 g/L, reduced fecundity at 0.29 g/L and decreased growth at 0.145 g/L (Khan, Halle, & Palmqvist, 2019). Other leachate effects include delayed larval development and decreased body mass in wood frogs (*Rana sylvatica*) (Camponelli, Casey, Snodgrass, Lev, & Landa, 2009); diminished photochemical conversion efficiency in marine algae

(*Ulva lactuca*) (Turner & Rice, 2010); and overall declines in larval mosquito (*Aedes albopictus* and *Aedes triseriatus*) population sizes and survival during their aquatic stages (Villena et al., 2017).

Studies often attributed the toxicity of these leachates to zinc as its concentration is often several orders of magnitude higher than other constituent metals (Camponelli et al., 2009; Capolupo et al., 2020; Gualtieri, Andrioletti, Mantecca, Vismara, & Camatini, 2005; Halle et al., 2021; Wik, Nilsson, Källqvist, Tobiesen, & Dave, 2009). Camponelli *et al.* showed that larval wood frogs (*Rana sylvatica*) accumulated a substantial amount of Zn within tissues (Camponelli et al., 2009). Other compounds connected to the toxicity of these leachates include benzothiazole (Capolupo et al., 2020), mercaptobenzothiazole (Chibwe et al., 2021) and N-(1,3-Dimethylbutyl)-N′-phenyl-p-phenylenediamine-quinone (6PPD-quinone) (Tian et al., 2020). Due to the complex chemical nature of the leachates and their potential synergistic and antagonistic interactions with each other, identifying the main chemicals responsible for leachate toxicity remains a challenge.

Recent studies have started to compare the toxicity of the leachate and TWP suspensions. Khan *et al.* found differences in acute toxicity between the two fractions: the TWP suspension had a sigmoidal concentration-response pattern with an LC50 of 1 g/L, but the leachate fraction did not fit a sigmoidal curve suggesting a difference in the mechanism of toxicity (Khan et al., 2019). Furthermore, these authors noted that at low concentrations, the leachate was more toxic, but at higher concentrations the particles exerted greater toxicity potentially due to the *in vivo* leaching of internal chemicals *i.e.*, a "Trojan horse" mechanism of toxicity. However, further studies are required to confirm their hypothesis. Another recent study by Halle *et al.* also observed a similar pattern of acute toxicity of worn tires where leachate and particles showed greater toxicity at low and high concentrations respectively (Halle et al., 2021). Liu *et al.* reported that their leachate was

more toxic than their TWP suspension to the marine-dwelling bacteria *Bacillus subtilis* (Y. Liu et al., 2022). Yang *et al.* obtained 96-hour LC50 values of 771.4 mg/L for their TWP suspension and 5.34 g/L for their leachate (Yang et al., 2022).

In the scientific literature most leachates contained micro-TWP or nano-TWP because the leachates were generated using filtration. The treatment was categorized as a leachate if (1) particle sizes were significantly smaller than those in the TWP suspension being compared, or (2) TWP were left in water for some time to allow chemicals to leach out (with or without filtration afterwards). As an example of the leachate classification based on size, Cunningham *et al.* referred to 3-day old filtered TWP suspensions containing 1 - 20 μm particles as a micro-TWP suspension, < 1 μm particles as a nano-TWP suspension, and < 0.02 μm particles as leachate (Cunningham, Harper, Brander, & Harper, 2022). As an example of leachate classification based on leaching time, Shin *et al.* incubated 1 g/L of TWP in artificial seawater for 3 days and filtered this suspension through a 45 μm filter to obtain their leachate (Shin et al., 2022). Studies which were able to separate the TWP from their leached chemicals used a Soxhlet extraction method to produce organic extracts, but this method involved the addition of organic solvents to the TWP suspension (Gualtieri, Andrioletti, Mantecca, et al., 2005; Mantecca et al., 2007). This lack of consistency in nomenclature and standardization of leachate generation methods presents challenges when comparing the findings of one study to another.

Size-dependent toxicity has also been reported. Cunningham found that their nano-TWP suspension and leachate were more toxic than their micro-TWP suspension to *Danio rerio* (Cunningham et al., 2022). Conversely, Siddiqui *et al.* found that their nano-TWP suspension (< 1 μm) significantly reduced the growth of *Menidia beryllina* but not the growth of *Americamysis bahia*, whereas their micro-TWP suspension (1 – 20 μm) significantly reduced growth for both

species (Siddiqui et al., 2022). Aggregation of TWP has also been found to affect the size of the particles in suspension, with larger, aggregated particles exerting less toxicity (Gualtieri, Andrioletti, Mantecca, et al., 2005).

Table 1 Summary of key findings for aquatic toxicity studies which used TWP leachates.

Fraction	Preparation	Size of Particles	Species	Exposure Concentration	Exposure Duration	Endpoints points	Results of Toxicity Tests	Reference
Particle suspension, Leachate	3 g of cryomilled tire tread were added to 300 mL of a 50g/L natural organic matter (NOM) suspension, then filtered (0.2 mm, 20 µm, 1 µm). Filtrate after the 1 µm filter labelled as the nano TWP fraction. 20 µm filter backflushed to form the micro TWP fraction. Nano TWP fraction filtered with a 30 K MWCO filter to get leachate.	TWP suspension: 1 - 20 µm, and < 1 µm Leachate: NA	*Americamysis bahia, Menidia beryllina*	TWP: 0.0038, 0.0378 and 3.778 mg/L Leachate: 0.014%	*A. bahia*: 7 days *M. beryllina*: 96 h	Growth, Swimming behavior (total distance, freezing, movement, in zone duration, in zone frequency, turn angle, meander), Internalization	Swimming behavior (freezing, positioning, total distance travelled) changed significantly for micro- and nano TWP, as well as for the leachate. Micro TWP caused a reduction in growth for both species. Nano TWP only reduced growth for *M. beryllina.* TWP were internalized.	(Siddiqui et al., 2022)
	3.25 g of cryomilled tire tread (new) were added to 300 mL of a 50g/L (NOM) suspension, autoclaved, shaken with glass beads for 3 days, then filtered (20 µm, 1 µm). Filtrate after the 1 µm filter labelled as the nano TWP fraction. The 1 µm filter was backflushed to get the micro TWP fraction. The nano TWP fraction filtered through a 20 nm filter to get the 100% leachate.	TWP suspension: 1 - 20 µm and < 1 µm Leachate: < 20 nm	*Danio rerio, Daphnia magna*	TWP: 0.63–81.18 mg/L Leachate:0-100%	*D. rerio:*120 h post-fertilization *D. magna:* 48 h	Mortality, Malformations, Behavioral response to touch	Nano fraction exerted greater toxicity than micro fraction as there was higher mortality and increased malformations to the nano fraction. Different mode of toxicity between particles and leached chemicals. Species-dependent toxicity observed.	(Cunningham et al., 2022)

	Crushed and pulverized tire rubber was dry sieved (78 µm). 10 g/L of pulverized rubber were mixed with artificial seawater for 35 days (with and without UV irradiation), then filtered (0.45 µm) to get the leachate. To get TWP used in toxicity tests, the leachate was oven dried.	TWP suspension: 6 - 130 µm Leachate: < 0.45 µm	*Bacillus subtilis, Bacillus cereus, Escherichia coli, Vibrio fischeri, Haliogiobus lutimaris,* *Bacillus* sp. LY- 1, *Bacillus* sp. LY-2, *Bacillus* sp. LY-3, *Geobacillus* sp. LY-4	TWP: 0.3 g/L Leachate: 10 g/L	12 h, 24 h, 36 h and 48 h	Cell viability	TWP can alter the composition of marine bacterial communities. Sensitivity of bacterial strains to leachate varied: *B. subtilis* was the most sensitive strain. Leachate more toxic than TWP.	(Y. Liu et al., 2022)
	Crushed and pulverized tire rubber was dry sieved (78 µm) to get TWP. 10 g/L of TWP were stirred at room temperature for 2 months, then filtered (0.45 µm) to get the leachate.	TWP suspension: 6 - 130 µm Leachate: < 0.45 µm	*Tigriopus japonicus*	TWP: 0, 320, 640, 1280, 2560 mg/L Leachate: 0.625, 1.25, 2.5, 5.0 and 10.0 g TWP/L	Acute: 96 h	Mortality	TWP 96-h LC50: 771.4 mg/L whereas Leachate 96-h LC50: 5.34 g/L. Toxicity mainly attributed to zinc. Antagonistic action of zinc and benzothiazole.	(Yang et al., 2022)
	TWP from grinding new and worn tires added to water with surfactant, then filtered (pore size 500 µm & 0.45 µm). Particles on 0.45 µm filter resuspended (particulate), filtrate collected (leachate).	Pristine TWP suspension: 210 ± 116 µm Worn TWP suspension: 176 ± 120 µm Leachate: < 0.45 µm*	*Hyallela azteca*	Acute: 0-37 g/L Chronic:0-0.13 g/L	Acute: 48 h Chronic: 21 d	Mortality Reproduction Growth	Particles caused growth inhibition at 0.127 g/L. Particles are more toxic than leachate at higher conc. Particles from new tires were more toxic than that from worn tires, but leachates from both were equally toxic.	(Halle et al., 2021)
	TWP from grinding worn tires added to water + surfactant, then filtered (pore size 500 µm & 1 µm). Particles on 1 µm filter resuspended (particulate), filtrate collected (leachate).	TWP suspension: 1 - 500 µm* Leachate: < 1 µm*	*Hyallela azteca*	Acute: 1 g/L Chronic: 00.58 g/L	Acute: 48 h Chronic: 21 d	Mortality Reproduction Growth Gut retention	Differences in acute toxicities of particles & leachate. Chronic study with particles only showed significant mortality, decreased fecundity & decreased growth at high TWP conc. (0.145-0.58 g/L). Gut retention time of 24-48h.	(Khan et al., 2019)

	50 g/L and 100 g/L of cryofractured tire tread shaken for 24 h to make TWP suspensions. 6 h Soxhlet extraction used to get TWP organic extracts.	TWP suspension: 1- 7 µm Organic Extracts: Not applicable	*Xenopus laevis,* Human lung A549 and human liver HepG2 cell line	TWP: 1%, 10%, 50% In vitro tests: 10-75 µg/L *X. laevis* test: 50-120 µg/L	*X. laevis*: 96 h HepG2 cells: 24 h A549 cells: 24 h , 48 h , 72 h	Cell viability, Comet length, Comet moment, Mortality, Malformations	50 g/L TWP suspension more toxic than 100 g/L due to less aggregation. Organic extracts altered morphology, higher mortality, more damaged DNA, more malformations.	(Gualtieri, Andrioletti, Mantecca, et al., 2005)
Leachate	3 tires (1 new, 2 used) were cut into 1-5 mm pieces and shaken in seawater for 14 days at room temperature. Suspension filtered (1.2 µm) and filtrate collected.	Leachate: < 1.2 µm	*Crassostrea gigas*	0 – 0.1 g/L	7 days	Clearance and respiration rates, Absorption efficiency, Histology	Respiration and filtration rates were reduced. No effect on absorption efficiency.	(Tallec, Gabriele, Paul-Pont, Alunno-Bruscia, & Huvet, 2022)
	1 g/L TWP suspension in 22 psu artificial sea water incubated and mixed at 42°C for 3 days. Suspension filtered (45 µm) and filtrate collected.	Leachate: < 45 µm	*Brachionus plicatilis*	0 – 1 g/L	Acute: 24 h Chronic: 9 days	Mortality, Reproduction, Growth, Oxidative stress, Transcriptome analysis	Leachate caused acute and chronic toxicity, oxidative stress and transcriptomic deregulation.	(Shin et al., 2022)
	10 g/L of cryogenically ground tire tread were used to create leachate. Leachate was left without agitation at 34°C for 1 day, 3 days, and 10 days. Leachate filtered either through a 1 mm filter was labelled as "unfiltered" and thorough a 0.45 µm filter as "filtered".	"Unfiltered" leachate: < 1mm "Filtered" leachate: < 0.45 µm	*Pimephales promelas*	10 g/L	5 days	Heart rate. Hatching success, Length, Malformations	Longer leaching time produced more toxic leachates. "Unfiltered" leachates are more toxic than "filtered" leachates. Toxicity correlated to benzothiazoles and aryl amines.	(Chibwe et al., 2021)
	80 g/L of car tire rubber granulates were shaken at room temperature in the dark, then filtered (0.2 µm) to get the leachate. Process was repeated with other microplastics like polypropylene (PP), polyethylene terephthalate (PET), polystyrene (PS) and polyvinyl chloride (PVC).	TWP: 1-2 mm	*Raphidocelis subcapitata, Skeletonema costatum,* Mytilus *galloprovincialis*	0.6,1, 2, 4, 6,10, 20, 40, 60, 80 and 100%	*R. subcapitata & S. costatum: 0 h, 24 h, 48 h & 72 h* *M. galloprovincialis: several different assays done at different life stages*	Growth inhibition, Lysosomal membrane stability, Gamete fertilization, Malformations	Car tire rubber and polyvinyl chloride had the highest concentrations of leached chemicals and are potentially the most toxic plastics to aquatic organisms.	(Capolupo et al., 2020)

	5 used tires of different brands were grated using a metal grater. TWP frozen, ground and filtered twice (both filters: pore size 500 µm) to obtain dry particles.	TWP: 10–586 µm	*Gammarus pulex, Asellus aquaticus Tubifex, Lumbriculus variegatus*	0 – 10% mass TWP in sediment (dry weight)	Chronic: 28 d	Survival Growth Feeding rate	For environmentally relevant concentrations of TWP no toxic effects on 4 different freshwater benthic macroinvertebrates were observed.	(Redondo-Hasselerharm, de Ruijter, Mintenig, Verschoor, & Koelmans, 2018)
	Tire was ground, filtered (0.59 mm), shaken in water for 1 week, filtered (0.2 µm), filtrate collected.	Leachate: < 0.2 µm*	*Aedes albopictus, Aedes triseriatus*	0-100 g/L	Dependent on eclosion of species	Population size Survival	*A. albopictus* larvae showed higher tolerance to leachate. General decline in both endpoints at as concentration increased.	(Villena et al., 2017)
	TRWPs collected on asphalt road simulator, added to sediment:water mixture, filtered, centrifuged, supernatant collected	Leachate: < 150 µm*	*Chironomus dilutes, Hyallela Azteca, Pimephales Promelas, Ceriodaphnia dubia*	10 g/kg soil	Chronic: 42 d	Survival Growth Reproduction Mortality	Mild growth inhibition in *C. dilutes* but not significant. No significant effects for *H. azteca*, *P. promelas* and *C. dubia*.	(Panko, Kreider, McAtee, & Marwood, 2013)
	TRWPs collected on asphalt road simulator, added to sediment:water mixture, filtered, centrifuged, supernatant collected	Leachate: < 150 µm*	*Pseudokirchneriella subcapita, Daphnia magna, Pimephales Promelas*	0.1-10 g/L	Acute: 48-96 h	Growth inhibition, Immobilization, Mortality	Acute tests with room temp. leachate showed EC/LC50 values >10 g/L. Leachate prepared at high temp (44 °C) more toxic than that prepared at room temperature.	(Marwood et al., 2011)
	20 End-of life tires filed, sieved (500 µm), TWP added to seawater, filtered (0.45 µm), filtrate collected & acidified.	Leachate: < 0.45 µm*	*Ulva lactuca*	0.5 g/L	Acute: 48 h	Photochemical energy conversion efficiency	Photochemical conversion efficiency decreased with increasing leachate conc.	(Turner & Rice, 2010)
	TWP from 3 abraded tires, added to water and leached for different times, filtered filtrate collected.	Leachate: < 185 mm*	*Ceriodaphnia dubia, Daphnia magna, Pseudokirchneriella subcapita, Danio rerio*	0.55-5 g/L	Acute: 24-48 h Chronic: 9 d	Growth inhibition, Immobilization, Survival, Reproduction	Most sensitive endpoint was *C. dubia* reproduction (EC50 0.013 g/L). Sequential leaching reduces toxicity of leachate.	(Wik et al., 2009)

	TWP filtered, added to soil:water mixture & aged for 8 months. Aliquot of sediment added to 3L water	Leachate: < 590 µm*	*Rana sylvatica*	83.8 g/kg soil in 3 L of water	Gosner stage 24 to stage 46	Time to metamorphosis, Tissue Zn conc.	Delayed development and reduced body mass at metamorphosis. Zn accumulation in tissues.	(Camponelli et al., 2009)
	Scrap tires cryo-fractured & organic extracts obtained in Soxhlet extraction apparatus	Not applicable	*Xenopus laevis*	0.05-0.14 g/L organic extract	Gosner stage 8 to stage 47	Malformations Histology	NOEC was 0.05 g/L. TC50 was 0.1446 g/L. Numerous severe malformations at high conc. of 0.12 & 0.14 g/L	(Mantecca et al., 2007)
	Tread of 25 tires abraded with rasp, added to water & leached for 72 h at 44 ℃. Unfiltered and filtered leachate used for exposures.	Not reported	*Daphnia magna*	0.5-10 g/L	Acute: 48 h	Immobilization	EC50s ranged from 0.5 to > 10 g/L depending on the brand of tire. Unfiltered leachate enhanced UV-phototoxicity for some tires, compared to leachate only. Highest EC_{50}: 0.5 g/L TWP	(Wik & Dave, 2006)
	16 g/L of grated tire tread were added to water and left for 3 days at 20±2℃. 12 different new tires were prepared separately.	Not reported	*Daphnia magna*	0.25, 0.5, 1, 2, 4, 8, 16 g/L	Acute: 24 h, 48 h	Immobilization	24 h EC50s: 0.29 – 32 g/L and 48 h EC50s: 0.0625 – 2.41 g/L. Toxicity for 4/12 tires increased after UV irradiation.	(Wik & Dave, 2005)
	New tire abraded with steel brush, TWP added directly to water to form leachate (i.e., no filtration).	Leachate: 10-80 µm	*Xenopus laevis, Rahidocelis subcapita, Daphnia magna*	50 & 100 g/L	Acute: 24, 72 h *X. laevis* Gosner stages 8-47	Growth inhibition, Mortality, Malformation	Teratogenicity to *X. laevis* at both concentrations. At high conc. aggregation of TWP reduces toxicity of leachate. New tires contain higher [Zn].	(Gualtieri, Andrioletti, Vismara, et al., 2005)

* Size of TWP was assumed based on smallest filter/membrane pore size used.

1.4 Knowledge Gaps

The generation of TWP varied greatly among studies from using abrasion techniques (road simulators, grinding stones, rasps, files) to cryo-fracturing and milling. Many of these studies did not perform physicochemical characterization on the TWP leachates generated. Therefore, it is imperative that future studies perform more thorough characterizations using multiple analytical techniques, to provide better insights into the fate and toxicity of TWP.

Although microplastics have the potential to cause physical damage to organisms such as blocking the gastrointestinal tract and damaging the intestinal wall (Matthews et al., 2021), nanoplastics potentially pose a greater risk because they have a higher affinity for cells (B. Zhang et al., 2021) and are able to disrupt cellular membranes (L. Liu et al., 2021). Toxic effects of nanoplastics also include inflammation (Brown, Wilson, MacNee, Stone, & Donaldson, 2001), oxidative stress (Bhattacharya, Lin, Turner, & Ke, 2010), mortality (Lee, Shim, Kwon, & Kang, 2013), decreased fecundity (Lee et al., 2013), developmental abnormalities (Della Torre et al., 2014), behavioral changes (Cedervall, Hansson, Lard, Frohm, & Linse, 2012), altered lipid metabolism (Cedervall et al., 2012), growth reductions (Besseling, Wang, Lürling, & Koelmans, 2014) and teratogenicity (Besseling et al., 2014). Many toxicity studies used particle suspensions/leachates containing a mixture of micrometer and nanometer-sized TWP, making it difficult to identify the size of the causative agent of toxicity.

Finally, although some of the more recent aquatic toxicity studies have begun to differentiate between the toxicity of the leachate and TWP suspension, these studies have not isolated the particle-specific effects from the chemical-specific effects. The fractionation of TWP leachates can help pinpoint which constituent of TWP leachates, i.e., particles or leached chemicals, is the primary cause of toxicity.

1.5 *Silurana tropicalis* as a Model Freshwater Organism for Toxicity Testing

To address these knowledge gaps, toxicity tests were performed using a model aquatic organism, *Silurana tropicalis* – the western-clawed frog formerly known as *Xenopus tropicalis* (Cannatella & Trueb, 1988). There are numerous advantages of using *S. tropicalis* for ecotoxicology experiments. Adult frog colonies can be maintained in the laboratory, and 1000-3000 embryos can be produced from one mating pair of frogs (Amaya, Offield, & Grainger, 1998). Ovulation and mating can be hormonally induced via the injection of human chorionic gonadotropin (hCG) into adult frogs, and breeding can be induced at any time of the year (ASTM International, 2013). During spawning, the eggs are released and fertilized *ex vivo*, and the embryos continue to develop externally thereby allowing researchers to monitor the early development of the organism (Khokha et al., 2002). Furthermore, the relatively large size of eggs and embryos facilitates their manipulation during experiments (Amaya et al., 1998). *S. tropicalis* is a diploid species meaning it has two homologous sets of chromosomes and is more practical for genetic analyses compared to the more widely used amphibian species, *Xenopus laevis*, which is a tetraploid species and has four sets of homologous chromosomes (Saka, 2010).

S. tropicalis is a freshwater vertebrate species that is often regarded as an indicator species of environmental health (Hayden et al., 2015; Simon, Puky, Braun, & Tóthmérész, 2011) as its permeable skin makes the animal highly susceptible to contaminants (Llewelyn, Berger, & Glass, 2019). *S. tropicalis* is a fully aquatic species, and contaminant exposure and uptake can occur throughout all stages of its life cycle. Chemical uptake can begin as early as egg deposition where chemicals can penetrate the thin egg membrane, and uptake can continue throughout the larval and tadpole stages via skin absorption and filter feeding (Sparling, Linder, Bishop, & Krest, 2000). In

addition to transdermal chemical uptake, other routes of exposure and uptake in adult frogs include respiration and dietary intake (Pinelli, Santillo, Chieffi Baccari, Falvo, & Di Fiore, 2019).

Once a chemical enters the body, it is processed by the liver and can either be used for metabolization, storage or excretion. Lipophilic chemicals which have a high octanol-water partition coefficient, (*i.e.,* $5 < \log K_{OW} \leq 9$) are likely to bioaccumulate within the lipid stores of the organism instead of being excreted and/or metabolized (Sparling et al., 2000). Benzothiazole, a vulcanization accelerant in the tire manufacturing process, has a log K_{OW} of 2.17 and is therefore less likely to bioaccumulate within organisms (Liao, Kim, & Kannan, 2018). Another tire compound which has been linked to acute toxicity in coho salmon, N-(1,3-Dimethylbutyl)-N′-phenyl-p-phenylenediamine-quinone (6PPD-quinone), has a log K_{OW} of 4.68 and also has a low likelihood of bioaccumulating in the organism (Tian et al., 2020).

Chemicals which are not metabolized or stored in the tissues of the amphibian are excreted in fecal matter or in the urine as nitrogenous waste. One previous study has found that fully aquatic amphibian species like *S. tropicalis* predominantly secrete waste in the form of ammonia, whereas amphibians which are both aquatic and terrestrial rely on the secretion of urea which is a less toxic excretory product (Cragg, Balinsky, & Baldwin, 1961). In copious amounts of freshwater, ammonia toxicity is mitigated via dilution, and the amphibian remains unaffected by the waste product (Sparling et al., 2000).

1.6 Thesis Objectives

The main goal of this study was to understand the relative toxicity of the chemical and particulate constituents of a TWP leachate by examining the acute (60-h) and 9-day effects on *S. tropicalis*. To accomplish this goal, a TWP leachate was separated into leached chemicals, nanoparticles and a combination of both (Figure 1) and the following objectives were assessed:

I. To determine if there is toxicity from each fraction of the TWP leachate
II. To determine whether the toxicity is the same for the three different fractions
III. To determine if there is a synergistic or antagonistic effect on toxicity from the leached chemicals and nanoparticles
IV. To investigate the connection between any behavioral effects caused by TWP leachate exposure and potential changes in brain morphometry

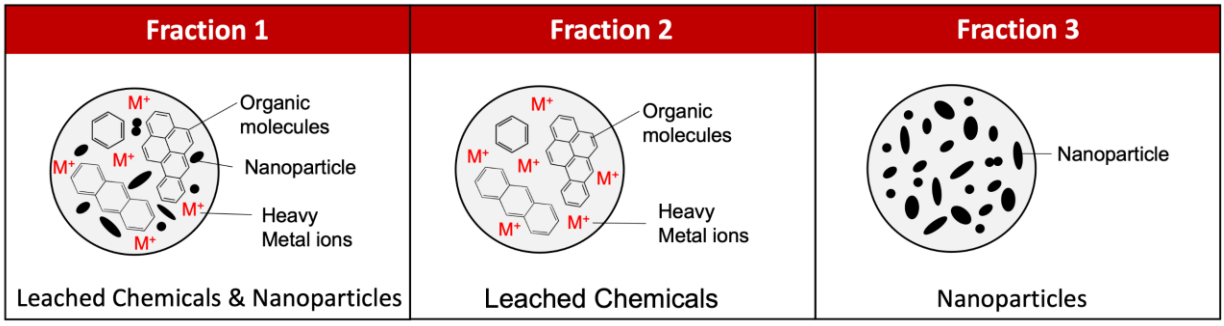

Figure 1 Separation of a tire-wear particle leachate into fraction 1 (leached chemicals and nanoparticles), fraction 2 (leached chemicals) and fraction 3 (nanoparticles).

We hypothesize that there will be toxicity from at least fraction 1 (i.e., the combined leached chemicals and nanoparticles fraction) as TWP leachate toxicity has been previously demonstrated using other aquatic organisms (Cunningham et al., 2022). We also predict that the toxicity of the three different fractions will not be the same since their constituents are different. If there is a synergistic or additive effect of the leached chemicals and the nanoparticles, then fraction 1 is likely to be the most toxic fraction among the three. However, if there is an antagonistic effect between the leached chemicals and nanoparticles, fraction 1 may not be the

most toxic fraction and either fractions 2 or 3 will be the most toxic. Finally, we hypothesize that alterations in swimming behavior are linked to changes in brain function and ultimately brain morphometry; regions of the brain such as the telencephalon and optic tectum are responsible for locomotion (Mai & Liao, 2019) and sensing of visual stimuli (Khakhalin, Koren, Gu, Xu, & Aizenman, 2014), respectively.

Chapter 2 provides details about the methodology (including tire-wear particle leachate generation and characterization, amphibian husbandry, 60-h and 9-day toxicity tests and statistical analyses), results, discussion, and conclusions of the experiments done with the amphibian *S. tropicalis* to address the thesis objectives and goal of the project.

Chapter 2: Nanoparticle-specific and Chemical-specific Effects of Tire-Wear Particle Leachate on Amphibian Early Life Stages

Authors: R. S. Cheong[1], E. Roubeau Dumont[1], P. E. Thomson[2], D. C. Castañeda-Cortés[2], L. M. Hernandez[1], X. Gao[3], J. Zheng[4], A. Baesu[4], J. R. Macairan[1], A. J. Smith[5], H-N. N. Bui[6], H. C. E. Larsson[6], S. Ghoshal[3], S. Bayen[4], V. S. Langlois[2], S. A. Robinson[7], N. Tufenkji[1]

[1] Department of Chemical Engineering, McGill University, Montreal, Quebec, Canada H3A 0C5
[2] Institut national de la recherche scientifique - Centre Eau Terre Environnement, Quebec City, Quebec Canada, G1K 9A9
[3] Department of Civil Engineering, McGill University, Montreal, Quebec, Canada H3A 0C3
[4] Department of Food Science and Agricultural Chemistry, McGill University, Sainte Anne de Bellevue, Quebec, Canada H9X 3V9
[5] Department of Biology, McGill University, Montreal, Quebec, Canada H3A 1B1
[6] Redpath Museum, McGill University, Montreal, Quebec, Canada H3A 2K6
[7] Environment and Climate Change Canada, Ecotoxicology and Wildlife Health Division, Ottawa, Ontario, Canada K1A 0H3

2.1 Introduction

Concomitant with the rapid expansion of the automotive industry and the exponential increase in production of the modern radial tire since the 1950s (Halle et al., 2020), tire-wear particles (TWP) have become a ubiquitous environmental contaminant that has been identified in the air, soil, and water (Dall'Osto et al., 2014; Gray, Wertz, Leads, & Weinstein, 2018). The generation of this contaminant is inevitable as TWP are formed from the abrasion of tire tread during the driving of automobiles (Baensch-Baltruschat et al., 2020; Boucher & Friot, 2017), with peak emissions typically occurring in urban areas adjacent to high traffic roadways (A. Wik & G. Dave, 2009). One study has estimated that over 5.9 million tons of TWP are released into the environment annually (Kole et al., 2017) and these particles can vary in size from the micrometer range (1 μm to 5 mm (Barbosa et al., 2020)) to the nanometer range (0.001 to 1 μm (Gigault et al., 2018)).

The fate and toxicity of TWP in freshwater ecosystems are especially concerning, firstly due to the potential for accumulation of particles in this environmental compartment (Unice et al., 2019), and secondly, to the release of a host of chemical additives from the particles once in an aqueous environment (Capolupo et al., 2020; Cunningham et al., 2022). Tire tread contains a proprietary formulation of natural and synthetic rubbers, fillers, softeners, vulcanization agents, antioxidants, plasticizers, *etc.* all in varying quantities depending on the brand, type, make, and model of tire (Baensch-Baltruschat et al., 2020; Sommer et al., 2018; Wik & Dave, 2006). In addition to the toxicity caused by the leached chemicals (Chibwe et al., 2021; Mantecca et al., 2007; Tallec et al., 2022), cytotoxicity may also result from the interaction of the particles with cellular and biomolecular entities leading to a disruption of physiological processes (Vineeth Kumar et al., 2022).

Most ecotoxicological studies have focused on the global effects of TWP leachate (Camponelli et al., 2009; Capolupo et al., 2020; Gualtieri, Andrioletti, Vismara, et al., 2005; Wik & Dave, 2006), and only a few recent studies have begun to isolate the particulate component and leached chemicals component to understand their respective contributions to the overall toxicity. Among these recent studies, Cunningham *et al.* found that their nano-TWP suspension (< 1 μm) and leachate (< 0.02 μm) produced different teratogenic effects on zebrafish (*Danio rerio*) larvae suggesting different modes of toxic action (Cunningham et al., 2022). A difference in the mechanism of toxicity between TWP suspension and leachate was also suggested by Khan *et al.* after these authors observed distinct differences in the acute (48 h) mortality of the freshwater amphipod *Hyallela azteca* upon exposure to the two treatments (Khan et al., 2019). Liu *et al.* reported that their leachate (< 0.45 μm) reduced the cell viability of the marine sediment-dwelling bacteria (*Bacillus subtilis*) compared to their TWP suspension (6 – 130 μm) (Y. Liu et al., 2022).

Finally, Halle *et al.* discovered that the relative toxicity of their leachate and TWP suspension to *H. azteca* varied based on the age of the tire and the particle concentration (Halle et al., 2021). Unfortunately, the lack of standardization in TWP leachate generation and nomenclature (i.e., TWP suspension versus leachate), makes inter-study analyses difficult. Despite these recent efforts, it is still unclear whether the toxicity of TWP in freshwater ecosystems is mainly attributable to the tire-wear chemical leachate, nanoparticulates or a combination of both.

The present study aims to address these knowledge gaps by performing toxicity tests using the model amphibian, *Silurana (Xenopus) tropicalis*. *S. tropicalis* is a highly fecund, diploid organism capable of being hormonally induced to breed at any time of the year (Amaya et al., 1998). *S. tropicalis* produces relatively large eggs that develop *ex vivo* facilitating direct observation of its early developmental stages (Khokha et al., 2002). Exposure to TWP leachates is likely to occur during the embryonic to metamorphic stages of development for most amphibians, and throughout adulthood for fully aquatic species like *S. tropicalis*. The presence of amphibian populations in the ecosystem is often an indication of good environmental health, since anurans are highly susceptible to contaminants in their surroundings as a result of their permeable skin (Qazi & Ashok, 2012). However, only a handful of studies have used amphibians to evaluate the toxicity of TWP leachates and all these studies found that TWP leachate is toxic to amphibians during their early development (Camponelli et al., 2009; Gualtieri, Andrioletti, Mantecca, et al., 2005; Gualtieri, Andrioletti, Vismara, et al., 2005; Mantecca et al., 2007). Among these studies, Gualtieri *et al.* began to distinguish the toxicity of TWP suspensions (50 and 100 g TWP/L stock concentrations) and organic extracts (0.05-0.12 g organic extract/L) to *Xenopus laevis*, but no conclusions were drawn regarding which component was mainly responsible for the toxic effects

observed (Gualtieri, Andrioletti, Mantecca, et al., 2005). Furthermore, no amphibian study has focused solely on the nano-TWP (< 0.2 µm) portion of TWP leachate.

In this study, *S. tropicalis* was exposed to different fractions of a TWP mixture (i.e., leached chemicals, nanoparticles (< 0.2 µm), and a combination of both) in 60-h and 9-day toxicity tests, and endpoints such as survival, malformations, swimming behavior and brain morphometry were analyzed. The objectives of this study were: 1) to elucidate the relative toxicity of these fractions in freshwater ecosystems, 2) to investigate any synergistic or antagonistic effect on toxicity from a combination of the particle and leached chemical constituents, and 3) to investigate the connection between any behavioral effects caused by TWP mixture exposure and potential changes in brain morphometry.

2.2 Materials and Methods

2.2.1 Generation and Characterization of Tire-Wear Particle Leachate Fractions

Figure 2 shows a schematic of the procedure used to generate the TWP leachate fractions. TWP were generated by abrading the tread of five different end-of-life tires (obtained from an auto repair shop in Montreal, Quebec, Canada) using a hand drill equipped with a diamond drill bit (Big Horn Diamond Burr Set, model number: 19391). Equal masses of particles from each tire were mixed to represent the variability of tire particles present in the environment. A concentration of 40 g/L TWP of moderately hard reconstituted water (MHRW) (Marking & Dawson, 1973) were stirred at room temperature for 7 days in the dark. The particle suspension was then sequentially filtered using a 1 mm sieve, followed by a 1.5 µm glass microfiber filter (Whatman) and finally a 0.20 µm nitrocellulose mixed ester filter (Advantec) to obtain fraction 1 (F1) containing leached chemicals and nanoparticles (< 0.2 µm). A portion of F1 was filtered through a 20 kDa GE osmonics flat sheet membrane (Sterlitech) in an Amicon® stirred cell (Millipore Sigma). The filtrate from the 20 kDa membrane, i.e., fraction 2 (F2), was collected, and the retentate was resuspended to obtain fraction 3 (F3, nanoparticles < 0.2 µm). Based on the results of Nanoparticle

Tracking Analysis (NTA) (LM14 instrument with 532 nm green laser, NanoSight Ltd.), F3 was diluted so that its particle number concentration was equivalent to that of F1. Most of the mass of TWP was removed by sequential filtration so that the actual concentration of TWP in the different fractions was markedly less than the initial 40 g/L TWP suspension. In addition to an unfiltered water control (Control), an F1 procedural control (PC F1) and an F3 procedural control (PC F3) were prepared in which MHRW was sequentially filtered in the same manner as F1 and F3, respectively. Finally, to ensure that the media was suitable for amphibian exposures salts were added to all treatments according to the Frog Embryo Teratogenesis Assay-Xenopus (FETAX) protocol (ASTM International, 2013). Fractions F1, F2 and F3 as prepared are referred to hereafter as stock suspensions.

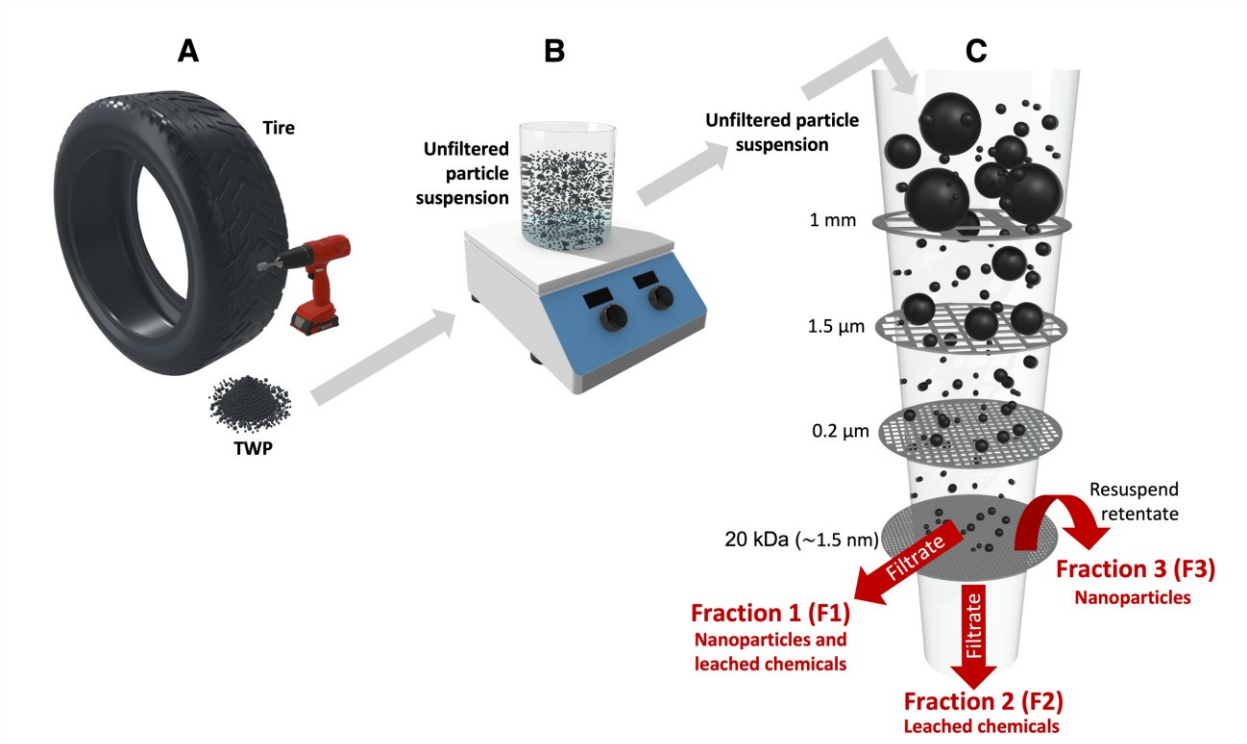

Figure 2 Procedure for generating the different tire-wear particle leachate fractions. (A) Five end-of-life tires were abraded using a drill with a diamond drill bit. (B) 40 g/L of TWP were stirred in moderately hard reconstituted water at room temperature for one week. (C) The TWP suspension was sequentially filtered using filters/membranes of reducing pore sizes to obtain the three different fractions of the tire-wear particle leachate. The media was converted to FETAX media prior to toxicity exposures.

Using dynamic light scattering (DLS, Zetasizer Ultra, Malvern Panalytical), the hydrodynamic diameter of particles in the stock suspensions was obtained. For DLS, styrene butadiene was selected as a proxy for rubber polymers present in the TWP leachate, and measurements were taken at room temperature.

For each treatment, five metal elements, ^{63}Cu, ^{208}Pb, ^{27}Al, ^{66}Zn, ^{111}Cd, were monitored using inductively coupled plasma – mass spectrometry (ICP-MS, Thermo iCAPQ c, quadrupole ICP-MS, Teledyne Cetac ASX-560 autosampler). Calibration standards (SCP Science Quality standard 4) between 20 ng/L and 1 mg/L were prepared in 2% nitric acid matrix. Linear relationship between counts and concentration for each metal element was achieved ($R^2 > 0.9999$). Quality control samples with known concentration were monitored at the middle and end of the ICP-MS sequence to ensure the accuracy of the measurement. To prepare samples for ICP-MS analysis, samples were first diluted with water (Optima™ LC/MS Grade, Fisher Chemical™), filtered through 0.22 μm filters (InnoSep™ SF13, 13 mm, CA, Syringe Filter) and acidified to 2-3% using concentrated nitric acid (70%, Thermo Scientific™).

Liquid chromatography-quadrupole time of flight mass spectrometry (LC-QTOF-MS) (Agilent 6545 LC/Q-TOF) was also performed to determine the concentration of organic chemicals. Fourteen organic chemicals were selected as targeted analytes in the present study, and detailed information about these analytes is shown in Table S1. Bisphenol AF-$^{13}C_{12}$ (BPAF-$^{13}C_{12}$; purity ≥ 98%) and bisphenol S-$^{13}C_{12}$ (BPS-$^{13}C_{12}$; purity ≥ 98%) analytical standards were purchased from Toronto Research Chemicals (Toronto, Canada). Bis(2-ethylhexyl) phthalate-d_{38} (DEHP-d_{38}; purity ≥ 98%), diethyl phthalate-d_{14} (DEP-d_{14}; purity ≥ 99%), diallyl phthalate-d_4 (DAP-d_4; purity ≥ 99%), butyl benzyl phthalate-d_4 (BBzP-d_4; purity ≥ 99%), di-n-octyl phahalte-d_4 (DnOP-d_4; purity ≥ 99%), diisobutyl phthalate-d_4, (DiBP-d_4; purity ≥ 99%), diisodecyl

phthalate-d_4 (DiDP-d_4; purity ≥ 99%), mono-n-butyl phahalte-d_4 (MBP-d_4; purity ≥ 99%), dicyclohexyl phthalate-d_4 (DcHP-d_4; purity ≥ 99%), and didecyl phthalate-d_4 (DDP-d_4; purity ≥ 99%) were purchased from CDN isotopes (Pointe-Claire, Canada). Bisphenol A-$^{13}C_{12}$ (BPA-$^{13}C_{12}$; purity ≥ 98%) was purchased from Cambridge Isotope Laboratoires (Tewksbury, USA). The isotope-labelled internal standard mixture solution (BPAF-$^{13}C_{12}$, BPS-$^{13}C_{12}$, BPA-$^{13}C_{12}$, BPF-$^{13}C_{12}$, DEP-d_{14}, DiBP-d_4, BBzP-d_4, DcHP-d_4, DEHP-d_{38}, DnOP-d_4, DAP-d_4, DiDP-d_4, MBP-d_4, DDP-d_4) was prepared at 1 μg mL^{-1} in methanol the day before use. For sample preparation, each water sample was filtered through a 0.22 μm PTFE filter (Fisher Scientific, Whitby, Canada), prepared in 25% methanol (water sample : methanol, 3:1 v/v) and stored in a glass vial. One milliliter of diluted water sample was transferred to a high-performance liquid chromatography (HPLC) glass vial, and 50 μL of internal standard mixture at 1 μg mL^{-1} was spiked into the water sample, followed by vortexing for 1 min. Detailed parameters for LC-QTOF-MS are provided in Table S2 and Table S3.

The morphology of raw particles generated from drilling (Figure 2A) was observed using a darkfield microscope (Olympus® BX43 microscope). Furthermore, enhanced darkfield hyperspectral imaging (CytoViva® hyperspectral microscope) was used to spatially map selected metals such as zinc, aluminum, and copper onto these raw TWP (Figure 2A). Spectral signatures of each metal were overlaid onto the corresponding TWP in ImageJ (Schneider, Rasband, & Eliceiri, 2012) so that all metals were displayed in one image. The morphology of nanoparticles in the different fractions was obtained using transmission electron microscopy (TEM) (Talos F200X G2 TEM, Thermo Fisher Scientific). For TEM, grids were prepared by pipetting 2 μL of the TWP fraction suspensions on a copper 400-mesh coated with a thin carbon film (CF-400-CU) followed

by water evaporation. The contrast of images was adjusted and standardized using ImageJ (version 1.53k) (Schneider et al., 2012).

2.2.2 Amphibian Husbandry

All experiments using the amphibian, *S. tropicalis*, were conducted at the Institut national de la recherche scientifique (INRS) (Quebec, Canada) (protocol #2201-02) in accordance with the guidelines of the Canadian Council on Animal Care (CCAC). To induce spawning, a healthy male and female adult frog were each injected with a priming dose of 12.5 international units (IU) of human chorionic gonadotropin hormone (hCG) (Sigma-Aldrich) in the dorsal lymph sac. About 20 h later, each frog was injected with a boosting dose of 200 IU of hCG. The male and female frogs were then paired and left in the dark to promote amplexus. The deposited eggs were de-jellied with 2% w/v L-cysteine solution (MP Biomedicals), and healthy, viable embryos were selected after two sorting phases (Bantle, Dumont, Finch, Linder, & Fort, 1991). All exposures were done in a climate controlled room at 27 ± 1 °C, 50% humidity with a 12 h day/12 h night cycle (ASTM International, 2013).

2.2.3 Acute Exposure Test

The FETAX protocol (ASTM International, 2013) with slight modifications was used as a guide for conducting the amphibian exposures. The treatments used were control (0%), PC F1 (0%), PC F3 (0%), F1 (10, 25, 50, 75, and 100%), F2 (10, 25, 50, 75, and 100%) and F3 (10, 25, 50, 75, and 100%). Treatment levels were expressed as volume percentages, for example, 100% treatment represents the undiluted stock suspension, whereas 75% treatment represents a 25% dilution of the stock suspension with FETAX salt media. All treatments were done in quadruplicate (n = 4). The pH of all stock suspensions was adjusted to 7.6-7.9 using hydrochloric acid and sodium hydroxide, followed by aeration whereby air was pumped through the media through a

glass Pasteur pipette. For the exposure, 15 embryos at Nieuwkoop-Faber (NF) stages 12-13 were haphazardly selected and placed in each experimental unit containing 30 mL of treatment media (Nieuwkoop & Faber, 1956). Following the FETAX protocol, all embryos were taken from a single mating pair to minimize genetic variability (ASTM International, 2013). The placement of the experimental units was randomized daily according to the results from a random number generator (randomizer.org), and at the end of each day dead individuals and debris were removed, and the media aerated manually with a glass Pasteur pipette. The acute exposure ended after 60 h when most of the tadpoles in the control group reached NF stage 46. The surviving tadpoles were euthanized by immersion in 0.2% w/v tricane methanesulfate (MS-222) solution (Sigma-Aldrich) and then fixed in 10% neutral buffered formalin (NBF) (Epredia). Survival and malformation data were obtained from the preserved tadpoles. Malformations were identified using the *Atlas of Abnormalities for Xenopus* (Bantle et al., 1991), and a tadpole was counted as malformed if it had at least one malformation (head, gut, tail or edema). Water samples from time 0 h and 60 h of the acute exposure were analyzed using ICP-MS and LC-QTOF-MS.

2.2.4 The 9-Day Exposure Test

A longer 9-day exposure was also conducted to assess the toxicity of low concentrations of the TWP leachate on *S. tropicalis* during the embryonic to early pre-metamorphic stages of development. This exposure lasted for 9 days post-fertilization. The treatments used were control (0%), PC F1 (0%), PC F3 (0%), F1 (1 and 10%), F2 (1 and 10%) and F3 (1 and 10%) with n = 4 replicates. Fifteen embryos at NF stages 12-13 were randomly selected and placed in each experimental unit initially containing 30 mL of treatment media. All embryos were from a single mating pair. The total volume of treatment media in the experimental units was gradually increased from 30 mL (day 0) to 100 mL (day 3) and finally 300 mL (day 6) with fresh treatment media. On

day 3, daily feeding of the tadpoles commenced. Tadpoles were fed 2 mg of powdered tadpole food (Ward's Science, VWR) twice a day. Dead tadpoles, food detritus and feces were removed daily. The placement of experimental units was randomized on days 0, 1, 2, 3 and 6. From day 3 onwards, the experimental units were aerated and covered to minimize evaporation.

At the end of the 9-day exposure, tadpole swimming behaviour was assessed with a startle response assay and a feeding assay. Swimming assays were developed according to the *Standard Guide for Behavioral Testing in Aquatic Toxicology* (ASTM International, 2020). The startle response is a useful metric for assessing the avoidance behavior of animals to a simulated predator; the normal response for tadpoles is to dart away from a predator (Berrill et al., 1993; Denver, 2010). The design of the startle response assay was based on that of previous behavioral studies (Carvan, Loucks, Weber, & Williams, 2004; Fong, Lambert, Hoagland, & Kurtz, 2018). Briefly, a tadpole was haphazardly selected from an experimental unit and transferred to a Petri dish (4 cm internal diameter) filled with 9 mL of its treatment media (1 cm liquid depth). Ten Petri dishes each with one tadpole were then placed on a light board and the tadpoles were left to acclimatize for 10 min, after which a rod was dropped from a height of 2.5 cm onto the center of the light board, exposing all animals to the same standardized vibrational force. The swimming behavior of the animals was recorded for 1 min using a video camera positioned above the animals (Figure S1). The tadpoles were then left to acclimatize for another 2 min, and the feeding assay was performed in which the animals' response to a food stimulus was tested. The tadpoles were not fed 24 h prior to the feeding assay. For this assay, 30 µL of Sera Micron tadpole food (5g/L) (Sera GmbH) was added to each Petri dish and the behaviour of the tadpoles was recorded for 1 min (Figure S2). The video analysis software, Kinovea (version 0.9.5), was used to track the swimming behavior of the tadpoles in each assay. From the video footage of both assays, the total swimming distance in 1 min after the

stimulus was introduced was obtained. More details of the experimental set up are described in the supplementary information. Water samples from the 9-day exposure were analyzed using ICP-MS and LC-QTOF-MS as previously described.

After completion of the swimming assays, the surviving tadpoles were euthanized by immersion in 0.2% w/v MS-222, and their spines were severed as a secondary physical method to confirm death. The animals were then fixed in 10% NBF. Preserved tadpoles were primarily imaged ventrally and laterally using a stereomicroscope (Olympus SZX16, Olympic Scientific Solutions), and these images were used to assess growth (head-to-tail body length, body width and tail length) and malformations. ImageJ was used to obtain growth measurements.

Next, X-Ray nano-computed tomography (CT) scans of haphazardly selected, similarly sized individuals from the control, 10% F1, F2 and F3 groups (n = 3) were taken using the Zeiss Xradia 520 Versa (Carl Zeiss Canada Limited). These tadpoles had no visible malformations. To prepare the samples for the CT scans, the fixed tadpoles were washed in deionized water, followed by 25, 50 and 70% ethanol, then stained with 1% phosphotungstic acid in 70% ethanol for about 2 weeks at 4 ℃. Immediately prior to imaging, the animals were washed in 70% ethanol and embedded in a 0.5% agarose gel. All scans were acquired at 3-4 μm resolution with 4× objective lens with 2 × 2 camera binning over a 360 degree-rotation. Each scan consisted of 1600 projections and taken at 60 kVp and 82 μA (Table S4). The scans obtained were used to construct 3D images in the Dragonfly image analysis software (Object Research Systems Inc.), and linear measurements of the brain were taken (Figure S3 and Figure S4) according to the procedure described previously (Cha, Uhrin, McClelland, & Woodley, 2021).

2.2.5 Statistical Analyses

Acute Exposure Data

R statistical software version 4.2.1 (R Core Team 2022) and RStudio software (RStudio Team 2022) with agricolae (de Mendiburu, 2021) and MASS packages (Venables & Ripley, 2002) were used to perform all statistical analyses. Normality was checked using the Shapiro-Wilk test, and a square-root transformation was applied to the response variables that did not meet the normality assumption. Comparisons between groups were done using two-way analysis of variance (ANOVA) with post-hoc Tukey HSD test with treatment and level as factors (Table S5). Differences were considered statistically significant at $p \leq 0.05$. For edema malformation data, a non-parametric Kruskal-Wallis test was applied when normality could not be met with data transformations. Concentration-response modelling and regression analyses were not often supported by the data; hence we used ANOVA's to provide consistent comparisons for the exposures and endpoints.

The 9-day Exposure Data

At exposure completion, survival and malformation data were analyzed using two-way ANOVAs as described previously. For all other endpoints such as morphometrics (i.e., growth and brain size) and swimming behavior, generalized linear mixed models (GLMM) were fitted to the data using the lme4 package (Bates, Machler, Bolker, & Walker, 2015) and lmerTest package (Kuznetsova, Brockhoff, & Christensen, 2017) in R and RStudio. This kind of modeling was selected as it incorporates both random effects of the experimental units (tadpoles in the same jar are not independent from each other) and additional biologically relevant fixed effects besides treatment and level like tadpole density and body length which significantly affected growth morphometrics and swimming behavior, respectively (Dyck et al., 2021; Robinson et al., 2017).

Data exploration and GLMM validation procedures were done following a previous study ensuring that the assumptions of homoscedasticity and homogeneity were met by each model (Zuur, Ieno, Walker, Saveliev, & Smith, 2009). The procedure for selecting the best GLMM for each endpoint is described in the supplementary information and in Table S6 and Table S7. Differences were considered statistically significant at $p < 0.05$.

For all boxplots, the thick horizontal bars represent the median values, and the upper and lower hinges of the boxplot represent the 75^{th} and 25^{th} percentiles, respectively. The upper whisker (vertical line) of the boxplot is 1.5 times the inter-quartile range (IQR), and the lower whisker is 1.5*IQR. Dots represent the average value of the response variable per replicate. The diamond (◇) represents the average of the four replicates per treatment level.

2.3 Results

2.3.1 Tire-Wear Particle Leachate Characterization

The particle concentration of F1 stock suspension was $3.5 \times 10^8 \pm 1.6 \times 10^7$ particles/mL from NTA analyses, and the concentrated F3 retentate was diluted to match this particle number concentration so that these two fractions had comparable particle numbers. Using NTA, no particles were detected in the controls nor in F2. From the NTA size distributions, the average diameter of nanoparticles in F1 was 275 ± 14 nm, and that of F3 was 139 ± 1 nm (Table S8). From DLS size distributions based on intensity, the average hydrodynamic diameter of the nanoparticles in F1 was 252 ± 12 nm, and that of F3 was 135 ± 11 nm for the most prominent peak (Figure 3A). The polydispersity index (PDI) of F1 was 0.16 ± 0.03, and F3 was slightly more polydisperse with a PDI of 0.42 ± 0.01.

The morphology of the TWP generated from drilling was examined (Figure S6), and the particles were found to be amorphous with a rough surface texture resembling TWP previously generated from mechanical abrasion processes (Roubeau Dumont et al., 2023; Tonegawa & Sasaki, 2021; Wagner et al., 2018). The imaging also confirmed that the method of abrasion used in this study produced particles that have similar morphologies to real-world environmental tire and road wear particles (Panko, Hitchcock, Fuller, & Green, 2019). TEM images of F1 and F3 confirmed the presence of nanoparticles in the leachate (Figure 3C-D and Figure S7). Using the NTA data regarding particle concentration and average particle hydrodynamic diameter, the mass concentrations of F1 and F3 were calculated to be 4.61 mg/L and 0.60 mg/L, respectively, assuming that the particles were spherical and had the density of rubber (1.2 g/cm^3) (Klöckner et al., 2019).

Hyperspectral microscopy (CytoViva) was successfully used as a rapid, qualitative method to chemically map metals on the surface of TWP. Selected metals such as zinc, aluminum, and copper were identified on the surface of the TWP (Figure 3E). Previous studies that used scanning electron microscopy - energy dispersive X-ray spectroscopy (SEM/EDX) also confirmed the presence of zinc, aluminum, and copper on tire tread and TWP (Kovochich et al., 2021; Sommer et al., 2018).

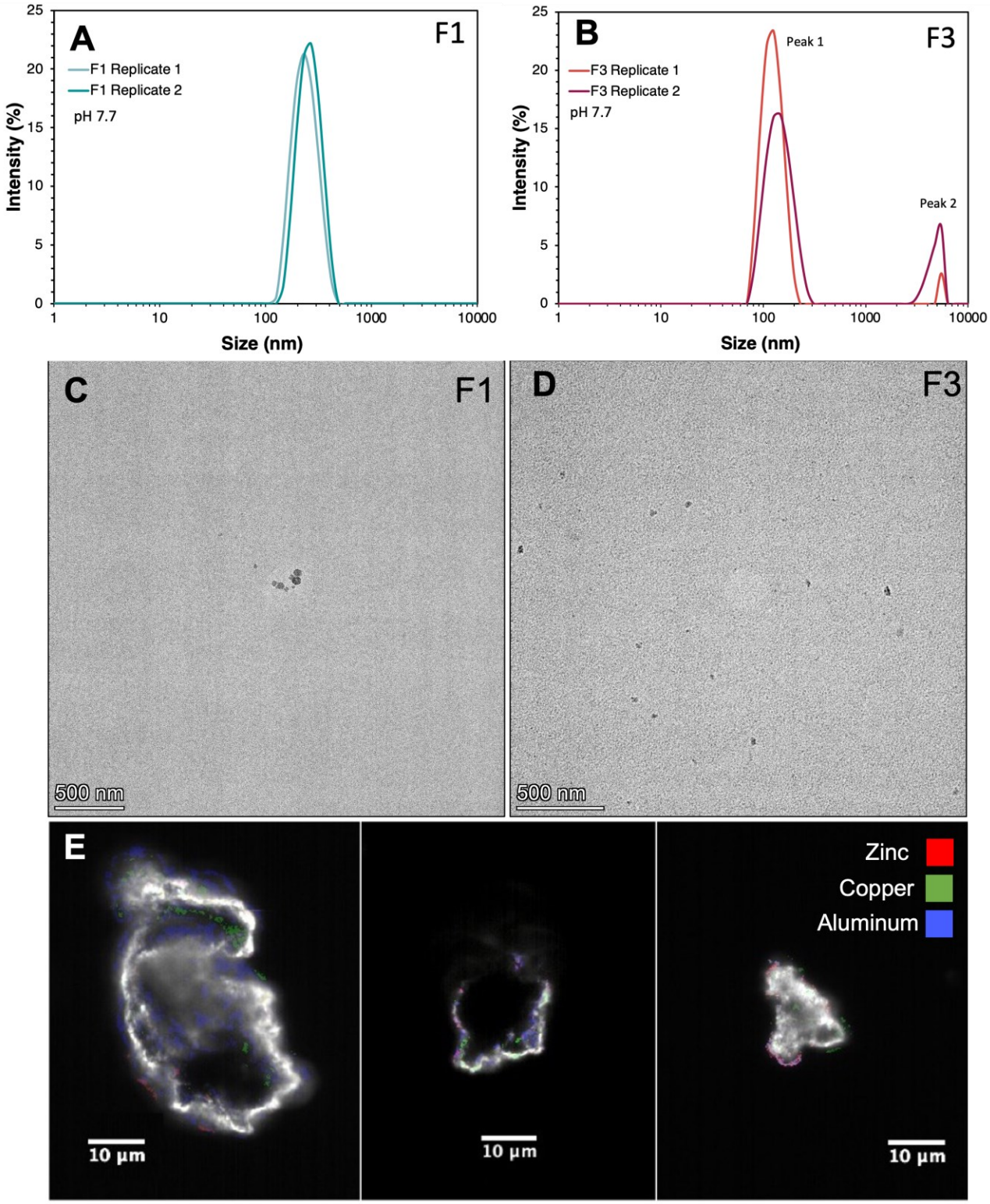

Figure 3. Particle characterization of the exposure fractions F1 and F3. (A) Hydrodynamic size distribution of particles in F1. (B) Hydrodynamic size distribution of particles in F3. (C) TEM image of nanoparticles in F1. (D) TEM images of nanoparticles in F3. (E) CytoViva® Enhanced Darkfield Hyperspectral Images showing spatially mapped metals on tire-wear particles. Metals such as zinc, copper, aluminum were identified on the surface of tire-wear particles.

ICP-MS analysis was used to quantify the metal concentrations in the 100% exposure treatments and controls, and the results are shown in Table 2. Overall, zinc was the most prominent heavy metal detected at concentrations of 3.04 mg/L and 2.21 mg/L in F1 and F2, respectively, and in trace amounts in F3 (0.151 mg/L). The same trends in zinc concentration were observed at the 10% treatment level used in the 9-day exposure (Figure S8). Aluminum, copper, cadmium, and lead were detected in trace amounts in F1 and F2 compared to the controls.

LC-QTOF-MS was utilized to quantify targeted organic compounds in the 100% exposure treatments and controls, and the results are shown in Table 2. Of the targeted compounds, benzothiazole, a vulcanization accelerator (J. Zhang et al., 2018), was the most abundant organic compound detected at concentrations of 1.15 mg/L and 1.01 mg/L in F1 and F2, respectively. Benzothiazole is often cited in literature as one of the key components of leachates derived from TWP (Chibwe et al., 2021; Ni, Lu, Luo, Tian, & Zeng, 2008; Reddy & Quinn, 1997; J. Zhang et al., 2018). Hexa(methoxymethyl) melamine (HMMM), another vulcanization agent (Johannessen, Helm, & Metcalfe, 2022; Rauert et al., 2020), was the second most concentrated chemical detected at concentrations of 1.035 mg/L and 0.865 mg/L in F1 and F2, respectively, and in trace quantities in F3. Mercaptobenzothiazole, a vulcanization accelerator (Wik & Dave, 2005), was detected in trace quantities for F1 and F2 only. Other targeted chemicals such as N-phenyl-N'-(1,3-dimethylbutyl)-p-phenylenediamine quinone (6-PPD quinone), dibutyl phthalate, diphenyl phthalate, diheptyl phthalate, dihexyl phthalate, di(2-ethylhexyl) phthalate (DEHP), decyl octyl phthalate, bisphenol A, Irganox 1081, Irganox 1330 and Irganox 1010 were not detected in any treatments. The results of these chemical characterizations demonstrate that most of the leached chemicals were successfully removed from F3, and that F1 and F2 retained most of the leached

chemicals. The concentration of organic chemicals at 0 h and 60 h of acute and 9-day exposures is recorded in Table S9.

Table 2 Concentration of metals and organic compounds (mean ± standard error, n = 4) in controls and 100% F1, F2 and F3.

		Control	PC F1	PC F3	F1	F2	F3
Metal	Aluminum (µg/L)	38 ± 2	26 ± 0.4	28 ± 2	72 ± 2	72 ± 3	27 ± 2
	Copper (µg/L)	33 ± 0.5	34 ± 0.9	35 ± 0.3	111 ± 3	101 ± 2	30 ± 1
	Zinc (µg/L)	24 ± 1	22 ± 0.2	36 ± 2	3035 ± 673	2208 ± 49	151 ± 14
	Cadmium (µg/L)	31 ± 13	24 ± 4	28 ± 2	86 ± 4	68 ± 4	13 ± 0.5
	Lead (µg/L)	8 ± 0.7	7 ± 0.1	8 ± 0.5	24 ± 0.1	24 ± 0.1	5 ± 0.02
Organic Compound	Benzothiazole (µg/L)	n.d.	n.d.	n.d.	1153 ± 20	1007 ± 45	n.d.
	Mercaptobenzothiazole (µg/L)	n.d.	n.d.	n.d.	7 ± 2	12 ± 0.3	n.d.
	Hexa(methoxymethyl) melamine (µg/L)	n.d.	n.d.	n.d.	1035 ± 37	865 ± 215	13 ± 3
	6-PPD quinone (µg/L)	n.d.	n.d.	n.d.	n.d.	n.d.	n.d.
	Dibutyl phthalate (µg/L)	n.d.	n.d.	n.d.	n.d.	n.d.	n.d.
	Dipentyl phthalate (µg/L)	n.d.	n.d.	n.d.	n.d.	n.d.	n.d.
	Diheptyl phthalate (µg/L)	n.d.	n.d.	n.d.	n.d.	n.d.	n.d.
	Dihexyl phthalate (µg/L)	n.d.	n.d.	n.d.	n.d.	n.d.	n.d.
	Di(2-ethylhexyl) phthalate (µg/L)	n.d.	n.d.	n.d.	n.d.	n.d.	n.d.
	Decyl octyl phthalate (µg/L)	n.d.	n.d.	n.d.	n.d.	n.d.	n.d.
	Bisphenol A (µg/L)	n.d.	n.d.	n.d.	n.d.	n.d.	n.d.
	Irganox 1081 (µg/L)	n.d.	n.d.	n.d.	n.d.	n.d.	n.d.
	Irganox 1330 (µg/L)	n.d.	n.d.	n.d.	n.d.	n.d.	n.d.
	Irganox 1010 (µg/L)	n.d.	n.d.	n.d.	n.d.	n.d.	n.d.

F1: Fractions 1; F2: Fraction 2; F3: Fraction 3; n. d.: not detected; PC F1: Procedural control for fraction 1; PC F3: Procedural control for fraction 3; 6-PPD quinone: N-phenyl-N'-(1,3-dimethylbutyl)-p-phenylenediamine quinone.

2.3.2 Acute Exposure

No dose-response effect on the survival of *S. tropicalis* was observed for any treatment. Most F1 and F2 treatments did not have a statistically significant effect on survival compared to the control (ANOVA, $p > 0.05$; Figure 4A; Table S5), and the mean survival rate was as low as 72% and 73% for F1 and F2, respectively. However, at all concentrations of F3, the survival rate was significantly lower than the control (ANOVA, $p < 0.05$; Figure 4A; Table S5), with the lowest mean survival rate at 47%.

For the proportion of malformed tadpoles, a roughly proportional increase with increasing concentrations of each treatment was observed, with the greatest number of malformed tadpoles found at the 100% treatment level (Figure 4B). When investigating the frequency of the different types of malformations, the proportion of tadpoles with gut abnormalities was significantly higher in the leached chemical-containing fractions compared to the control (i.e., 75 - 100% F1 and 50 - 100% F2) (ANOVA, $p < 0.05$; Figure 4C; Table S5). Tadpoles in F3, did not show significant gut malformations when compared to the control (ANOVA, $p > 0.05$; Figure 4C; Table S5). Head malformations were significant at 100% F1 and 25% - 100% F2 (ANOVA, $p < 0.05$; Figure 4E; Table S5), but not for F3 (ANOVA, $p > 0.05$; Figure 4E; Table S5). Similar trends were observed for the proportion of edematous tadpoles, in which F1 and F2 tadpoles exhibited higher average rates of edema compared to F3, though none of the treatments were significantly different from the control according to the results of the Kruskal Wallis test (Kruskal Wallis, $p > 0.05$; Figure 4D). At almost all treatment levels for F1, F2 and F3, tail malformations were significantly higher than the control (ANOVA, $p < 0.05$; Figure 4F; Table S5).

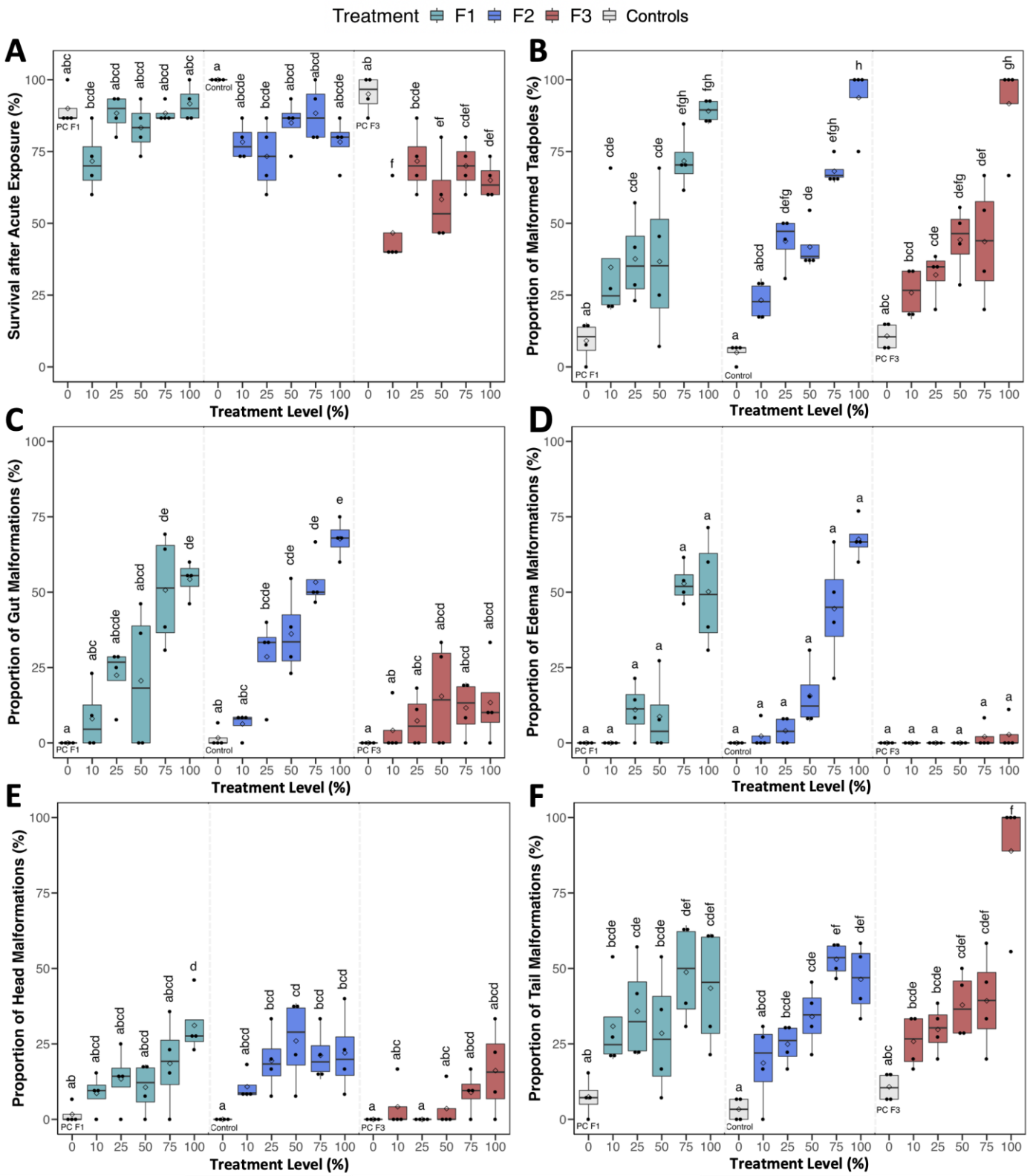

Figure 4. Treatment comparisons of *S. tropicalis* percent survival and malformations after 60 h acute exposure to tire-wear particle leachate fractions. Boxplot of proportion of (A) surviving tadpoles; (B) surviving tadpoles that were malformed; (C) surviving tadpoles with gut malformations; (D) surviving

tadpoles with edema; (E) surviving tadpoles with head malformations; and (F) surviving tadpoles with tail malformations. Treatments were control (0%), PC F1 (0%), PC F3 (0%), F1 (10, 25, 50, 75, and 100%), F2 (10, 25, 50, 75, and 100%) and F3 (10, 25, 50, 75, and 100%). For (A), (B), (C), (E) and (F) letters correspond to significant differences ($p < 0.05$) according to two-way ANOVA with treatment (F1/F2/F3) and level (0-100%) as factors. For better visualization of trends, boxplots are grouped according to treatment. Boxplots with the same letter are not considered significantly different ($p > 0.05$) by Tukey-HSD test. For (D) no significant differences were found using the Kruskal-Wallis test.

2.3.3 The 9-Day Exposure

Compared to the control, almost all treatments significantly decreased the rate of survival of *S. tropicalis* after a 9-day exposure period (ANOVA, $p < 0.05$; Figure 5A; Table S5). Survival rates were comparable between 1% and 10% treatments levels for all fractions (ANOVA, $p > 0.05$; Figure 5A; Table S5), and at each respective treatment level there was no significant difference among the fractions (ANOVA, $p > 0.05$; Figure 5A; Table S5), though the mean survival rate dropped to approximately 50% in F2 and F3, and to 62% in F1.

For the proportion of malformed tadpoles, there was no significant effect of any treatment compared to the control, likely due to the death of highly malformed animals (ANOVA, $p > 0.05$; Figure 5B; Table S5). Categories of malformations (i.e., head, gut, tail and edema) are shown in Figure S9.

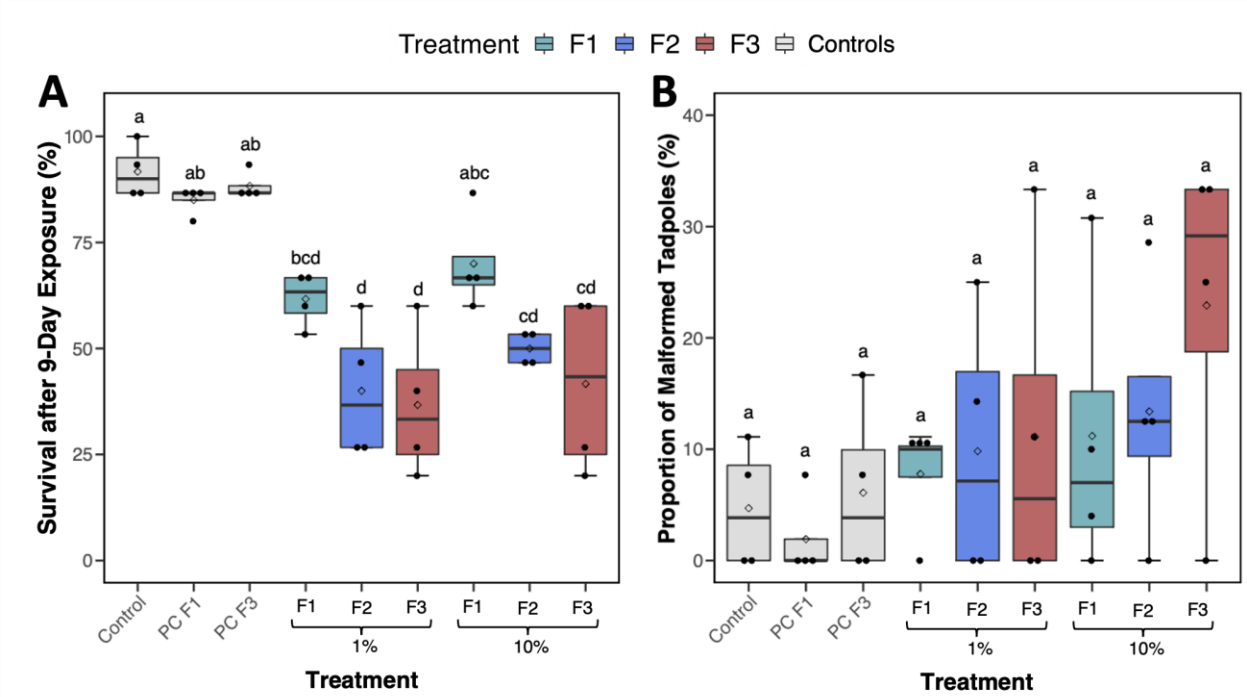

Figure 5 Treatment comparisons of *S. tropicalis* percent survival and malformations after 9-day exposure to tire-wear particle leachate fractions. Boxplots of (A) percentage of surviving tadpoles; and (B) proportion of surviving tadpoles that were malformed. Treatments were control (0%), PC F1 (0%), PC F3 (0%), F1 (1 and 10%), F2 (1 and 10%) and F3 (1 and 10%). Letters correspond to significant differences ($p < 0.05$) according to two-way ANOVA with treatment (F1/F2/F3) and level (0 - 10%) as factors. Boxplots with the same letter are not considered significantly different ($p > 0.05$) by Tukey-HSD test.

Regarding morphometry, 9-day exposure to all fractions of TWP leachate did not significantly affect the body length of the tadpoles when compared to the controls (GLMM, $p > 0.05$; Figure 6A; Table S7). However, the density of tadpoles in the experimental unit did significantly affect the growth rate in an inverse manner – the lower the tadpole density in the experimental unit, the higher the growth rate (GLMM, $p < 0.05$; Table S7). The relationship between tadpole density and growth rate has previously been reported (Gillespie, 2002). Similar results were obtained for other growth morphometrics such as tail length and body width (Figure S10A-B). Measurements were obtained by one individual, and the mean coefficient of variance for 20 repeated morphological measurements for five different tadpoles was ≤ 0.01 for the tail length, body length and body width measurements (Hayek, Heyer, & Gascon, 2001).

For brain morphometry (Figure S3 and Figure S4), exposure to 10% F3 significantly increased the size of the telencephalon width (Figure 6B), diencephalon width (Figure S10C), optic tectum width (Figure S10D), and medulla width (Figure S10E) (GLMM, $p < 0.05$; Table S7). These results indicate that the brains were significantly larger for tadpoles that were exposed to F3. Similarly, measurements were obtained by one individual, and the mean coefficient of variance for 20 repeated morphological measurements for five different tadpoles was ≤ 0.01 for all brain width measurements.

Regarding swimming behavior during the startle response assay, at the 10% treatment level tadpoles exposed to F1 and F2 swam significantly less than those exposed to the controls, but there was no significant difference in swimming between tadpoles in F3 and those in the controls (GLMM, $p < 0.05$; Figure 6C; Table S7). However, the trend was different at the 1% treatment level in which F3 was the only treatment that was significantly different from the controls (GLMM, $p < 0.05$; Figure 5C; Table S7). For the total distance travelled while feeding, only 10% F2 was significantly different from the control, as these tadpoles exhibited lower feeding activity (Figure 6D).

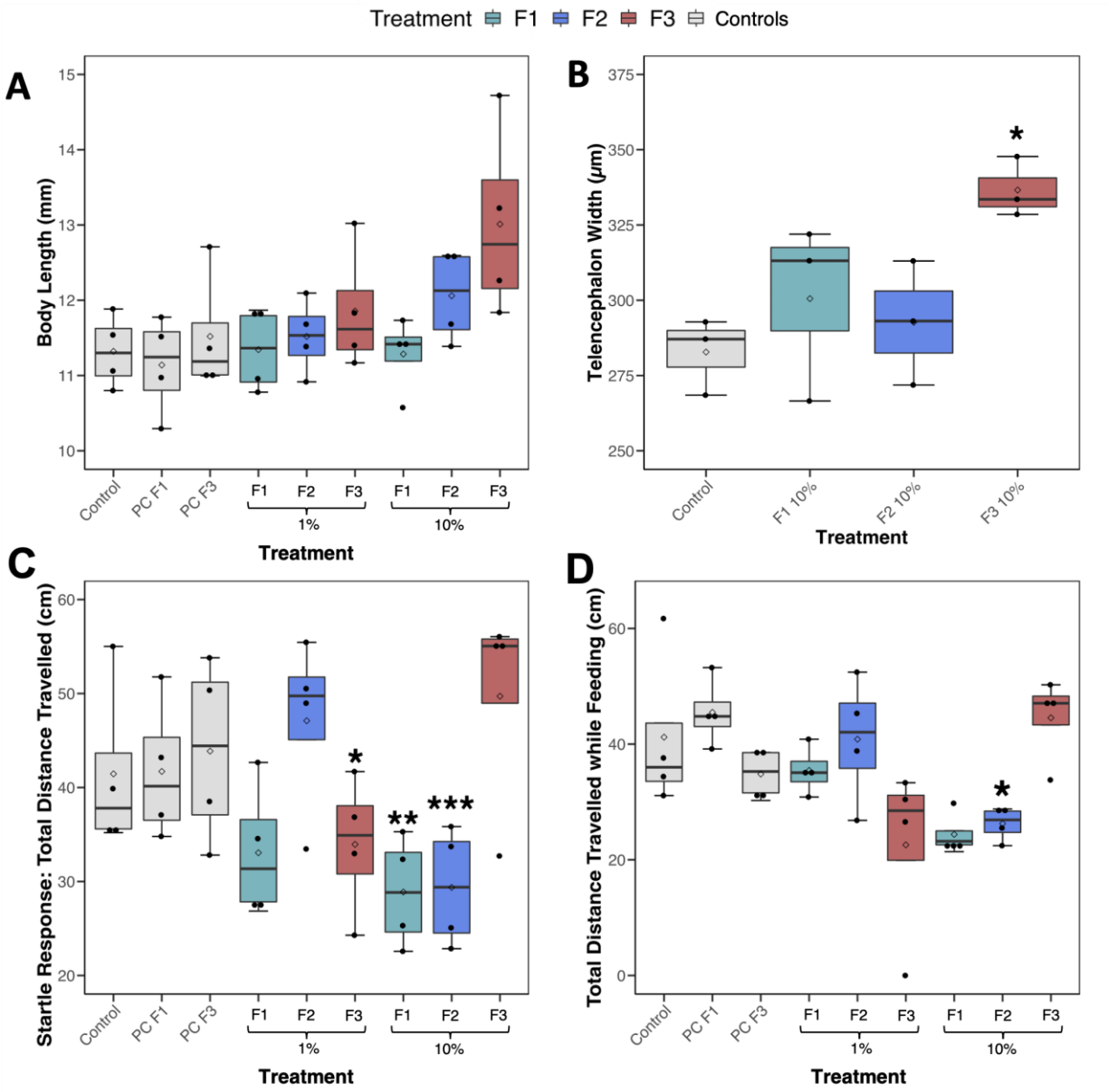

Figure 6 Morphometrics and locomotory behavior of *S. tropicalis* tadpoles after 9-day exposure to tire-wear particle leachate fractions. Boxplots of (A) total body length; (B) telencephalon width; (C) total distance travelled during the startle response assay; and (D) total distance travelled while feeding. Statistical analyses were conducted using generalized linear mixed models (GLMM). Significance codes correspond to p values as follows: *** $0 \leq p \leq 0.001$; ** $0.001 < p \leq 0.01$; * $0.01 < p \leq 0.05$ when compared to the control.

2.4 Discussion

2.4.1 Tire-Wear Particle Stability

Both DLS and NTA results confirmed that mean particle diameter was larger in F1 than in F3. The greater extent of particle aggregation in F1 was likely caused by a more extensive metal-polymer complexation related to the higher concentration of multivalent metal cations and organic compounds present in that fraction (Santo, Vishnyakov, Kumar, & Neimark, 2018; Shupe, Boenisch, Harper, Brander, & Harper, 2021). Chemical characterization results confirmed elevated concentrations of the heavy metal zinc and organic compounds like benzothiazole and HMMM in F1 compared to F3. Several other studies have reported similar findings whereby zinc was the most concentrated heavy metal in TWP leachate (Halle et al., 2021; Shin et al., 2022; Yang et al., 2022). Zinc is used as vulcanization agent in the tire manufacturing process (Sommer et al., 2018). Trace amounts of aluminum, copper, cadmium, and lead were also detected in F1 and F2, and these metals, among others, have also been previously identified in TWP (Capolupo et al., 2020; Ma et al., 2021). In a recent study, concentrations of HMMM > 1 μg/L were detected in surface waters near highways, and environmental HMMM has been associated with additives in tires and plastics (Johannessen et al., 2022). Another possible reason for the smaller particle sizes in F3 is that some of the larger nanoparticles may have remained embedded in the 20 kDa membrane during resuspension of the retentate (Figure 2C).

2.4.2 Impact on Survival

Overall, exposure to F3 caused a significant decrease in the survival of *S. tropicalis* tadpoles after both acute and 9-day exposures. Though F1 and F2 were generally not acutely toxic to this species after a 60-h exposure period, these two fractions did significantly reduce survival after a 9-day exposure period at low concentrations.

When comparing particle-containing fractions, F3 appeared to exert greater toxicity compared to F1. One hypothesis is that the larger, aggregated particles in F1 caused them to be less bioavailable to the organism; thereby reducing its uptake and cytotoxicity (Vineeth Kumar et al., 2022). A similar pattern of size-dependent toxicity has been previously observed in which exposure to a 100 g/L TWP suspension resulted in lower acute toxicity to embryos of the amphibian *X. laevis* when compared to a 50 g/L TWP suspension - these authors attributed the reduced toxicity to enhanced aggregation at the higher concentration (Gualtieri, Andrioletti, Mantecca, et al., 2005; Gualtieri, Andrioletti, Vismara, et al., 2005). Mantecca *et al.* concluded that particle size and surface area play crucial roles in the toxicity of TWP as these physical properties can elicit different mechanisms of toxicity (Mantecca et al., 2009). Numerous other studies have concluded that smaller particles generally cause more cytotoxic responses in living organisms compared to larger particles (Beddoes, Case, & Briscoe, 2015; Cunningham et al., 2022; Dong et al., 2020). The exact mechanism of toxicity of nano-TWP remains to be elucidated in addition to demonstrating uptake within the organism using advanced imaging techniques.

When comparing chemical constituent fractions, there was no statistically significant difference in survival between F1 (particles and leached chemicals) and F2 (leached chemicals) for both the acute and 9-day exposures. Cunningham *et al.* reported different findings whereby their TWP suspension was more toxic than their leachate to *D. rerio* (zebrafish) embryos and *D. magna* (crustacean) (Cunningham et al., 2022). However, their nanoparticle (< 1 μm) concentrations ranged from $0 – 3.6 \times 10^9$ particles/mL compared to the nanoparticle (< 0.2 μm) concentrations in the present study which ranged from $0 – 3.5 \times 10^8$ particles/mL.

Though not acutely toxic, F2 significantly diminished survival after 9-day exposure with the average survival being almost as low as that of F3. These results indicate that a chemical-

induced mode of toxicity comes into play with longer exposure time (Tennekes & Sánchez-Bayo, 2013). The increased mortality may be associated with genotoxic mechanisms such as damage to DNA/RNA/proteins or oxidative stress (Burgos-Aceves, Faggio, Betancourt-Lozano, González-Mille, & Ilizaliturri-Hernández, 2022), however, further studies are needed to reveal the precise mechanism of toxic action in *S. tropicalis* since this objective was beyond the scope of this study. Based on the TWP leachate generated in this study, nanoparticles were more toxic to *S. tropicalis* compared to the leached chemicals after a 60-h exposure period.

The results showed that there was a general lack of significant acute toxicity for the chemical constituent fractions (i.e., F1 and F2), and one possible reason for this is that the concentration of leached chemicals may be near the non-observable effect concentration (NOEC) for this exposure time, though this metric could not be obtained for this study due to the lack of a dose-response effect for survival. Even at the 100% treatment level, average survival was greater than 75%. For *X. laevis*, an amphibian species closely related to *S. tropicalis* (Amaya et al., 1998), Mantecca *et al.* reported a NOEC of 50 mg/L of concentrated organic extracts from tire debris (Mantecca et al., 2007), but did not report the concentrations of metals and organic compounds within their organic extracts. In the present study, concentrations of most leached metals and organic chemicals were either not detected or in the μg/L range for both F1 and F2. Only zinc, benzothiazole and HMMM reached concentrations in the low mg/L range (< 3.04 mg/L) for F1 and F2.

2.4.3 Impact on Malformations

After the 9-day exposure, there was no significant difference in the proportion of living, malformed tadpoles between the control and treatment groups (Figure 5B). Conversely, for the acute exposure, trends in the overall proportion of malformed tadpoles were similar for F1, F2 and

F3 – malformations were higher with increasing concentration (Figure 4B). A similar trend of increasing *X. laevis* tadpole malformations with increasing concentrations of tire-wear particle leachates after 120 h exposure has been previously observed (Gualtieri, Andrioletti, Vismara, et al., 2005).

Distinct differences between fractions were observed when examining the frequency of single malformations. Fractions with leached chemicals (i.e., F1 and F2) had significantly higher gut and head malformations, and on average higher instances of edema compared to F3. Gut and head abnormalities have been previously identified as common malformations in *X. laevis* tadpoles upon exposure to organic extracts from tire debris (Mantecca et al., 2007). These authors concluded that organic extracts were potent teratogens causing abnormal morphogenesis in larval amphibians, and in the present study both F1 and F2 contained organic chemicals. For another freshwater species, *D. rerio*, pericardial edema has been observed in larvae after exposure to nano TWP suspensions (< 1000 nm, EC_{50} = 8.05×10^8 particles/mL) and leachate (EC_{50} = 84.1%) (Cunningham et al., 2022). Chibwe *et al.* found higher instances of severely malformed fathead minnow (*Pimephales promelas*) embryos upon exposure to TWP leachate (Chibwe et al., 2021). A higher frequency of malformations has previously been linked to DNA damage (Ralph & Petras, 1997) or changes in enzymatic activities (Egea-Serrano, Relyea, Tejedo, & Torralva, 2012).

Due to the complex composition of the leachate, pinpointing the main chemicals responsible for these teratogenic effects remains a challenge, especially for amphibians. Furthermore, in combination, chemicals could exert antagonistic or synergistic effects based on their relative concentrations as seen with the combinations of zinc and benzothiazole (Yang et al., 2022), and zinc and lead (Herkovits & Pérez-Coll, 1991).

2.4.4 Impact on Body Morphometrics after 9-Day Exposure

For the 9-day exposure, TWP leachates had no significant effect on any growth parameter. However, the inverse relationship between tadpole density and growth was significant along the body and tail lengths (craniocaudal axis), but not along the body width (mediolateral axis). Gillespie also reported increased tadpole growth along the craniocaudal axis with lower tadpole densities (Gillespie, 2002). A recent study, reported that nano-TWP suspensions did not affect the growth of mysid shrimp (*Americamysis bahia*), but did reduce growth of Inland Silverside fish (*Menidia beryllina*) at higher particle concentrations (Siddiqui et al., 2022). Siddiqui *et al.* also found that leached chemicals did not have a significant impact on growth for both these species.

Further investigations into brain morphometrics at the 10% treatment level revealed that tadpoles exposed to F3 had significantly larger brains compared to the control - the telencephalon, diencephalon, optic tectum, and medulla were all larger in width. According to the Cognitive Buffer Hypothesis, one possible explanation for the increased brain size is to confer greater locomotory abilities to compensate for environmental stressors (Luo et al., 2017). We acknowledge that the increased growth in treatments with reduced survival may be related to density effects that were not fully captured in the statistical models, and we recommend that future studies be performed with treatment levels that support higher survival or with one animal per experimental unit.

2.4.5 Impact on Swimming Behavior after 9-Day Exposure

The startle response of tadpoles is an ecologically relevant endpoint. When exposed to a predator, tadpoles exhibit a sharp, jerking motion accompanied by accelerated swimming to avoid predation (Berrill, Bertram, McGillivray, Kolohon, & Pauli, 1994; Jung & Jagoe, 1995). At the 10% treatment level, tadpoles in F1 and F2 showed significantly lower swimming activity when

compared to the controls, indicating a potentially diminished ability for predator avoidance. Tadpoles in F3 were on average more active at this concentration compared to those in F1 and F2, possibly due to stress (Burgos-Aceves et al., 2022) or the F3 tadpoles' increased brain size - a larger telencephalon in anurans may lead to improved navigation and cognitive function (Mai & Liao, 2019). One possible cellular mechanism of toxic action that could be responsible for the increased swimming activity is overstimulation of the cholinergic system which controls movement (Burgos-Aceves et al., 2022). At the 1% treatment level, however, the tadpoles in F3 swam significantly less than the controls. A similar trend was observed when comparing the feeding activity, though only 10% F2 was significantly lower than the controls, and this reduction in locomotion may have negative implications on the animal's ability to forage for food.

Overall, chemical constituent fractions (*i.e.*, F1 and F2) had a negative impact on swimming behavior at the 10% treatment, but the trend was not so obvious at the lower 1% treatment. From an extensive behavioral study, Siddiqui *et al.* reported significant behavioral changes for two different estuarine species, *A. bahia* and *M. beryllina*, upon exposure to both the leached chemicals and nano-sized TWP (< 1 μm) at particle concentrations of 60, 6,000 and 60,000 particles/mL (Siddiqui et al., 2022).

2.5 Conclusion

Prolonged 9-day exposure to low concentrations of all fractions of tire-wear particle leachate (F1, F2, and F3) at almost all treatment levels significantly decreased the survival of the amphibian *S. tropicalis* during its embryonic to larval stages. However, the nanoparticulate fraction (F3) was the most acutely lethal fraction, likely due to the presence of smaller, more bioavailable nanoparticles exerting greater cytotoxic effects. Enhanced aggregation of particles in F1 may be responsible for its lower acute toxicity compared to the other nanoparticle-containing fraction, F3. For the acute exposure, the frequency of malformed tadpoles increased in a roughly proportional manner to increasing concentrations of all fractions. Distinct differences between fractions were observed for single malformations, whereby the fractions containing leached chemicals (*i.e.*, F1 and F2) exhibited higher instances of head, gut, and edema malformations suggesting that the leached chemicals exerted a more teratogenic than lethal effect at the concentrations used in the present study. Prolonged 9-day exposure to F1 and F2 also had significant negative effects on both the tadpole startle response and feeding activity at the 10% treatment though the results were different at the 1% treatment. This altered behavior is a sign of reduced individual fitness that could have ramifications at the population level. Brain morphometrics (telencephalon width, diencephalon width, optic tectum width and medulla width), were impacted after 9 days, and tadpoles in F3 had significantly larger brains indicative of exposure to a higher degree of environmental stress according to the cognitive brain hypothesis. The larger brain size appeared to enhance swimming ability.

These results reveal that there are distinct adverse effects associated with the nanoparticle and leached chemicals in TWP leachate, and that the relative proportion of these constituents in the environment will influence the overall toxicity to freshwater organisms. The leached chemicals

and nanoparticles have different modes of toxic action, but further research is needed to elucidate the precise cellular mechanisms of toxicity of these different constituents, as well as to identify the specific chemicals driving toxicity.

Chapter 3: Conclusions and Future Work

Despite recent efforts to distinguish between the toxicity of TWP suspensions and leachates, a key knowledge gap still exists whereby the particle-specific effects and the chemical-specific effects of tire-wear particle leachate are still poorly understood. Furthermore, most aquatic toxicity studies used tire-wear particle suspensions/leachates which contained a mixture of micrometer- and nanometer-sized TWP, precluding the deduction of any size-related effects in the nanometer range. These knowledge gaps were addressed in the present study by exposing an environmentally relevant amphibian model, *S. tropicalis*, to various fractions of a TWP leachate (leached chemicals, nanoparticles < 0.2 μm, or a combination of both).

Overall, all fractions of this contaminant were found to be lethal and teratogenic to *S. tropicalis* after acute exposure and caused significant mortality after a prolonged 9-day exposure during the embryonic and larval stages of development. These findings are consistent with those in the scientific literature in which effects of TWP leachate exposure ranged from mortality to teratogenicity for several different aquatic species including amphibians. Such impacts on individual fitness may translate to smaller amphibian populations in the environment.

In addition to these global effects, chemical-specific and particle-specific effects of TWP leachate toxicity were revealed in both 60-h and 9-day exposures. The fractions containing higher concentrations of leached chemicals (F1 and F2) were generally more teratogenic to *S. tropicalis* and caused the development of more head, gut, and edema abnormalities during its early developmental stages. These leached chemicals fractions also significantly hindered swimming performance after prolonged exposure. The nanoparticulate fraction exhibited higher acute mortality likely due to smaller particle size distribution, but no fraction-specific differences were observed after prolonged 9-day exposure. Brain size was also increased in tadpoles exposed to the

nanoparticulate fraction and the change in brain morphology appears to increase swimming activity. Results were inconclusive as to whether there was a synergistic or antagonistic effect on toxicity from the leached chemicals and nanoparticles.

The results of this study motivate action to be taken to mitigate the effects of this ubiquitous environmental contaminant especially to aquatic organisms. Preventative measures can be taken whereby less toxic chemical additives can be employed in the tire manufacturing process. On the other hand, the generation of tire debris is inevitable, therefore, corrective measures such as installing drainage and filtration systems near high traffic roadways could be implemented to minimize the exposure of aquatic organisms to TWP. The discharge of road runoff directly into water bodies is one of the primary routes of transportation of micro- and nano-TWP to these environmental compartments.

There are both strengths and limitations to the present study. Some of the strengths include 1) demonstrating an effective method for generating TWP in the laboratory and separating nanoparticles from leached chemicals in TWP leachates, 2) performing a thorough physicochemical characterization of the TWP leachate components using techniques such as LC-QTOF-MS, ICP-MS, enhanced darkfield hyperspectral imaging, DLS, and TEM, and 3) exploring a range of ecotoxicological endpoints such as mortality, malformations, growth metrics and swimming parameters to get a broad overview of the impact of the different components of TWP leachate on a model freshwater vertebrate. Despite these strengths, some of the limitations are 1) the inability to directly link the main chemicals to the toxic effects observed, and 2) the lack of a direct physiological link between altered swimming behavior and brain physiology.

This work provides a basic framework for understanding the toxicity of such a complex environmental contaminant on *S. tropicalis*, and future research can be conducted to address the

limitations of this study. Future work can include the identification of the specific mechanisms of toxicity which are responsible for these unique anatomical and physiological changes to *S. tropicalis*, for example, the generation of reactive oxygen species, alterations to enzymatic activities, or damage to DNA. The link between tadpole behavior and brain functionality can be investigated by monitoring neuronal activity with *in vivo* calcium ion imaging. More research can also be done to demonstrate the internalization and translocation of the micro- and nano-TWP in tadpoles. Finally, due to the complex cocktail of chemicals present in tire-wear particles and their potentially synergistic and antagonistic interactions, it remains a challenge to pinpoint the principal agents of toxicity, hence more work is needed to address this knowledge gap.

References

Amaya, E., Offield, M. F., & Grainger, R. M. (1998). Frog genetics: Xenopus tropicalis jumps into the future. *Trends in Genetics, 14*(7), 253-255. doi:https://doi.org/10.1016/S0168-9525(98)01506-6

ASTM International. (2013). Standard Guide for Conducting the Frog Embryo Teratogenesis Assay-Xenopus (FETAX). In *ASTM E1439-12(2013)*. West Conshohocken, PA.

ASTM International. (2020). Standard Guide for Behavioral Testing in Aquatic Toxicology. In *ASTM E1604-20(2020)*. West Conshohocken, PA.

Baensch-Baltruschat, B., Kocher, B., Stock, F., & Reifferscheid, G. (2020). Tyre and road wear particles (TRWP) - A review of generation, properties, emissions, human health risk, ecotoxicity, and fate in the environment. *Science of The Total Environment, 733*, 137823. doi:https://doi.org/10.1016/j.scitotenv.2020.137823

Bantle, J. A., Dumont, J. N., Finch, R. A., Linder, G., & Fort, D. J. (1991). *Atlas of abnormalities : a guide for the performance of FETAX* (Second ed.): Printing Services, Oklahoma State University.

Barbosa, F., Adeyemi, J. A., Bocato, M. Z., Comas, A., & Campiglia, A. (2020). A critical viewpoint on current issues, limitations, and future research needs on micro- and nanoplastic studies: From the detection to the toxicological assessment. *Environmental Research, 182*, 109089. doi:https://doi.org/10.1016/j.envres.2019.109089

Bates, D., Machler, M., Bolker, B., & Walker, S. (2015). Fitting Linear Mixed-Effects Models Using lme4. Journal of Statistical Software 67(1): 1-48 doi:10.18637/jss/v067.i01.

Beddoes, C. M., Case, C. P., & Briscoe, W. H. (2015). Understanding nanoparticle cellular entry: A physicochemical perspective. *Advances in Colloid and Interface Science, 218*, 48-68. doi:https://doi.org/10.1016/j.cis.2015.01.007

Berrill, M., Bertram, S., McGillivray, L., Kolohon, M., & Pauli, B. (1994). Effects of low concentrations of forest use pesticides on frog embryos and tadpoles. *Environmental Toxicology and Chemistry, 13*(4), 657-664. doi:10.1897/1552-8618(1994)13[657:eolcof]2.0.co;2

Berrill, M., Bertram, S., Wilson, A., Louis, S., Brigham, D., & Stromberg, C. (1993). Lethal and sublethal impacts of pyrethroid insecticides on amphibian embryos and tadpoles. *Environmental Toxicology and Chemistry, 12*(3), 525-539. doi:10.1897/1552-8618(1993)12[525:lasiop]2.0.co;2

Besseling, E., Wang, B., Lürling, M., & Koelmans, A. A. (2014). Nanoplastic Affects Growth of S. obliquus and Reproduction of D. magna. *Environmental Science & Technology, 48*(20), 12336-12343. doi:10.1021/es503001d

Bhattacharya, P., Lin, S., Turner, J. P., & Ke, P. C. (2010). Physical Adsorption of Charged Plastic Nanoparticles Affects Algal Photosynthesis. *The Journal of Physical Chemistry C, 114*(39), 16556-16561. doi:10.1021/jp1054759

Boucher, J., & Friot, D. (2017). *Primary microplastics in the oceans: a global evaluation of sources* (Vol. 10): Iucn Gland, Switzerland.

Brown, D. M., Wilson, M. R., MacNee, W., Stone, V., & Donaldson, K. (2001). Size-Dependent Proinflammatory Effects of Ultrafine Polystyrene Particles: A Role for Surface Area and Oxidative Stress in the Enhanced Activity of Ultrafines. *Toxicology and Applied Pharmacology, 175*(3), 191-199. doi:https://doi.org/10.1006/taap.2001.9240

Burgos-Aceves, M. A., Faggio, C., Betancourt-Lozano, M., González-Mille, D. J., & Ilizaliturri-Hernández, C. A. (2022). Ecotoxicological perspectives of microplastic pollution in amphibians. *Journal of Toxicology and Environmental Health, Part B, 25*(8), 405-421. doi:10.1080/10937404.2022.2140372

Cai, H., Xu, E. G., Du, F., Li, R., Liu, J., & Shi, H. (2021). Analysis of environmental nanoplastics: Progress and challenges. *Chemical Engineering Journal, 410*, 128208. doi:https://doi.org/10.1016/j.cej.2020.128208

Camponelli, K. M., Casey, R. E., Snodgrass, J. W., Lev, S. M., & Landa, E. R. (2009). Impacts of weathered tire debris on the development of Rana sylvatica larvae. *Chemosphere, 74*(5), 717-722. doi:https://doi.org/10.1016/j.chemosphere.2008.09.056

Cannatella, D. C., & Trueb, L. (1988). Evolution of pipoid frogs: intergeneric relationships of the aquatic frog family Pipidae (Anura). *Zoological Journal of the Linnean Society, 94*(1), 1-38.

Capolupo, M., Sørensen, L., Jayasena, K. D. R., Booth, A. M., & Fabbri, E. (2020). Chemical composition and ecotoxicity of plastic and car tire rubber leachates to aquatic organisms. *Water Research, 169*, 115270. doi:https://doi.org/10.1016/j.watres.2019.115270

Carvan, M. J., 3rd, Loucks, E., Weber, D. N., & Williams, F. E. (2004). Ethanol effects on the developing zebrafish: neurobehavior and skeletal morphogenesis. *Neurotoxicology and Teratology, 26*(6), 757-768. doi:10.1016/j.ntt.2004.06.016

Cedervall, T., Hansson, L.-A., Lard, M., Frohm, B., & Linse, S. (2012). Food Chain Transport of Nanoparticles Affects Behaviour and Fat Metabolism in Fish. *PLOS ONE, 7*(2), e32254. doi:10.1371/journal.pone.0032254

Cha, E. S., Uhrin, M. T., McClelland, S. J., & Woodley, S. K. (2021). Brain plasticity in response to short-term exposure to corticosterone in larval amphibians. *Canadian Journal of Zoology, 99*(9), 839-844. doi:10.1139/cjz-2021-0031

Chibwe, L., Parrott, J., Shires, K., Khan, H., Clarence, S., Lavalle, C., . . . Rochman, C. (2021). A Deep Dive into the Complex Chemical Mixture and Toxicity of Tire Wear Particle Leachate in Fathead Minnow. *Environmental Toxicology and Chemistry, 41*. doi:10.1002/etc.5140

Cragg, M. M., Balinsky, J., & Baldwin, E. (1961). A comparative study of nitrogen excretion in some amphibia and reptiles. *Comparative Biochemistry and Physiology, 3*(4), 227-235.

Cunningham, B., Harper, B., Brander, S., & Harper, S. (2022). Toxicity of micro and nano tire particles and leachate for model freshwater organisms. *Journal of Hazardous Materials, 429*, 128319. doi:https://doi.org/10.1016/j.jhazmat.2022.128319

Dall'Osto, M., Beddows, D. C. S., Gietl, J. K., Olatunbosun, O. A., Yang, X., & Harrison, R. M. (2014). Characteristics of tyre dust in polluted air: Studies by single particle mass spectrometry (ATOFMS). *Atmospheric Environment, 94*, 224-230. doi:https://doi.org/10.1016/j.atmosenv.2014.05.026

de Mendiburu, F. (2021). _agricolae: Statistical Procedures for Agricultural Research_. R package version 1.3-5,. Retrieved from <https://CRAN.R-project.org/package=agricolae>.

Degaffe, F. S., & Turner, A. (2011). Leaching of zinc from tire wear particles under simulated estuarine conditions. *Chemosphere, 85*(5), 738-743. doi:https://doi.org/10.1016/j.chemosphere.2011.06.047

Della Torre, C., Bergami, E., Salvati, A., Faleri, C., Cirino, P., Dawson, K. A., & Corsi, I. (2014). Accumulation and Embryotoxicity of Polystyrene Nanoparticles at Early Stage of Development of Sea Urchin Embryos Paracentrotus lividus. *Environmental Science & Technology, 48*(20), 12302-12311. doi:10.1021/es502569w

Denver, R. J. (2010). Tadpole Behavior and Metamorphosis. In M. D. Breed & J. Moore (Eds.), *Encyclopedia of Animal Behavior* (pp. 375-378). Oxford: Academic Press.

Dong, X., Wu, Z., Li, X., Xiao, L., Yang, M., Li, Y., . . . Sun, Z. (2020). The size-dependent cytotoxicity of amorphous silica nanoparticles: a systematic review of in vitro studies. *International journal of nanomedicine, 15*, 9089. doi:10.2147/IJN.S276105

Dyck, A., Robinson, S. A., Young, S. D., Renaud, J. B., Sabourin, L., Lapen, D. R., & Pick, F. R. (2021). The Effects of Ditch Management in Agroecosystems on Embryonic and Tadpole Survival, Growth, and Development of Northern Leopard Frogs (Lithobates pipiens). *Archives of Environmental Contamination and Toxicology, 81*(1), 107-122. doi:10.1007/s00244-021-00836-0

Egea-Serrano, A., Relyea, R. A., Tejedo, M., & Torralva, M. (2012). Understanding of the impact of chemicals on amphibians: a meta-analytic review. *Ecology and Evolution, 2*(7), 1382-1397. doi:10.1002/ece3.249

European Automobile Manufacturers Association. (2019). World Motor Vehicle Production. Retrieved from https://www.acea.be/statistics/tag/category/world-production

Fong, P. P., Lambert, O. J., Hoagland, M. L., & Kurtz, E. R. (2018). Differential sensitivity to the antifouling chemical medetomidine between wood frog and American toad tadpoles with evidence for low-dose stimulation and high-dose inhibition of metamorphosis. *Environmental Science and Pollution Research, 25*(20), 19470-19479. doi:10.1007/s11356-018-2168-y

Gigault, J., Halle, A. t., Baudrimont, M., Pascal, P.-Y., Gauffre, F., Phi, T.-L., . . . Reynaud, S. (2018). Current opinion: What is a nanoplastic? *Environmental Pollution, 235*, 1030-1034. doi:https://doi.org/10.1016/j.envpol.2018.01.024

Gillespie, G. R. (2002). Impacts of sediment loads, tadpole density, and food type on the growth and development of tadpoles of the spotted tree frog Litoria spenceri: an in-stream experiment. *Biological Conservation, 106*(2), 141-150. doi:https://doi.org/10.1016/S0006-3207(01)00127-6

Gray, A. D., Wertz, H., Leads, R. R., & Weinstein, J. E. (2018). Microplastic in two South Carolina Estuaries: Occurrence, distribution, and composition. *Marine Pollution Bulletin, 128*, 223-233. doi:https://doi.org/10.1016/j.marpolbul.2018.01.030

Gualtieri, M., Andrioletti, M., Mantecca, P., Vismara, C., & Camatini, M. (2005). Impact of tire debris on in vitro and in vivo systems. *Particle and Fibre Toxicology, 2*(1), 1. doi:10.1186/1743-8977-2-1

Gualtieri, M., Andrioletti, M., Vismara, C., Milani, M., & Camatini, M. (2005). Toxicity of tire debris leachates. *Environment International, 31*(5), 723-730. doi:https://doi.org/10.1016/j.envint.2005.02.001

Halle, L. L., Palmqvist, A., Kampmann, K., Jensen, A., Hansen, T., & Khan, F. R. (2021). Tire wear particle and leachate exposures from a pristine and road-worn tire to Hyalella azteca: Comparison of chemical content and biological effects. *Aquatic Toxicology, 232*, 105769. doi:https://doi.org/10.1016/j.aquatox.2021.105769

Halle, L. L., Palmqvist, A., Kampmann, K., & Khan, F. R. (2020). Ecotoxicology of micronized tire rubber: Past, present and future considerations. *Science of The Total Environment, 706*, 135694. doi:https://doi.org/10.1016/j.scitotenv.2019.135694

Hayden, M. T., Reeves, M. K., Holyoak, M., Perdue, M., King, A. L., & Tobin, S. C. (2015). Thrice as easy to catch! Copper and temperature modulate predator-prey interactions in larval dragonflies and anurans. *Ecosphere, 6*(4), art56. doi:https://doi.org/10.1890/ES14-00461.1

Hayek, L.-A., Heyer, W. R., & Gascon, C. (2001). Frog Morphometrics: A cautionary Tale. *Alytes: International Journal of Batrachology, 18*, 153-177.

Herkovits, J., & Pérez-Coll, C. S. (1991). Antagonism and synergism between lead and zinc in amphibian larvae. *Environmental Pollution, 69*(2), 217-221. doi:https://doi.org/10.1016/0269-7491(91)90145-M

Johannessen, C., Helm, P., & Metcalfe, C. D. (2022). Runoff of the Tire-Wear Compound, Hexamethoxymethyl-Melamine into Urban Watersheds. *Archives of Environmental Contamination and Toxicology, 82*(2), 162-170. doi:10.1007/s00244-021-00815-5

Jung, R. E., & Jagoe, C. H. (1995). Effects of low pH and aluminum on body size, swimming performance, and susceptibility to predation of green tree frog (Hyla cinerea) tadpoles. *Canadian Journal of Zoology-Revue Canadienne De Zoologie, 73*(12), 2171-2183. doi:10.1139/z95-257

Khakhalin, A. S., Koren, D., Gu, J., Xu, H., & Aizenman, C. D. (2014). Excitation and inhibition in recurrent networks mediate collision avoidance in Xenopus tadpoles. *European Journal of Neuroscience, 40*(6), 2948-2962. doi:https://doi.org/10.1111/ejn.12664

Khan, F. R., Halle, L. L., & Palmqvist, A. (2019). Acute and long-term toxicity of micronized car tire wear particles to Hyalella azteca. *Aquatic Toxicology, 213*, 105216. doi:https://doi.org/10.1016/j.aquatox.2019.05.018

Khokha, M. K., Chung, C., Bustamante, E. L., Gaw, L. W. K., Trott, K. A., Yeh, J., . . . Grammer, T. C. (2002). Techniques and probes for the study of Xenopus tropicalis development. *Developmental Dynamics, 225*(4), 499-510. doi:https://doi.org/10.1002/dvdy.10184

Klaine, S. J., Koelmans, A. A., Horne, N., Carley, S., Handy, R. D., Kapustka, L., . . . von der Kammer, F. (2012). Paradigms to assess the environmental impact of manufactured nanomaterials. *Environmental Toxicology and Chemistry, 31*(1), 3-14. doi:https://doi.org/10.1002/etc.733

Klöckner, P., Reemtsma, T., Eisentraut, P., Braun, U., Ruhl, A. S., & Wagner, S. (2019). Tire and road wear particles in road environment - Quantification and assessment of particle dynamics by Zn determination after density separation. *Chemosphere, 222*, 714-721. doi:10.1016/j.chemosphere.2019.01.176

Knight, L. J., Parker-Jurd, F. N. F., Al-Sid-Cheikh, M., & Thompson, R. C. (2020). Tyre wear particles: an abundant yet widely unreported microplastic? *Environmental Science and Pollution Research, 27*(15), 18345-18354. doi:10.1007/s11356-020-08187-4

Koelmans, A. A., Besseling, E., & Shim, W. J. (2015). Nanoplastics in the Aquatic Environment. Critical Review. In M. Bergmann, L. Gutow, & M. Klages (Eds.), *Marine Anthropogenic Litter* (pp. 325-340). Cham: Springer International Publishing.

Kole, P. J., Löhr, A. J., Van Belleghem, F. G. A. J., & Ragas, A. M. J. (2017). Wear and Tear of Tyres: A Stealthy Source of Microplastics in the Environment. *International journal of environmental research and public health, 14*(10), 1265. doi:10.3390/ijerph14101265

Kolomijeca, A., Parrott, J., Khan, H., Shires, K., Clarence, S., Sullivan, C., . . . Rochman, C. M. (2020). Increased Temperature and Turbulence Alter the Effects of Leachates from Tire Particles on Fathead Minnow (Pimephales promelas). *Environmental Science & Technology, 54*(3), 1750-1759. doi:10.1021/acs.est.9b05994

Kontrick, A. V. (2018). Microplastics and Human Health: Our Great Future to Think About Now. *Journal of Medical Toxicology, 14*(2), 117-119. doi:10.1007/s13181-018-0661-9

Kovochich, M., Liong, M., Parker, J. A., Oh, S. C., Lee, J. P., Xi, L., . . . Unice, K. M. (2021). Chemical mapping of tire and road wear particles for single particle analysis. *Science of The Total Environment, 757*, 144085. doi:https://doi.org/10.1016/j.scitotenv.2020.144085

Kuznetsova, A., Brockhoff, P. B., & Christensen, R. H. B. (2017). lmerTest Package: Tests in Linear Mixed Effects Models. *Journal of Statistical Software, 82(13):1-26*. doi:10.18637/jss.v082.i13

Lee, K.-W., Shim, W. J., Kwon, O. Y., & Kang, J.-H. (2013). Size-Dependent Effects of Micro Polystyrene Particles in the Marine Copepod Tigriopus japonicus. *Environmental Science & Technology, 47*(19), 11278-11283. doi:10.1021/es401932b

Liao, C., Kim, U.-J., & Kannan, K. (2018). A Review of Environmental Occurrence, Fate, Exposure, and Toxicity of Benzothiazoles. *Environmental Science & Technology, 52*(9), 5007-5026. doi:10.1021/acs.est.7b05493

Liu, L., Xu, K., Zhang, B., Ye, Y., Zhang, Q., & Jiang, W. (2021). Cellular internalization and release of polystyrene microplastics and nanoplastics. *Science of The Total Environment, 779*, 146523. doi:https://doi.org/10.1016/j.scitotenv.2021.146523

Liu, Y., Zhou, H., Yan, M., Liu, Y., Ni, X., Song, J., & Yi, X. (2022). Toxicity of tire wear particles and the leachates to microorganisms in marine sediments. *Environmental Pollution, 309*, 119744. doi:https://doi.org/10.1016/j.envpol.2022.119744

Llewelyn, V. K., Berger, L., & Glass, B. D. (2019). Permeability of frog skin to chemicals: effect of penetration enhancers. *Heliyon, 5*(8), e02127-e02127. doi:10.1016/j.heliyon.2019.e02127

Luo, Y., Zhong, M. J., Huang, Y., Li, F., Liao, W. B., & Kotrschal, A. (2017). Seasonality and brain size are negatively associated in frogs: evidence for the expensive brain framework. *Scientific Reports, 7*(1), 16629. doi:10.1038/s41598-017-16921-1

Ma, Y., Mummullage, S., Wijesiri, B., Egodawatta, P., McGree, J., Ayoko, G. A., & Goonetilleke, A. (2021). Source quantification and risk assessment as a foundation for risk management of metals in urban road deposited solids. *Journal of Hazardous Materials, 408*, 124912. doi:https://doi.org/10.1016/j.jhazmat.2020.124912

Mai, C. L., & Liao, W. B. (2019). Brain size evolution in anurans: a review. *Animal Biology, 69*(3), 265-279. doi:https://doi.org/10.1163/15707563-00001074

Malaysian Rubber Export Promotion Council, M. (2021). World Rubber Production, Consumption and Trade. Retrieved from http://www.myrubbercouncil.com/industry/world_production.php

Mantecca, P., Gualtieri, M., Andrioletti, M., Bacchetta, R., Vismara, C., Vailati, G., & Camatini, M. (2007). Tire debris organic extract affects Xenopus development. *Environment International, 33*(5), 642-648. doi:https://doi.org/10.1016/j.envint.2007.01.007

Mantecca, P., Sancini, G., Moschini, E., Farina, F., Gualtieri, M., Rohr, A., . . . Camatini, M. (2009). Lung toxicity induced by intratracheal instillation of size-fractionated tire particles. *Toxicology Letters, 189*(3), 206-214. doi:https://doi.org/10.1016/j.toxlet.2009.05.023

Marking, L. L., & Dawson, V. K. (1973). *Toxicity of quinaldine sulfate to fish* (48). Retrieved from http://pubs.er.usgs.gov/publication/ifc48

Marwood, C., McAtee, B., Kreider, M., Ogle, R. S., Finley, B., Sweet, L., & Panko, J. (2011). Acute aquatic toxicity of tire and road wear particles to alga, daphnid, and fish. *Ecotoxicology, 20*(8), 2079. doi:10.1007/s10646-011-0750-x

Matthews, S., Xu, E. G., Roubeau Dumont, E., Meola, V., Pikuda, O., Cheong, R. S., . . . Tufenkji, N. (2021). Polystyrene micro- and nanoplastics affect locomotion and daily activity of Drosophila melanogaster. *Environmental Science: Nano*. doi:10.1039/D0EN00942C

Ni, H.-G., Lu, F.-H., Luo, X.-L., Tian, H.-Y., & Zeng, E. Y. (2008). Occurrence, Phase Distribution, and Mass Loadings of Benzothiazoles in Riverine Runoff of the Pearl River Delta, China. *Environmental Science & Technology, 42*(6), 1892-1897. doi:10.1021/es071871c

Nieuwkoop, P. D., & Faber, J. (1956). *Normal Tables of Xenopus laevis (Daudin)* (Second ed.). North Holland, Amsterdam.

Panko, J. M., Hitchcock, K. M., Fuller, G. W., & Green, D. (2019). Evaluation of Tire Wear Contribution to PM2.5 in Urban Environments. *Atmosphere, 10*(2), 99. doi:https://doi.org/10.3390/atmos10020099

Panko, J. M., Kreider, M. L., McAtee, B. L., & Marwood, C. (2013). Chronic toxicity of tire and road wear particles to water- and sediment-dwelling organisms. *Ecotoxicology, 22*(1), 13-21. doi:10.1007/s10646-012-0998-9

Park, I., Kim, H., & Lee, S. (2018). Characteristics of tire wear particles generated in a laboratory simulation of tire/road contact conditions. *Journal of Aerosol Science, 124*, 30-40. doi:https://doi.org/10.1016/j.jaerosci.2018.07.005

Pinelli, C., Santillo, A., Chieffi Baccari, G., Falvo, S., & Di Fiore, M. M. (2019). Effects of chemical pollutants on reproductive and developmental processes in Italian amphibians. *Molecular Reproduction and Development, 86*(10), 1324-1332. doi:https://doi.org/10.1002/mrd.23165

Plastics-Europe. (2020). Plastics – the Facts 2020. An analysis of European latest plastics production, demand and waste data. *Plastics Europe: Association of Plastic Manufacturers: Brussels, Belgium*, 16.

Pochron, S. T., Fiorenza, A., Sperl, C., Ledda, B., Lawrence Patterson, C., Tucker, C. C., . . . Panico, N. (2017). The response of earthworms (Eisenia fetida) and soil microbes to the crumb rubber material used in artificial turf fields. *Chemosphere, 173*, 557-562. doi:https://doi.org/10.1016/j.chemosphere.2017.01.091

Qazi, A. H., & Ashok, K. (2012). Global amphibian declines: a review. *International Journal of Biodiversity and Conservation, 4*(10), 348-357.

R Core Team 2022. R: A language and environment for statistical computing. R Foundation for Statistical Computing, Vienna, Austria. URL. Retrieved from https://www.R-project.org/

Ralph, S., & Petras, M. (1997). Genotoxicity monitoring of small bodies of water using two species of tadpoles and the alkaline single cell gel (comet) assay. *Environmental and Molecular Mutagenesis, 29*(4), 418-430. doi:https://doi.org/10.1002/(SICI)1098-2280(1997)29:4<418::AID-EM11>3.0.CO;2-H

Rauert, C., Kaserzon, S. L., Veal, C., Yeh, R. Y., Mueller, J. F., & Thomas, K. V. (2020). The first environmental assessment of hexa(methoxymethyl)melamine and co-occurring cyclic amines in Australian waterways. *Science of The Total Environment, 743*, 140834. doi:https://doi.org/10.1016/j.scitotenv.2020.140834

Reddy, C. M., & Quinn, J. G. (1997). Environmental Chemistry of Benzothiazoles Derived from Rubber. *Environmental Science & Technology, 31*(10), 2847-2853. doi:10.1021/es970078o

Redondo-Hasselerharm, P. E., de Ruijter, V. N., Mintenig, S. M., Verschoor, A., & Koelmans, A. A. (2018). Ingestion and Chronic Effects of Car Tire Tread Particles on Freshwater Benthic Macroinvertebrates. *Environmental Science & Technology, 52*(23), 13986-13994. doi:10.1021/acs.est.8b05035

Reed, M. D., Iceman, K. E., Harris, M. B., & Taylor, B. E. (2018). The rostral medulla of bullfrog tadpoles contains critical lung rhythmogenic and chemosensitive regions across metamorphosis. *Comp Biochem Physiol A Mol Integr Physiol, 225*, 7-15. doi:10.1016/j.cbpa.2018.05.024

Robinson, S. A., Richardson, S. D., Dalton, R. L., Maisonneuve, F., Trudeau, V. L., Pauli, B. D., & Lee-Jenkins, S. S. Y. (2017). Sublethal effects on wood frogs chronically exposed to environmentally relevant concentrations of two neonicotinoid insecticides. *Environmental Toxicology and Chemistry, 36*(4), 1101-1109. doi:https://doi.org/10.1002/etc.3739

Roubeau Dumont, E., Gao, X., Zheng, J., Macairan, J.-R., Hernandez Rodriguez, L., Baesu, A., . . . Tufenkji, N. (2023). Unraveling the Toxicity of Tire Wear Contamination in Three Freshwater Species: From Chemical Mixture to Nanoparticles. Under Review. doi:https://dx.doi.org/10.2139/ssrn.4369138

RStudio Team 2022. RStudio: Integrated Development Environment for R. RStudio, PBC, Boston, MA URL Retrieved from http://www.rstudio.com/.

Saka, M. (2010). Acute toxicity of rice paddy herbicides simetryn, mefenacet, and thiobencarb to Silurana tropicalis tadpoles. *Ecotoxicol Environ Saf, 73*(6), 1165-1169. doi:10.1016/j.ecoenv.2010.05.008

Santo, K. P., Vishnyakov, A., Kumar, R., & Neimark, A. V. (2018). Elucidating the Effects of Metal Complexation on Morphological and Rheological Properties of Polymer Solutions by a Dissipative Particle Dynamics Model. *Macromolecules, 51*(14), 4987-5000. doi:10.1021/acs.macromol.8b00493

Schneider, C. A., Rasband, W. S., & Eliceiri, K. W. (2012). NIH Image to ImageJ: 25 years of image analysis. *Nature Methods, 9*(7), 671-675. doi:10.1038/nmeth.2089

Shin, H., Sukumaran, V., Yeo, I.-C., Shim, K.-Y., Lee, S., Choi, H.-K., . . . Lee, J.-S. (2022). Phenotypic toxicity, oxidative response, and transcriptomic deregulation of the rotifer Brachionus plicatilis exposed to a toxic cocktail of tire-wear particle leachate. *Journal of Hazardous Materials, 438*, 129417. doi:10.1016/j.jhazmat.2022.129417

Shupe, H. J., Boenisch, K. M., Harper, B. J., Brander, S. M., & Harper, S. L. (2021). Effect of Nanoplastic Type and Surface Chemistry on Particle Agglomeration over a Salinity Gradient. *Environmental Toxicology and Chemistry, 40*(7), 1820-1826. doi:https://doi.org/10.1002/etc.5030

Siddiqui, S., Dickens, J. M., Cunningham, B. E., Hutton, S. J., Pedersen, E. I., Harper, B., . . . Brander, S. M. (2022). Internalization, reduced growth, and behavioral effects following exposure to micro and nano tire particles in two estuarine indicator species. *Chemosphere, 296*, 133934. doi:https://doi.org/10.1016/j.chemosphere.2022.133934

Simon, E., Puky, M., Braun, M., & Tóthmérész, B. (2011). Frogs and toads as biological indicators in environmental assessment. *Frogs: Biology, Ecology and Uses*, 141-150.

Sommer, F., Dietze, V., Baum, A., Sauer, J., Gilge, S., Maschowski, C., & Gieré, R. (2018). Tire Abrasion as a Major Source of Microplastics in the Environment. *Aerosol and Air Quality Research, 18*(8), 2014-2028. doi:10.4209/aaqr.2018.03.0099

Sparling, D., Linder, G., Bishop, C., & Krest, S. K. (2000). Ecotoxicology of Amphibians and Reptiles. *Recent Advancements in Amphibian and Reptile Ecotoxicology*, 1-13. doi:10.1201/EBK1420064162

Tallec, K., Gabriele, M., Paul-Pont, I., Alunno-Bruscia, M., & Huvet, A. (2022). Tire rubber chemicals reduce juvenile oyster (Crassostrea gigas) filtration and respiration under experimental conditions. *Marine Pollution Bulletin, 181*, 113936. doi:10.1016/j.marpolbul.2022.113936

Tennekes, H. A., & Sánchez-Bayo, F. (2013). The molecular basis of simple relationships between exposure concentration and toxic effects with time. *Toxicology, 309*, 39-51. doi:10.1016/j.tox.2013.04.007

Tian, Z., Zhao, H., Peter, K. T., Gonzalez, M., Wetzel, J., Wu, C., . . . Kolodziej, E. P. (2020). A ubiquitous tire rubber–derived chemical induces acute mortality in coho salmon. *Science*, eabd6951. doi:10.1126/science.abd6951

Tire America. (2021). Tire Science & History. Retrieved from https://www.tireamerica.com/resource/history-of-tire-innovation

Tonegawa, Y., & Sasaki, S. (2021). Development of Tire-Wear Particle Emission Measurements for Passenger Vehicles. *Emission Control Science and Technology*. doi:10.1007/s40825-020-00181-z

Turner, A., & Rice, L. (2010). Toxicity of tire wear particle leachate to the marine macroalga, Ulva lactuca. *Environmental Pollution, 158*(12), 3650-3654. doi:https://doi.org/10.1016/j.envpol.2010.08.001

Unice, K. M., Weeber, M. P., Abramson, M. M., Reid, R. C. D., van Gils, J. A. G., Markus, A. A., . . . Panko, J. M. (2019). Characterizing export of land-based microplastics to the estuary - Part I: Application of integrated geospatial microplastic transport models to assess tire and road wear particles in the Seine watershed. *Science of The Total Environment, 646*, 1639-1649. doi:https://doi.org/10.1016/j.scitotenv.2018.07.368

Venables, W., & Ripley, B. (2002). Modern Applied Statistics with S, Fourth edition. Springer, New York. ISBN 0-387-95457-0, .

Villena, O. C., Terry, I., Iwata, K., Landa, E. R., LaDeau, S. L., & Leisnham, P. T. (2017). Effects of tire leachate on the invasive mosquito Aedes albopictus and the native congener Aedes triseriatus. *PeerJ, 5*, e3756. doi:10.7717/peerj.3756

Vineeth Kumar, C. M., Karthick, V., Kumar, V. G., Inbakandan, D., Rene, E. R., Suganya, K. S. U., . . . Sowmiya, P. (2022). The impact of engineered nanomaterials on the environment: Release mechanism, toxicity, transformation, and remediation. *Environmental Research, 212*, 113202. doi:https://doi.org/10.1016/j.envres.2022.113202

Wagner, S., Hüffer, T., Klöckner, P., Wehrhahn, M., Hofmann, T., & Reemtsma, T. (2018). Tire wear particles in the aquatic environment - A review on generation, analysis, occurrence, fate and effects. *Water Research, 139*, 83-100. doi:https://doi.org/10.1016/j.watres.2018.03.051

Wik, A., & Dave, G. (2005). Environmental labeling of car tires—toxicity to Daphnia magna can be used as a screening method. *Chemosphere, 58*(5), 645-651. doi:https://doi.org/10.1016/j.chemosphere.2004.08.103

Wik, A., & Dave, G. (2006). Acute toxicity of leachates of tire wear material to Daphnia magna—Variability and toxic components. *Chemosphere, 64*(10), 1777-1784. doi:https://doi.org/10.1016/j.chemosphere.2005.12.045

Wik, A., & Dave, G. (2009). Occurrence and effects of tire wear particles in the environment – A critical review and an initial risk assessment. *Environmental Pollution, 157*(1), 1-11. doi:https://doi.org/10.1016/j.envpol.2008.09.028

Wik, A., & Dave, G. (2009). Occurrence and effects of tire wear particles in the environment--a critical review and an initial risk assessment. *Environmental Pollutution, 157*(1), 1-11. doi:10.1016/j.envpol.2008.09.028

Wik, A., Nilsson, E., Källqvist, T., Tobiesen, A., & Dave, G. (2009). Toxicity assessment of sequential leachates of tire powder using a battery of toxicity tests and toxicity identification evaluations. *Chemosphere, 77*(7), 922-927. doi:https://doi.org/10.1016/j.chemosphere.2009.08.034

Xu, E. G., Lin, N., Cheong, R. S., Ridsdale, C., Tahara, R., Du, T. Y., . . . Tufenkji, N. (2019). Artificial turf infill associated with systematic toxicity in an amniote vertebrate. *Proceedings of the National Academy of Sciences, 116*(50), 25156-25161. doi:10.1073/pnas.1909886116

Yang, K., Jing, S., Liu, Y., Zhou, H., Liu, Y., Yan, M., . . . Liu, R. (2022). Acute toxicity of tire wear particles, leachates and toxicity identification evaluation of leachates to the marine copepod, Tigriopus japonicus. *Chemosphere, 297*, 134099. doi:https://doi.org/10.1016/j.chemosphere.2022.134099

Zhang, B., Chao, J., Chen, L., Liu, L., Yang, X., & Wang, Q. (2021). Research progress of nanoplastics in freshwater. *Science of The Total Environment, 757*, 143791. doi:https://doi.org/10.1016/j.scitotenv.2020.143791

Zhang, J., Zhang, X., Wu, L., Wang, T., Zhao, J., Zhang, Y., . . . Mao, H. (2018). Occurrence of benzothiazole and its derivates in tire wear, road dust, and roadside soil. *Chemosphere, 201*, 310-317. doi:https://doi.org/10.1016/j.chemosphere.2018.03.007

Zuur, A. F., Ieno, E. N., Walker, N. J., Saveliev, A. A., & Smith, G. M. (2009). *Mixed effects models and extensions in ecology with R* (Vol. 574): Springer.

Appendix: Supplementary Materials

Liquid Chromatography-Quadrupole Time of Flight Mass Spectrometry (LC-QTOF-MS)

Table S1 Targeted analytes for Liquid Chromatography-Quadrupole Time of Flight Mass Spectrometry

Analyte	Molecular formula	*m/z*	Retention time (min)
ESI+			
Hexa(methoxymethyl)melamine	$C_{15}H_{30}N_6O_6$	391.2305	7.788
Benzothiazole	C_7H_5NS	136.0221	7.134
Mercaptobenzothiazole	$C_7H_5NS_2$	167.9941	7.390
Dibutyl phthalate	$C_{16}H_{22}O_4$	279.1596	8.748
6-PPD quinone	$C_{18}H_{22}N_2O_2$	299.1760	8.732
Dipentyl phthalate	$C_{18}H_{26}O_4$	307.1909	9.030
Dihexyl phthalate	$C_{20}H_{30}O_4$	335.2222	9.154
Diheptyl-phthalate	$C_{22}H_{34}O_4$	363.2535	9.477
Bis(2-ethylhexyl) phthalate	$C_{24}H_{38}O_4$	391.2848	9.579
Decyl octyl phthalate	$C_{26}H_{42}O_4$	419.3161	9.932
ESI−			
BPA	$C_{15}H_{16}O_2$	227.1072	7.676
Irganox 1081	$C_{22}H_{30}O_2S$	357.1894	9.257
Irganox 1330	$C_{54}H_{78}O_3$	773.5878	10.598
Irganox 1010	$C_{73}H_{108}O_{12}$	1175.7768	10.842

Table S2 Liquid Chromatography-Quadrupole Time of Flight Mass Spectrometry Instrument analysis parameters for targeted analytes

Parameter	Details
Separation Column	InfinityLab Poroshell 120 (Pheny-Hexyl, 3.0 x 100 mm, 2.7 µm, Agilent Technologies) with a Poroshell (4.6 mm) Phenyl Hexyl pre-column
Column Temperature (°C)	30 °C
Mobile Phases for ESI+ Mode	**(A)** 0.1% formic acid in water **(B)** 0.1% formic acid in methanol
Mobile Phases for ESI− Mode	**(A)** 5 mM ammonium acetate in water **(B)** 5 mM ammonium acetate in methanol
Flow Rate (mL/min)	0.3 mL/min for both ESI+ and ESI− modes
Gradient (%)	For both ionization modes an incremental increase in gradient was applied from **(A)** 5% to **(B)** 100% at time 0 min to 7 min and maintained at **(B)** 100% at time 7 min to 12 min. Between time 12 min to 12.5 min the gradient was decreased to **(B)** 5% and maintained at **(B)** 5% between time 12.5 min to 13 min.
Injection Volume (µL)	10 µL for ESI + mode and 20 µL for ESI – mode
Data Collection Mode	Full-scan mode between 80 and 1700 m/z for ESI+ & ESI−
Mass Spectrometry Parameters for ESI+ Mode	Drying gas temperature: 150°C Drying gas flow rate: 11 L/min Sheath gas temperature: 375°C Sheath gas flow rate: 12 L/min Nebulizer pressure: 30 psi Capillary voltage: 4000 V Nozzle voltage: 1000 V Fragmentor voltage: 125 V Skimmer voltage: 45 V
Mass Spectrometry Parameters for ESI− Mode	Drying gas temperature: 175°C Drying gas flow rate: 10 L/min Sheath gas temperature: 375°C Sheath gas flow rate: 12 L/min n Nebulizer pressure: 30 psi Capillary voltage: 4000 V Nozzle voltage: 2000 V Fragmentor voltage: 125 V Skimmer voltage: 40 V

Table S3 Liquid Chromatography-Quadrupole Time of Flight Mass Spectrometry Instrument analysis parameters for non-targeted suspects.

Parameter	Details
Method of Analysis for MS/MS data for Non-targeted Suspects	The same method used for targeted analytes was applied. The "Targeted Feature Extraction" mode was used to get full-scan MS raw datasets from which molecular features were extracted.
Instrument	Agilent MassHunter Profinder B.10.00
Collision Energies (V)	10 V, 20 V, and 40 V
***m/z* Range and Acquisition Rate (spectra/s)**	70 – 1700 at 5 spectra/s 40 – 1700 at 4 spectra/s
Charge State (Z)	Z = 1 for targeted list setting Delta retention time: 0.5 min *Iso width* ~ 1.3 *m/z*
Peak Height Filter (counts)	≥ 300 counts
Allowed Positive Ion Species	$[M+H]^+$, $[M+Na]^+$, $[M+K]^+$, $[M+NH_4]^+$
Allowed Negative Ion Species	$[M-H]^-$, $[M+CH_3COO]^-$
Allowed Neutral Loss Ion Species	$[M-H_2O]$
Retention Time Tolerance (min)	± 0.25 min
Mass Tolerance (ppm)	10.00 ppm + 2.00mDa
Chemical Annotation	Agilent Extractables & Leachables PCDL (1006 compounds)

Experimental Design of Behavioral Assays

Diagrams of the experimental set up of the startle response assay and feeding assay are shown in Figure S1 and Figure S2, respectively. The aim of the startle response assay was to expose the tadpoles to a standard vibrational force in an isolated environment. To do so, a metal rod was dropped from a height of 2.5 cm above the light board within a black box. The rod did not bounce upon hitting the light board. To eliminate the effect of visual stimuli during the startle response assay, tadpoles were partitioned from the experimenter and each other using external and internal black boards, respectively. Note that the height of the internal partition separating tadpoles on the light board was reduced in the diagram for visualization of the tadpoles in the back row. In fact, this internal partition completely covered the falling rod. For video tracking analyses, the total swimming distance was obtained for one min after the rod hit the light board.

Once the startle response assay was completed, the tadpoles were left to acclimatize for 2 min, then the front door of the box was opened, and the experimenter pipetted one drop (30 μL) of tadpole food into each Petri dish starting from the back row from left to right. The box was then closed, and their behavior recorded for 1 min. For video tracking analyses, the total swimming distance and burst swimming distance (i.e., the greatest swimming speed immediately after the introduction of the stimulus) were obtained for 1 min after the droplet of food entered the corresponding Petri dish.

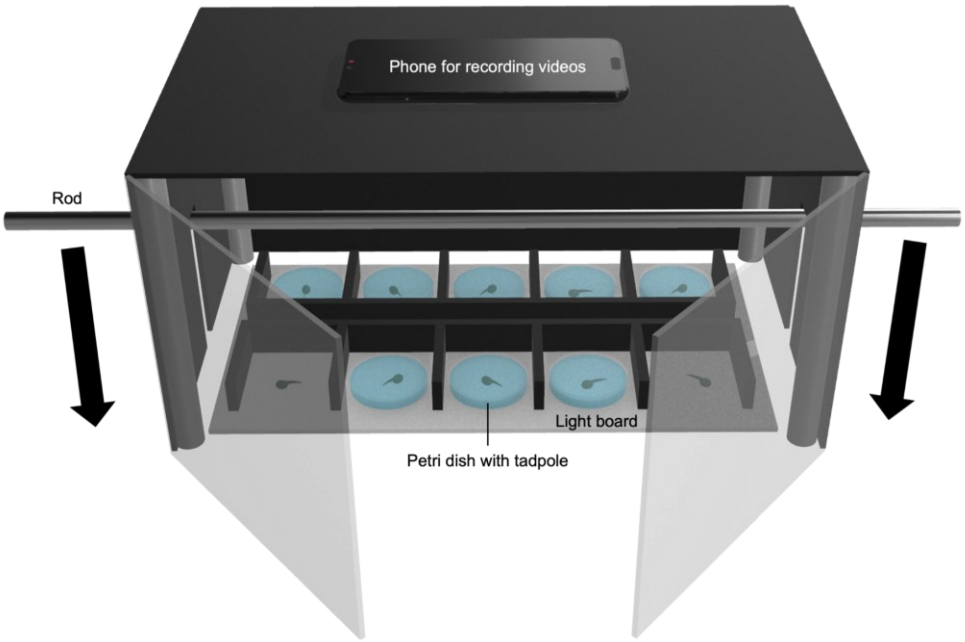

Figure S1 Diagram of the experimental set up of the startle response assay. Ten tadpoles were simultaneously exposed to a standardized vibrational stimulus in the form of a falling rod dropped from a fixed height. Swimming behavior was recorded for 1 min after the stimulus was introduced.

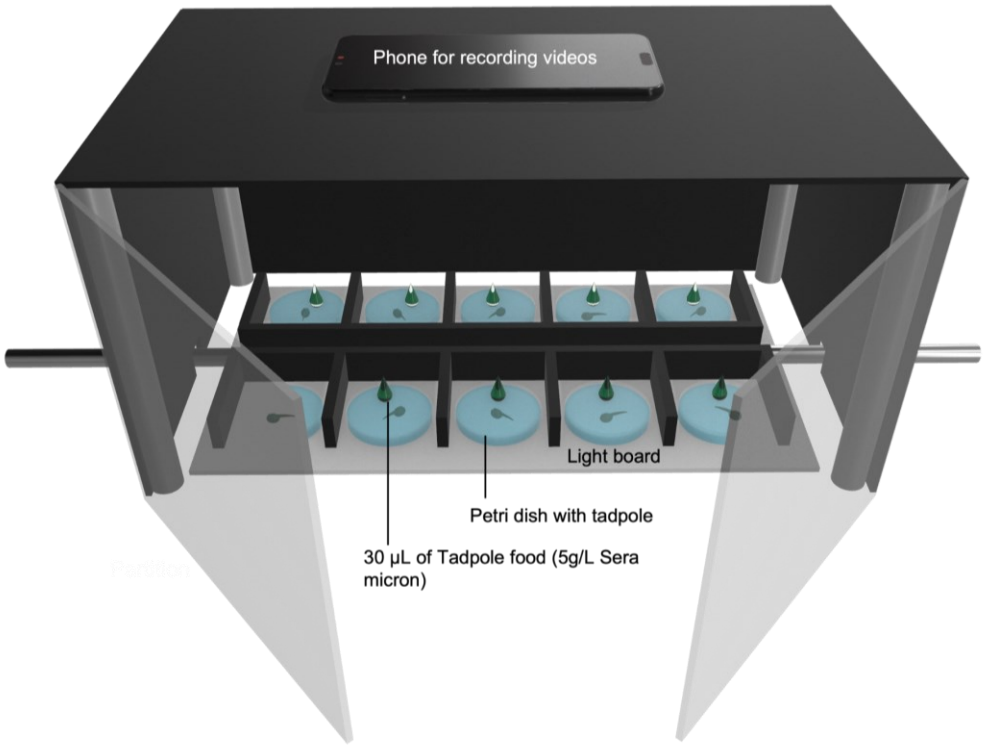

Figure S2 Diagram of the experimental set up of the feeding assay. A drop (30 µL) of tadpole food was added to each Petri dish and the swimming behavior was recorded for 1 min.

Tadpole Nano CT Scanning Parameters

The X-ray nano CT scanning parameters used for each tadpole is shown in Table S4.

Table S4 X-ray nano CT scanning parameters used for each tadpole.

Sample Number	**Nano CT scanning Parameters**
Tadpole 1 (Control)	[Det Assembly Info] Optical Magnification = 4.002400 [Image Info] Current = 84.000000 Data Type = ushort Dto R A Distance = 22795.841797 Exp Times = 1.000000 Image Height = 1014 Image Width = 994 Images Taken = 998 Optical Magnification = 4.002400 Pixel Size = 3.610723 Sto R A Distance = 26253.095703 Voltage = 60.000000
Tadpole 2 (Control)	[Det Assembly Info] Optical Magnification = 4.002400 [Image Info] Current = 84.000000 Data Type = ushort Dto R A Distance = 23812.900391 Exp Times = 1.000000 Image Height = 1014 Image Width = 993 Images Taken = 997 Optical Magnification = 4.002400 Pixel Size = 3.537653 Sto R A Distance = 26257.458984 Voltage = 60.000000
Tadpole 3 (Control)	[Det Assembly Info] Optical Magnification = 4.002400 [Image Info] Current = 83.000000 Data Type = ushort Dto R A Distance = 23812.900391 Exp Times = 1.000000 Image Height = 1014 Image Width = 994 Images Taken = 998 Optical Magnification = 4.002400 Pixel Size = 3.537653 Sto R A Distance = 26257.458984 Voltage = 60.000000

Tadpole 4 (10% F1)	[Det Assembly Info] Optical Magnification = 4.002400 [Image Info] Current = 83.000000 Data Type = ushort Dto R A Distance = 21848.023438 Exp Times = 1.000000 Image Height = 1014 Image Width = 993 Images Taken = 998 Optical Magnification = 4.002400 Pixel Size = 3.405545 Sto R A Distance = 22274.062500 Voltage = 60.000000
Tadpole 5 (10% F1)	[Det Assembly Info] Optical Magnification = 4.002400 [Image Info] Current = 83.000000 Data Type = ushort Dto R A Distance = 21848.023438 Exp Times = 1.000000 Image Height = 1014 Image Width = 994 Images Taken = 998 Optical Magnification = 4.002400 Pixel Size = 3.405545 Sto R A Distance = 22274.062500 Voltage = 60.000000
Tadpole 6 (10% F1)	[Det Assembly Info] Optical Magnification = 4.002400 [Image Info] Current = 83.000000 Data Type = ushort Dto R A Distance = 21848.025391 Exp Times = 1.000000 Image Height = 1014 Image Width = 993 Images Taken = 998 Optical Magnification = 4.002400 Pixel Size = 3.805648 Sto R A Distance = 28277.982422 Voltage = 60.000000
Tadpole 7 (10% F2)	[Det Assembly Info] Optical Magnification = 4.002400 [Image Info] Current = 83.000000 Data Type = ushort Dto R A Distance = 19423.222656

	Exp Times = 1.000000 Image Height = 1014 Image Width = 994 Images Taken = 996 Optical Magnification = 4.002400 Pixel Size = 5.023427 Sto R A Distance = 56644.253906 Voltage = 60.000000
Tadpole 8 (10% F2)	[Det Assembly Info] Optical Magnification = 4.002400 [Image Info] Current = 83.000000 Data Type = ushort Dto R A Distance = 19423.220703 Exp Times = 1.000000 Image Height = 1014 Image Width = 994 Images Taken = 998 Optical Magnification = 4.002400 Pixel Size = 3.903129 Sto R A Distance = 26667.615234 Voltage = 60.000000
Tadpole 9 (10% F2)	[Det Assembly Info] Optical Magnification = 4.002400 [Image Info] Current = 84.000000 Data Type = ushort Dto R A Distance = 31416.931641 Exp Times = 1.000000 Image Height = 1014 Image Width = 993 Images Taken = 997 Optical Magnification = 4.002400 Pixel Size = 3.273552 Sto R A Distance = 29619.779297 Voltage = 60.000000
Tadpole 10 (10% F3)	[Det Assembly Info] Optical Magnification = 4.002400 [Image Info] Current = 84.000000 Data Type = ushort Dto R A Distance = 16453.037109 Exp Times = 0.500000 Image Height = 1014 Image Width = 990 Images Taken = 1000 Optical Magnification = 4.002400 Pixel Size = 3.294381

	Sto R A Distance = 15703.734375 Voltage = 60.000000
Tadpole 11 (10% F3)	[Det Assembly Info] Optical Magnification = 4.002400 [Image Info] Current = 83.000000 Data Type = ushort Dto R A Distance = 13459.353516 Exp Times = 0.750000 Image Height = 1014 Image Width = 994 Images Taken = 998 Optical Magnification = 4.002400 Pixel Size = 4.643678 Sto R A Distance = 29730.130859 Voltage = 60.000000
Tadpole 12 (10% F3)	[Det Assembly Info] Optical Magnification = 4.002400 [Image Info] Current = 83.000000 Data Type = ushort Dto R A Distance = 13459.351563 Exp Times = 0.750000 Image Height = 1014 Image Width = 994 Images Taken = 1000 Optical Magnification = 4.002400 Pixel Size = 4.237989 Sto R A Distance = 22743.789063 Voltage = 60.000000

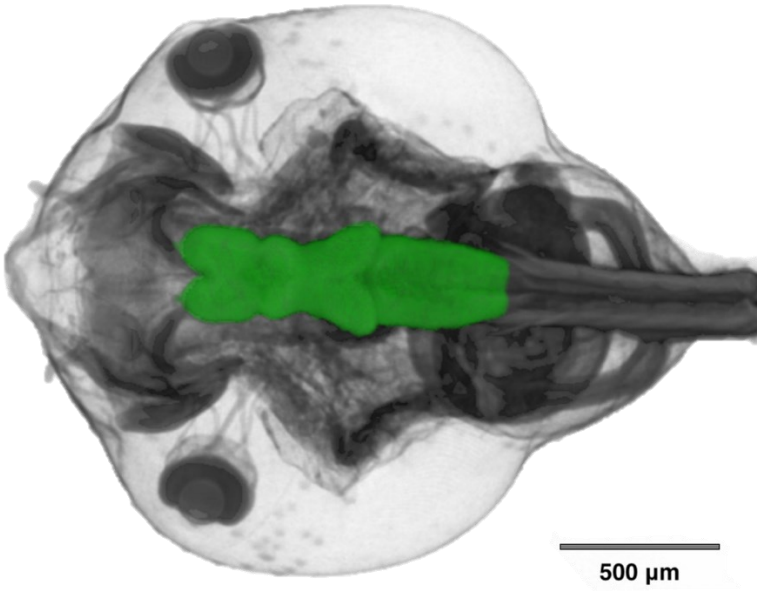

Figure S3 Doral view of the head of a 9-day old tadpole with the brain region highlighted in green.

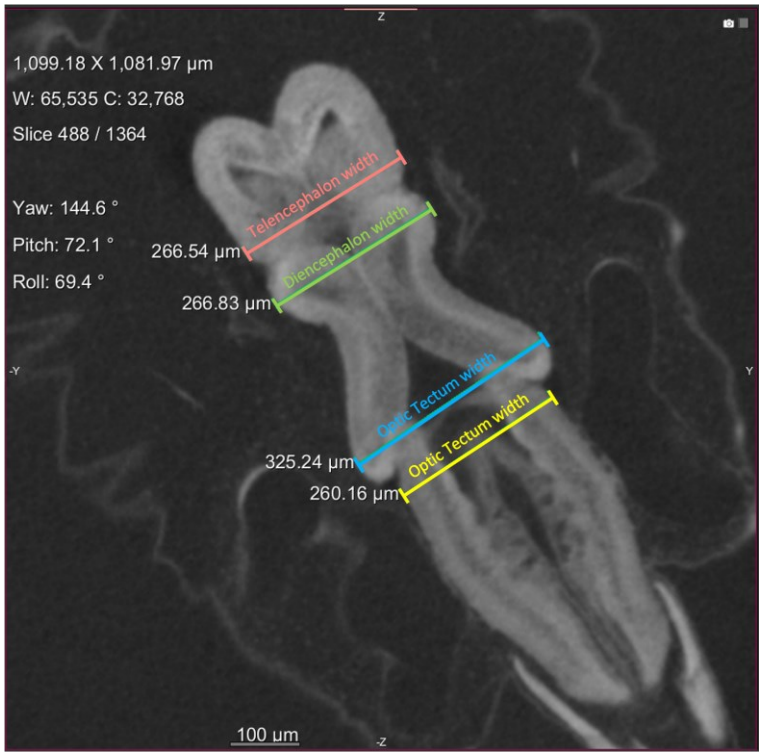

Figure S4 Computed tomography (CT) image through the horizontal plane of the brain. Measurements of the telencephalon width, diencephalon width, optic tectum width and medulla width are shown.

Analysis of Variance (ANOVA) Methodology and Results

Table S5 Analysis of Variance Results on the different response variables such as acute and 9-day survival and malformations. Differences were considered statistically significant at $p \leq 0.05$.

Exposure	Endpoint	Factor	Df	F value	P value
Acute	Survival	Level	5	13.440	1.61×10^{-8}
		Treatment	4	17.838	2.18×10^{-9}
		Level: Treatment	8	2.027	0.0603
		Residuals	54		
Acute	Malformations*	Level	5	49.655	$< 2\times10^{-16}$
		Treatment	4	1.140	0.348
		Level: Treatment	8	1.175	0.331
		Residuals	54		
Acute	Gut Malformations	Level	5	26.448	2.10×10^{-13}
		Treatment	4	15.269	2.06×10^{-8}
		Level: Treatment	8	3.796	0.00135
		Residuals	54		
Acute	Head Malformations*	Level	5	9.880	9.53×10^{-7}
		Treatment	4	7.874	4.48×10^{-5}
		Level: Treatment	8	0.975	0.465
		Residuals	54		
Acute	Tail Malformations	Level	5	21.620	8.14×10^{-12}
		Treatment	4	1.354	0.26212
		Level: Treatment	8	3.726	0.00156
		Residuals	54		
9-Day	Survival	Level	2	42.432	4.64×10^{-9}
		Treatment	4	5.661	0.00192
		Level: Treatment	2	0.091	0.91350
		Residuals	27		
9-Day	Malformations	Level	2	3.295	0.0524
		Treatment	4	0.565	0.6903
		Level: Treatment	2	0.376	0.6904
		Residuals	27		

* A square-root transformation was applied to the response variable to meet the normality assumption.

Generalized Linear Mixed Models (GLMMs) Procedure

The procedure for selecting the GLMM follows that described by Zuur, A.F., *et al.*, *Mixed effects models and extensions in ecology with R*. Vol. 574. 2009: Springer (Zuur et al., 2009). Briefly:

1. Different GLMMs incorporating the most relevant fixed effects for each response variable were run in R software version 4.2.1 (R Core Team 2022) and RStudio software (RStudio Team 2022) using the lme4 package (Bates et al., 2015) and lmerTest package (Kuznetsova et al., 2017).
2. Fixed effects which did not have a significant effect on the response variable were removed from the GLMMs and step 1 was repeated.
3. The GLMM with the smallest Akaike information criterion (AIC) value was selected (Table S6). For models with the same AIC value, the simpler model with fewer fixed effects was selected.
4. The selected model was checked for homoscedasticity and homogeneity.
5. If model fit was poor, different transformations on the response variable were performed (e.g., log and square-root transformations) and steps 1 – 4 were repeated. Final models selected are shown in Table S7.

For body length and tail length, the GLMM fixed effects were treatment, level, as well as survival to account for the effect of different tadpole densities in the experimental units (Table S6). The GLMM random effect of jar was included since tadpoles raised in the same experimental were not considered to be independent from each other. For body width, the GLMM only included treatment, level, and jar, as survival did not have a significant effect on this endpoint. For all brain morphometrics, the GLMM fixed effects were treatment, and the random effect was jar (Table S6). Body width did not have a significant effect on this response variable.

For the total distance travelled during the startle response and feeding assays, square-root transformation was ultimately applied to the response variable as this transformation provided the best model fit (Table S6). The GLMM for the total distance travelled during the startle response had fixed effects of treatment (e.g., F1 10%) and body length, and the random effect of jar (Table S6). The GLMM for the total distance travelled during the feeding assay had fixed effects of treatment, level and body length, and the random effect of jar (Table S6). The GLMM for burst swimming speed had the fixed effects of treatment and total length, and the random effect of jar (Table S6).

For growth and swimming data, controls were re-categorized as follows: Control → 0% F2, PC F1 → 0% F1, PC F3 → 0% F3 in the fixed effect "Treatment" to ensure a 3 × 3 factorial design for statistical analyses (Table S6). When there were no significant differences between the water control and procedural controls, the controls were pooled together into one control group to increase the power of the statistical analysis (Green, J. and J.R. Wheeler, The use of carrier solvents in regulatory aquatic toxicology testing: Practical, statistical and regulatory considerations. Aquatic Toxicology, 2013. 144-145: p. 242-249. Green, J.W., Power and control choice in aquatic experiments with solvents. Ecotoxicology and Environmental Safety, 2014. 102: p. 142-146.). As shown in Table S6, the variable labelled "Treatment_pooledCTRLs" represents data whereby the controls were pooled together; this model was only selected if it had the smallest AIC value.

After the best model was selected, if applicable, a post-hoc analysis was done to obtain the treatment:level pair-wise comparisons using the emmeans package in R software (Lenth R (2022). _emmeans: Estimated Marginal Means, aka Least-Squares Means_. R package version 1.8.0, <https://CRAN.R-project.org/package=emmeans>.). Compared to the control, differences were considered statistically significant at $p \leq 0.05$.

Table S6 Comparisons of Akaike information criterion (AIC) value for different general(ized) mixed models (GLMMs) with relevant predictor variables such as tire-wear particle leachate treatment level, tadpole density/survival, and tadpole length. Jar was included as a random variable in the GLMMs since tadpoles raised in the same jar were not considered independent from each other. For each endpoint the GLMM with the lowest AIC value is highlighted in bold. For models with the same AIC value, the simpler model (i.e., fewer fixed effects) was selected. ΔAIC represents the difference between the AIC of that model and the model with the lowest AIC value.

Model	AIC
Model 1: Body length	
1. Treatment_pooledCTRLs + survival_count + 1|Jar	1250.545
2. Treatment + level + survival_count + 1|Jar	**1247.738**
3. Treatment * level + survival_count + 1|Jar	1252.819
Model 2: Tail length	
1. Treatment_pooledCTRLs + survival_count + 1|Jar	1024.111
2. Treatment + level + survival_count + 1|Jar	**1020.780**
3. Treatment * level + survival_count + 1|Jar	1025.975
Model 3: Body width	
1. Treatment_pooledCTRLs + 1|Jar	307.7200
2. Treatment + level + 1|Jar	**305.7402**
3. Treatment * level + 1|Jar	310.9819
Model 4: sqrt(Startle response total swimming distance)	
1. Treatment_pooledCTRLs + total_length + 1|Jar	**1089.920**
2. Treatment + level + total_length + 1|Jar	1096.675
3. Treatment * level + total_length + 1|Jar	1093.340
Model 5: Startle response burst swimming speed	
1. Treatment_id + total_length + 1|Jar	**-1152.827**
2. Treatment + level + total_length + 1|Jar	-1146.792
3. Treatment * level + total_length + 1|Jar	-1152.827
Model 6: sqrt(Total swimming distance while feeding)	
1. Treatment_pooledCTRLs + total_length + 1|Jar	1074.983
2. Treatment + level + total_length + 1|Jar	1079.411
3. Treatment * level + total_length + 1|Jar	**1074.073**
Model 7: Telencephalon width	
1. Treatment_id + 1|Jar	**112.8714**
2. Treatment + level + 1|Jar	112.8714
3. Treatment * level + 1|Jar	112.8714
Model 8: Diencephalon width	
1. Treatment_id + 1|Jar	**103.7085**
2. Treatment + level + 1|Jar	103.7085

3. Treatment * level + 1|Jar	103.7085
Model 9: Optic tectum width	
1. Treatment_id + 1|Jar	**117.6778**
2. Treatment + level + 1|Jar	117.6778
3. Treatment * level + 1|Jar	117.6778
Model 10: Medulla width	
1. Treatment_id + 1|Jar	**107.8125**
2. Treatment + level + 1|Jar	107.8125
3. Treatment * level + 1|Jar	107.8125

[***Treatment_id***]: unique treatment and level identification e.g., F1 10%; [***Treatment***]: tire-wear particle leachate treatments (F1/F2/F3) with controls re-categorized as Control → 0% F2, PC F1 → 0% F1, PC F3 → 0% F3 to ensure a 3 × 3 factorial design for statistical analyses; [***Treatment_pooledCTRLs***]: tire-wear particle leachate treatments with pooled controls if there was no statistical difference between the controls; [***survival_count***]: tadpole density per experimental unit; and [***total_length***]: tadpole body length

Table S7 Results of generalized linear mixed models analyzing *S. tropicalis* tadpole growth parameters, swimming behavior and brain morphometrics after 9-day exposure to tire-wear particle leachate treatments (replicates, n = 4).

Model		β Estimate ± SE	df	*t* value	*p* value	Variance	SD
Model 1: Body length ~ Treatment + level + survival_count + 1|Jar							
Fixed Effects	(Intercept)	13.71525 ± 0.89598	38.40793	15.308	$< 2\times10^{-16}$ [a]		
	Treatment (Reference: F1, 0%)						
	F2	0.11608 ± 0.25158	27.59381	0.461	0.64813		
	F3	0.40845 ± 0.26338	25.98018	1.551	0.13305		
	Level 1%	-0.87571± 0.42221	30.66319	-2.074	0.04656[a]		
	Level 10%	-0.31880 ± 0.36351	27.96028	-0.877	0.38795		
	Survival_count	-0.19101 ± 0.06155	44.02457	-3.103	0.00334[a]		
Random Effects	Jar (Intercept)					0.0378	0.1944
	Residual					2.7697	1.6643
Number of observations = 320							
Model 2: Tail length ~ Treatment + level + survival_count + 1|Jar							
Fixed Effects	(Intercept)	9.31457 ± 0.63775	38.02949	14.605	$< 2\times10^{-16}$ [a]		
	Treatment (Reference: F1, 0%)						
	F2	0.10243 ± 0.17961	27.43092	0.570	0.57310		
	F3	0.26134 ± 0.18815	25.88058	1.389	0.17666		
	Level 1%	-0.68896 ± 0.30113	30.42015	-2.288	0.02926[a]		
	Level 10%	-0.21973 ± 0.25948	27.87087	-0.847	0.40431		
	Survival_count	-0.14119 ± 0.04376	43.50722	-3.226	0.00238[a]		
Random Effects	Jar (Intercept)					0.02464	0.157
	Residual					1.35762	1.165
Number of observations = 320							
Model 3: Body width ~ Treatment + level + 1|Jar							
Fixed Effects	(Intercept)	2.733496 ± 0.052162	24.158888	52.404	$< 2\times10^{-16}$ [a]		
	Treatment (Reference: F1, 0%)						
	F2	0.054411 ± 0.060753	29.869272	0.896	0.3776		
	F3	0.115107 ± 0.062314	30.790990	1.847	0.0743		

	Level 1%	-0.009524 ± 0.062679	33.184566	-0.152	0.8801		
	Level 10%	0.048891 ± 0.060288	29.197129	0.811	0.4240		
Random Effects	Jar (Intercept)					0.006509	0.08068
	Residual					0.142689	0.37774
Number of observations = 320							

Model 4: sqrt(Startle response total distance travelled) ~ Treatment_pooledCTRLs + total_length + 1\|Jar

Fixed Effects	(Intercept)	3.46748 ± 0.69367	263.45575	4.999	1.05×10^{-6} [a]		
	Treatment (Reference: Pooled Controls, 0%)						
	F1 1%	-0.63024 ± 0.35297	23.96705	-1.786	0.086836		
	F1 10%	-1.22380 ± 0.34450	22.07682	-3.552	0.001778[a]		
	F2 1%	-0.06475 ± 0.41647	40.92650	-0.155	0.877203		
	F2 10%	-1.45916 ± 0.37824	32.01876	-3.858	0.000521[a]		
	F3 1%	-1.04457 ± 0.43119	46.27274	-2.423	0.019385[a]		
	F3 10%	-0.08626 ± 0.42772	44.73822	-0.202	0.841083		
	Total_length	0.25540 ± 0.05870	272.54268	4.351	1.92×10^{-5} [a]		
Random Effects	Jar (Intercept)					0.08241	0.2871
	Residual					2.64585	1.6266
Number of observations = 281							

Model 5: Startle response burst swimming speed ~ Treatment_id + total_length + 1\|Jar

Fixed Effects	(Intercept)	$-2.452\times10^{-2} \pm 1.330\times10^{-2}$	271	-1.844	0.0662
	Treatment (Reference: Control, 0%)				
	F1 1%	$1.227\times10^{-2} \pm 6.975\times10^{-3}$	271	1.759	0.0797
	F1 10%	$-4.279\times10^{-4} \pm 6.833\times10^{-3}$	271	-0.063	0.9501
	F2 1%	$1.406\times10^{-2} \pm 8.058\times10^{-3}$	271	1.745	0.0821
	F2 10%	$1.705\times10^{-2} \pm 7.427\times10^{-3}$	271	2.296	0.0224[a]
	F3 1%	$1.615\times10^{-3} \pm 8.321\times10^{-3}$	271	0.194	0.8462
	F3 10%	$1.150\times10^{-2} \pm 8.259\times10^{-3}$	271	1.393	0.1647
	PC F1	$1.704\times10^{-2} \pm 7.027\times10^{-3}$	271	2.425	0.0159[a]
	PC F3	$1.043\times10^{-2} \pm 6.832\times10^{-3}$	271	1.527	0.1279

	Total_length	$6.952\times10^{-3} \pm 1.084\times10^{-3}$	271	6.413	6.33×10^{-10} [a]		
Random Effects	Jar (Intercept)					0.0000000	0.00000
	Residual					0.0009214	0.03035
Number of observations = 281							
Model 6: sqrt(Total distance while feeding) ~ Treatment * level + total_length + 1|Jar							
Fixed Effects	(Intercept)	2.54748 ± 0.71374	200.80949	3.569	0.000448[a]		
	Treatment (Reference: F1, 0%)						
	F2	-0.37630 ± 0.42173	22.68904	-0.892	0.381614		
	F3	-0.83506 ± 0.42379	23.11252	-1.970	0.060878		
	Level 1%	-0.87310 ± 0.43015	24.26837	-2.030	0.053481		
	Level 10%	-1.81338 ± 0.42361	23.05561	-4.281	0.000278[a]		
	Total_length	0.35305 ± 0.05691	270.79255	6.204	2.06×10^{-9} [a]		
	Treatment F2: Level 1%	0.51872 ± 0.63788	28.36936	0.813	0.422882		
	Treatment F3: Level 1%	0.40059 ± 0.64809	30.06974	0.618	0.541156		
	Treatment F2: Level 10%	0.16961 ± 0.61049	24.96218	0.278	0.783432		
	Treatment F3: Level 10%	1.91253 ± 0.64137	28.90654	2.982	0.005763[a]		
Random Effects	Jar (Intercept)					0.08933	0.2989
	Residual					2.47850	1.5743
Number of observations = 281							
Model 7: Telencephalon width ~ Treatment_id + 1|Jar							
Fixed Effects	(Intercept)	282.790 ± 11.444	8.000	24.711	7.69×10^{-9} [a]		
	Treatment (Reference: Control, 0%)						
	F1 10%	17.747 ± 16.184	8.000	1.097	0.3047		
	F2 10%	9.873 ± 16.184	8.000	0.610	0.5587		
	F3 10%	53.813 ± 16.184	8.000	3.325	0.0105[a]		
Random Effects	Jar (Intercept)					0.0	0.00
	Residual					392.9	19.82
Number of observations = 12							
Model 8: Diencephalon width ~ Treatment_id + 1|Jar							
Fixed Effects	(Intercept)	266.530 ± 7.812	8.000	34.118	5.95×10^{-10} [a]		

	Treatment (Reference: Control, 0%)						
	F1 10%	21.233 ± 11.048	8.000	1.922	0.09085		
	F2 10%	10.300 ± 11.048	8.000	0.932	0.37846		
	F3 10%	39.500 ± 11.048	8.000	3.575	0.00724[a]		
Random Effects	Jar (Intercept)					0.0	0.00
	Residual					183.1	13.53
Number of observations = 12							
Model 9: Optic tectum width ~ Treatment_id + 1|Jar							
Fixed Effects	(Intercept)	359.070 ± 13.981	8.000	25.682	5.67×10^{-9} [a]		
	Treatment (Reference: Control, 0%)						
	F1 10%	9.787 ± 19.773	8.000	0.495	0.6339		
	F2 10%	-2.373 ± 19.773	8.000	-0.120	0.9074		
	F3 10%	56.680 ± 19.773	8.000	2.867	0.0209[a]		
Random Effects	Jar (Intercept)					0.0	0.00
	Residual					586.4	24.22
Number of observations = 12							
Model 10: Medulla width ~ Treatment_id + 1|Jar							
Fixed Effects	(Intercept)	272.103 ± 9.269	8.000	29.356	1.96×10^{-9} [a]		
	Treatment (Reference: Control, 0%)						
	F1 10%	18.887 ± 13.108	8.000	1.441	0.18761		
	F2 10%	24.473 ± 13.108	8.000	1.867	0.09886		
	F3 10%	56.240 ± 13.108	8.000	4.290	0.00265[a]		
Random Effects	Jar (Intercept)					0.0	0.00
	Residual					257.7	16.05
Number of observations = 12							

[a] Statistically significant at $p \leq 0.05$. SE = standard error; SD = standard deviation; PC = Procedural control. [***Treatment_id***]: unique treatment and level identification e.g., F1 10%; [***Treatment***]: tire-wear particle leachate treatments with controls re-categorized as Control → 0% F2, PC F1 → 0% F1, PC F3 → 0% F3 to ensure a 3 × 3 factorial design for statistical analyses; [***Treatment_pooledCTRLs***]: tire-wear particle leachate treatments with pooled controls if there was no statistical difference between the controls; [***survival_count***]: tadpole density per experimental unit; and [***total_length***]: tadpole body length. [1|Jar]: random variable to account for tadpoles raised in the same jar. The number of observations represents the sample size used for each model.

Particle Size Characterization Results

Table S8 Mean hydrodynamic sizes (± standard error) for particles in F1 and F3 using different characterization techniques. The particle size for F3 corresponds to the mean size of peak 1 in Figure S5(B).

Fraction	Dynamic Light Scattering (DLS)	Nanoparticle Tracking Analysis (NTA)
F1	252 ± 12 nm	275 ± 14 nm
F3	135 ± 11 nm	139 ± 1 nm

The DLS hydrodynamic size distributions of particles in F1 and F3 are shown in Figure S5. For F3, the more prominent peak 1 is used as the metric for particle size of the nanoparticles fraction (Figure S5B). Styrene butadiene rubber (SBR) was used as the reference material for DLS measurements as it one of the main constituents for tire tread.

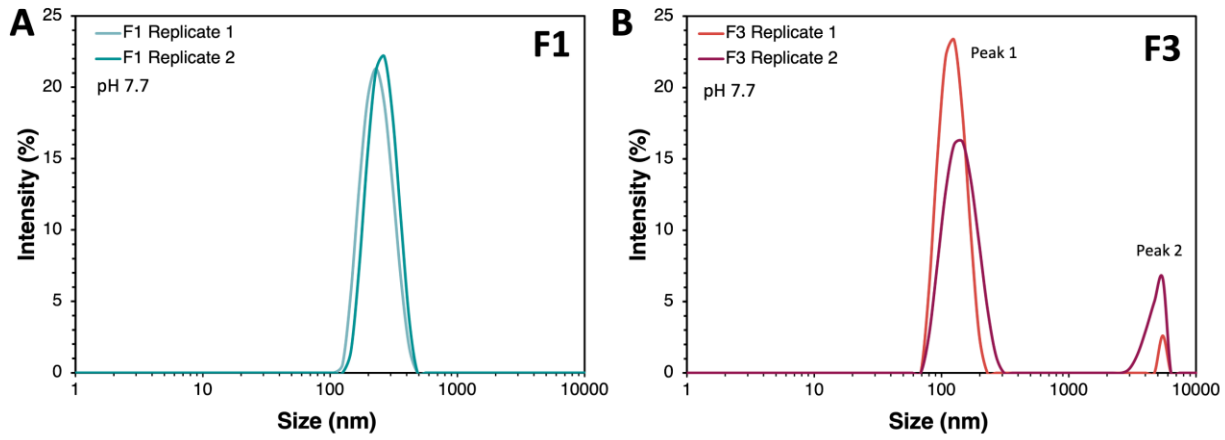

Figure S5 Hydrodynamic size distribution of particles in F1 and F3 are shown in (A) and (B) respectively.

Particle Morphology

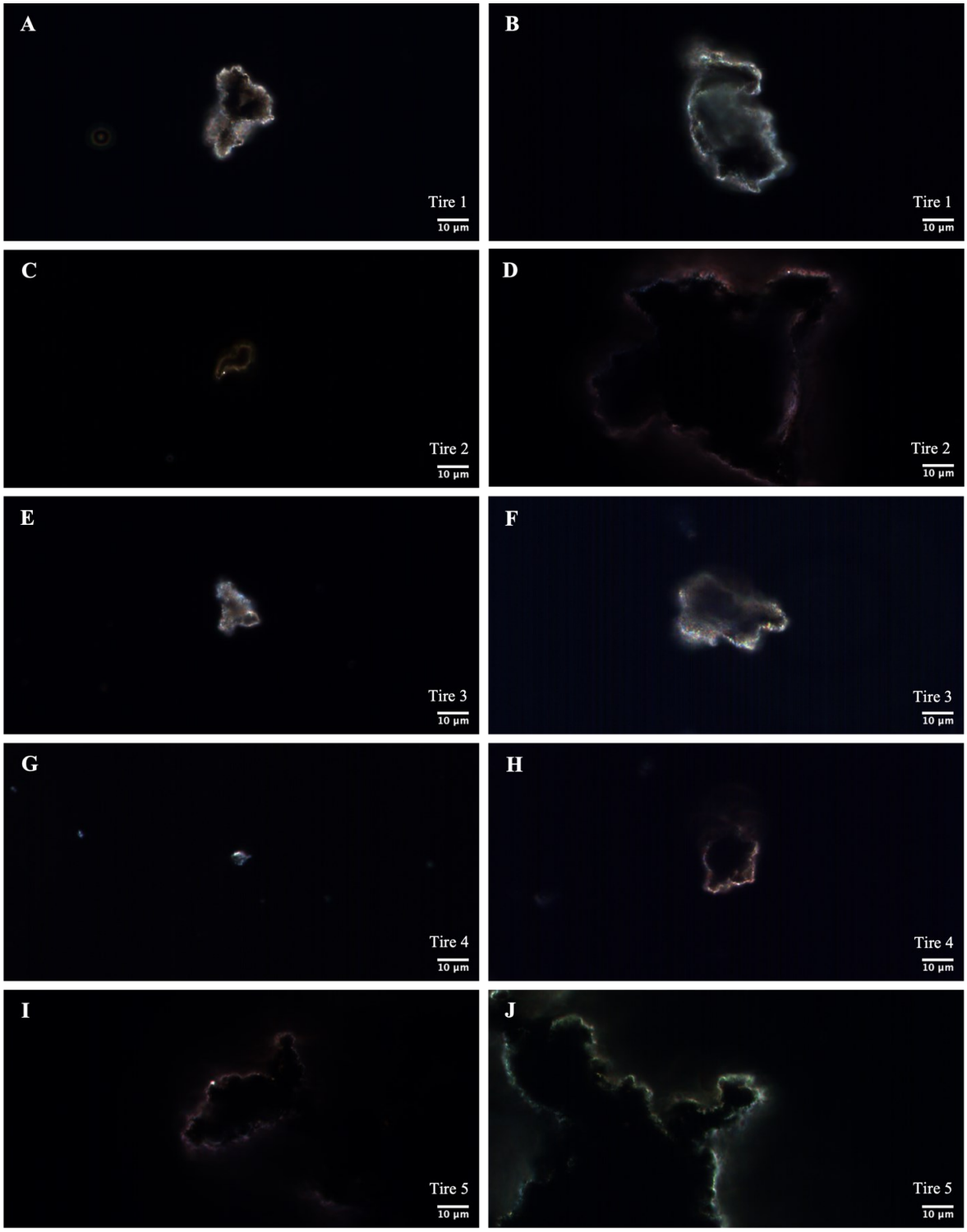

Figure S6 Darkfield images of tire-wear particles generated from drilling process.

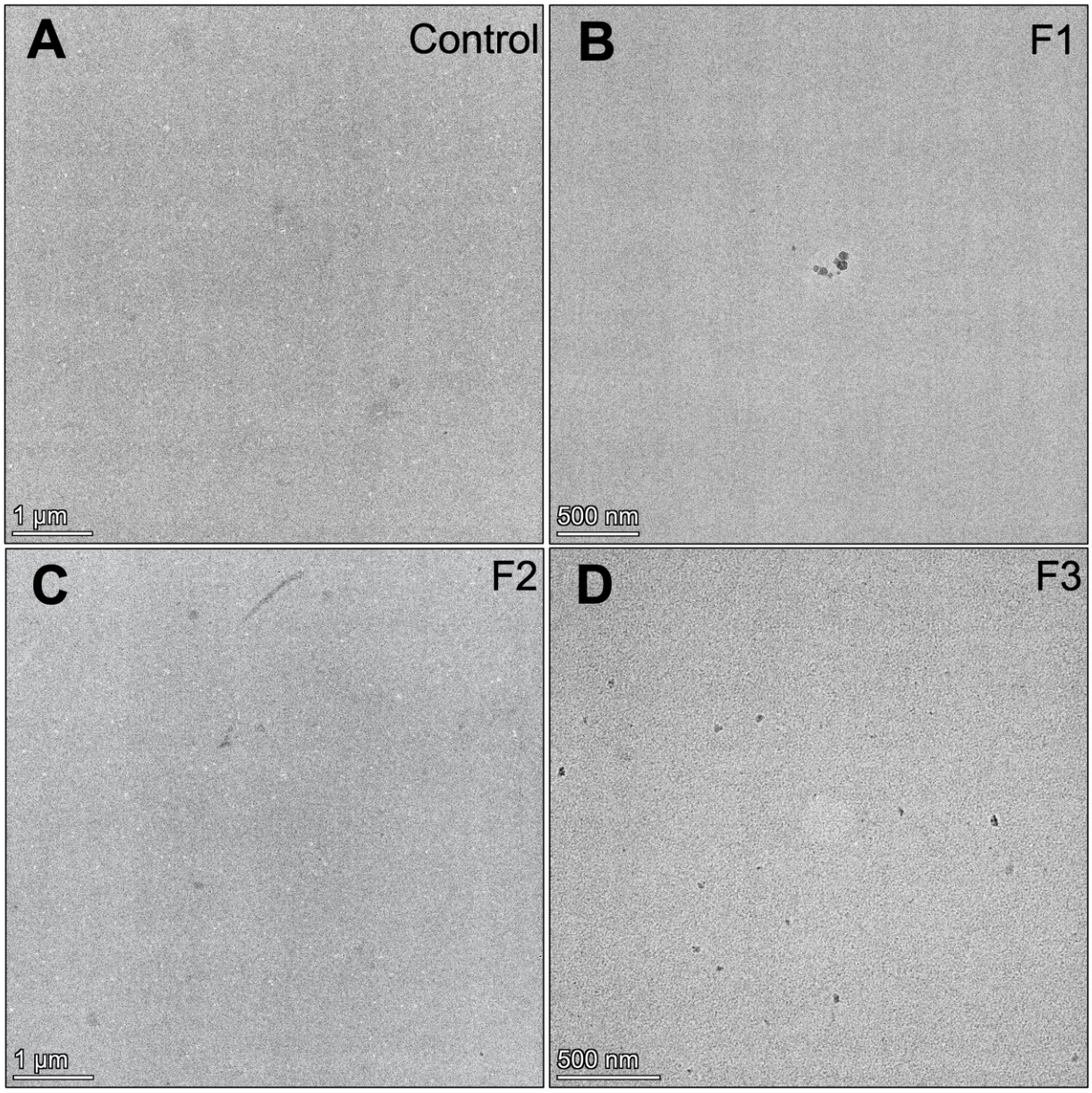

Figure S7 TEM images of (A) Control, (B) F1, (C) F2 and (D) F3.

Metal and Organic Chemicals Characterization Results

The concentrations of metals at the 10% treatment level used for the 9-day exposure are shown in Figure S8.

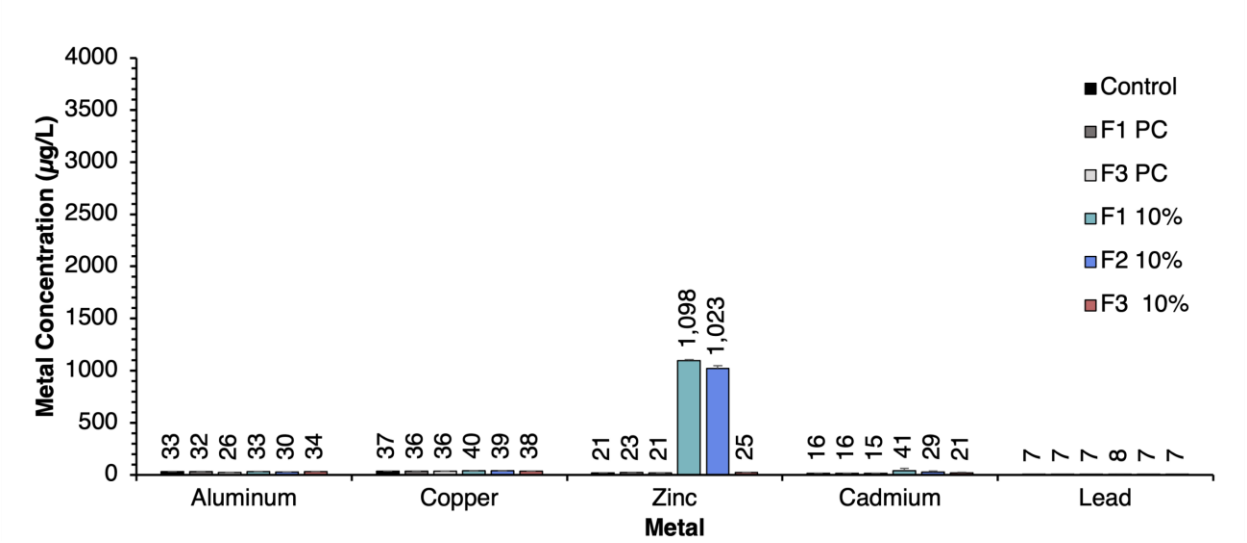

Figure S8 Metal concentration of 10% treatments and controls used in the 9-day exposure. The numbers above the bars represent the mean metal concentration in µg/L. The vertical line on top of each bar represents the standard error from 4 replicates (n = 4). Zinc was the most prominent metal in fractions which contained leached chemicals (i.e., F1 and F2).

Table S9 Concentration of organic chemicals (mean ± standard error, n = 4) in day 0 and day 3 water samples from acute and 9-day exposures.

Exposure	Treatment	Level (%)	Day	BT (µg/L)	MBT (µg/L)	HMMM (µg/L)	6-PPD quinone (µg/L)	Dibutyl phthalate (µg/L)	Dipentyl phthalate (µg/L)	Diheptyl phthalate (µg/L)
Acute	Control	0	0	0 ± 0	0 ± 0	0 ± 0	n.d.	n.d.	n.d.	n.d.
Acute	F1 PC	0	0	0 ± 0	0 ± 0	0 ± 0	n.d.	n.d.	n.d.	n.d.
Acute	F3 PC	0	0	0 ± 0	0 ± 0	0 ± 0	n.d.	n.d.	n.d.	n.d.
Acute	F1	100	0	1153 ± 20	7 ± 2	1035 ± 37	n.d.	n.d.	n.d.	n.d.
Acute	F2	100	0	1007 ± 45	11 ± 0.3	865 ± 215	n.d.	n.d.	n.d.	n.d.
Acute	F3	100	0	0 ± 0	0 ± 0	13 ± 3	n.d.	n.d.	n.d.	n.d.
Acute	Control	0	3	0 ± 0	0 ± 0	0 ± 0	n.d.	n.d.	n.d.	n.d.
Acute	F1 PC	0	3	0 ± 0	0 ± 0	0 ± 0	n.d.	n.d.	n.d.	n.d.
Acute	F3 PC	0	3	0 ± 0	0 ± 0	0 ± 0	n.d.	n.d.	n.d.	n.d.
Acute	F1	100	3	690 ± 39	12 ± 1	1071 ± 27	n.d.	n.d.	n.d.	n.d.
Acute	F2	100	3	956 ± 102	11 ± 1	1094 ± 44	n.d.	n.d.	n.d.	n.d.
Acute	F3	100	3	0 ± 0	0 ± 0	22 ± 3	n.d.	n.d.	n.d.	n.d.
9-Day	Control	0	0	0 ± 0	0 ± 0	0 ± 0	n.d.	n.d.	n.d.	n.d.
9-Day	F1 PC	0	0	101 ± 25	0 ± 0	0 ± 0	n.d.	n.d.	n.d.	n.d.
9-Day	F3 PC	0	0	144 ± 92	0 ± 0	0 ± 0	n.d.	n.d.	n.d.	n.d.
9-Day	F1	10	0	279 ± 103	2 ± 0.3	187 ± 29	n.d.	n.d.	n.d.	n.d.
9-Day	F2	10	0	246 ± 59	3 ± 0.1	187 ± 48	n.d.	n.d.	n.d.	n.d.
9-Day	F3	10	0	68 ± 56	0 ± 0	0 ± 0	n.d.	n.d.	n.d.	n.d.
9-Day	Control	0	3	0 ± 0	0 ± 0	0 ± 0	n.d.	n.d.	n.d.	n.d.
9-Day	F1 PC	0	3	0 ± 0	0 ± 0	0 ± 0	n.d.	n.d.	n.d.	n.d.
9-Day	F3 PC	0	3	0 ± 0	0 ± 0	0 ± 0	n.d.	n.d.	n.d.	n.d.
9-Day	F1	10	3	61 ± 8	0 ± 0	243 ± 75	n.d.	n.d.	n.d.	n.d.
9-Day	F2	10	3	46 ± 9	0 ± 0	221 ± 45	n.d.	n.d.	n.d.	n.d.
9-Day	F3	10	3	0 ± 0	0 ± 0	0 ± 0	n.d.	n.d.	n.d.	n.d.

Exposure	Treatment	Level (%)	Day	Dihexyl phthalate (µg/L)	DEHP (µg/L)	Decyl octyl phthalate (µg/L)	BPA (µg/L)	Irganox 1081 (µg/L)	Irganox 1330 (µg/L)	Irganox 1010 (µg/L)
Acute	Control	0	0	n.d.	n.d.	n.d.	n.d.	n.d.	n.d.	n.d.
Acute	F1 PC	0	0	n.d.	n.d.	n.d.	n.d.	n.d.	n.d.	n.d.
Acute	F3 PC	0	0	n.d.	n.d.	n.d.	n.d.	n.d.	n.d.	n.d.
Acute	F1	100	0	n.d.	n.d.	n.d.	n.d.	n.d.	n.d.	n.d.
Acute	F2	100	0	n.d.	n.d.	n.d.	n.d.	n.d.	n.d.	n.d.
Acute	F3	100	0	n.d.	n.d.	n.d.	n.d.	n.d.	n.d.	n.d.
Acute	Control	0	3	n.d.	n.d.	n.d.	n.d.	n.d.	n.d.	n.d.
Acute	F1 PC	0	3	n.d.	n.d.	n.d.	n.d.	n.d.	n.d.	n.d.
Acute	F3 PC	0	3	n.d.	n.d.	n.d.	n.d.	n.d.	n.d.	n.d.
Acute	F1	100	3	n.d.	n.d.	n.d.	n.d.	n.d.	n.d.	n.d.
Acute	F2	100	3	n.d.	n.d.	n.d.	n.d.	n.d.	n.d.	n.d.
Acute	F3	100	3	n.d.	n.d.	n.d.	n.d.	n.d.	n.d.	n.d.
9-Day	Control	0	0	n.d.	n.d.	n.d.	n.d.	n.d.	n.d.	n.d.
9-Day	F1 PC	0	0	n.d.	n.d.	n.d.	n.d.	n.d.	n.d.	n.d.
9-Day	F3 PC	0	0	n.d.	n.d.	n.d.	n.d.	n.d.	n.d.	n.d.
9-Day	F1	10	0	n.d.	n.d.	n.d.	n.d.	n.d.	n.d.	n.d.
9-Day	F2	10	0	n.d.	n.d.	n.d.	n.d.	n.d.	n.d.	n.d.
9-Day	F3	10	0	n.d.	n.d.	n.d.	n.d.	n.d.	n.d.	n.d.
9-Day	Control	0	3	n.d.	n.d.	n.d.	n.d.	n.d.	n.d.	n.d.
9-Day	F1 PC	0	3	n.d.	n.d.	n.d.	n.d.	n.d.	n.d.	n.d.
9-Day	F3 PC	0	3	n.d.	n.d.	n.d.	n.d.	n.d.	n.d.	n.d.
9-Day	F1	10	3	n.d.	n.d.	n.d.	n.d.	n.d.	n.d.	n.d.
9-Day	F2	10	3	n.d.	n.d.	n.d.	n.d.	n.d.	n.d.	n.d.
9-Day	F3	10	3	n.d.	n.d.	n.d.	n.d.	n.d.	n.d.	n.d.

BT: Benzothiazole; MBT: Mercaptobenzothiazole; HMMM: Hexa (methoxymethyl) melamine; 6-PPD: N-(1,3-dimethylbutyl)-N′-phenyl-p-phenylenediamine; BPA: Bisphenol A; n.d.: Not Detected

9-Day Exposure – Additional Information

The main categories of malformations identified in the acute and 9-day exposures are shown in the representative image in Figure S9. Edema included abdominal, thoracic, and ophthalmic edema as well as blistering. Head malformations encompassed both eye and face abnormalities such as microphthalmia, abnormal head shape/size, optic fissures *etc*. Bantle's *et al.* "Atlas of Abnormalities: a Guide for the Performance of FETAX" was used as a guide for the identification of the different types of malformations in larval amphibians (Bantle et al., 1991).

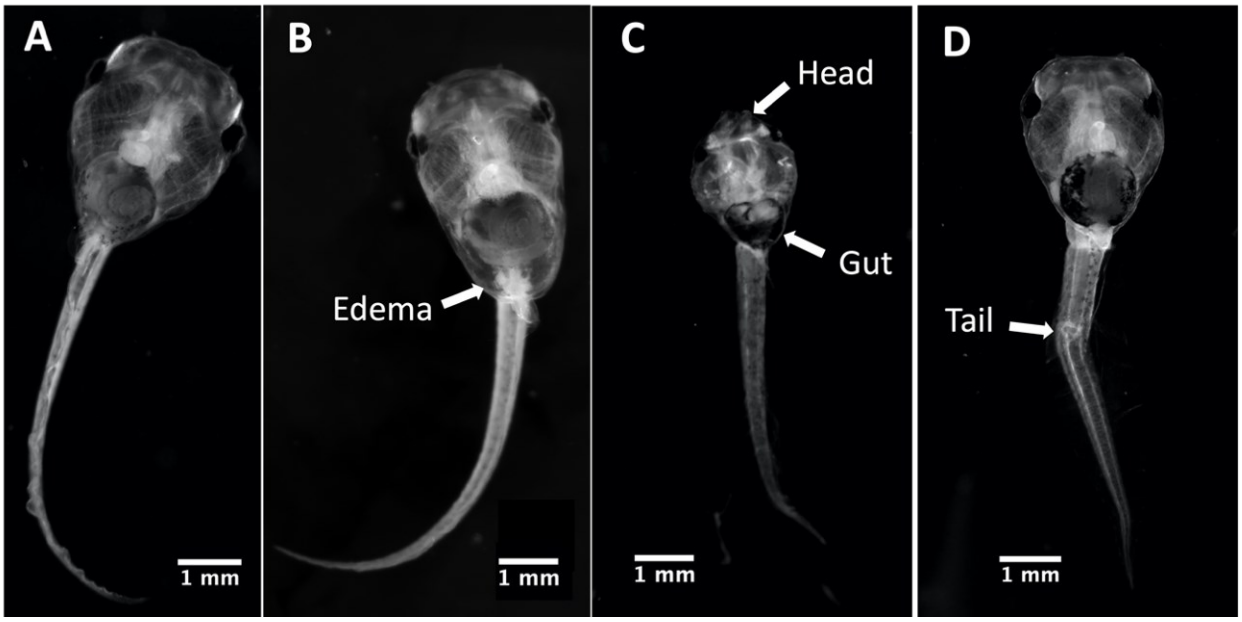

Figure S9 Ventral views of representative normal and malformed premetamorphic *S. tropicalis* tadpoles after 9-day exposure to low concentrations of tire-wear particle leachate. (A) normal tadpole; (B) tadpole with edema in the abdominal region; (C) tadpole with head and gut abnormalities; and (D) tadpole with tail abnormality.

Other body morphometrics such as the tail length, body width, diencephalon width, optic tectum and medulla width are shown in Figure S10. The burst swimming speed (i.e., the highest swimming speed after the vibrational stimulus was introduced in the startle response assay) was also analyzed. The dorsal view of the head of a 9-day old tadpole with the brain highlighted is shown in Figure S3. Measurements of the various brain regions (telencephalon, diencephalon,

optic tectum, and medulla) are illustrated in Figure S4. The telencephalon plays a key role in amphibian locomotion (Mai & Liao, 2019). The optic tectum allows the animal to sense visual stimuli (Khakhalin et al., 2014). The medulla is important for respiration in amphibians (Reed, Iceman, Harris, & Taylor, 2018).

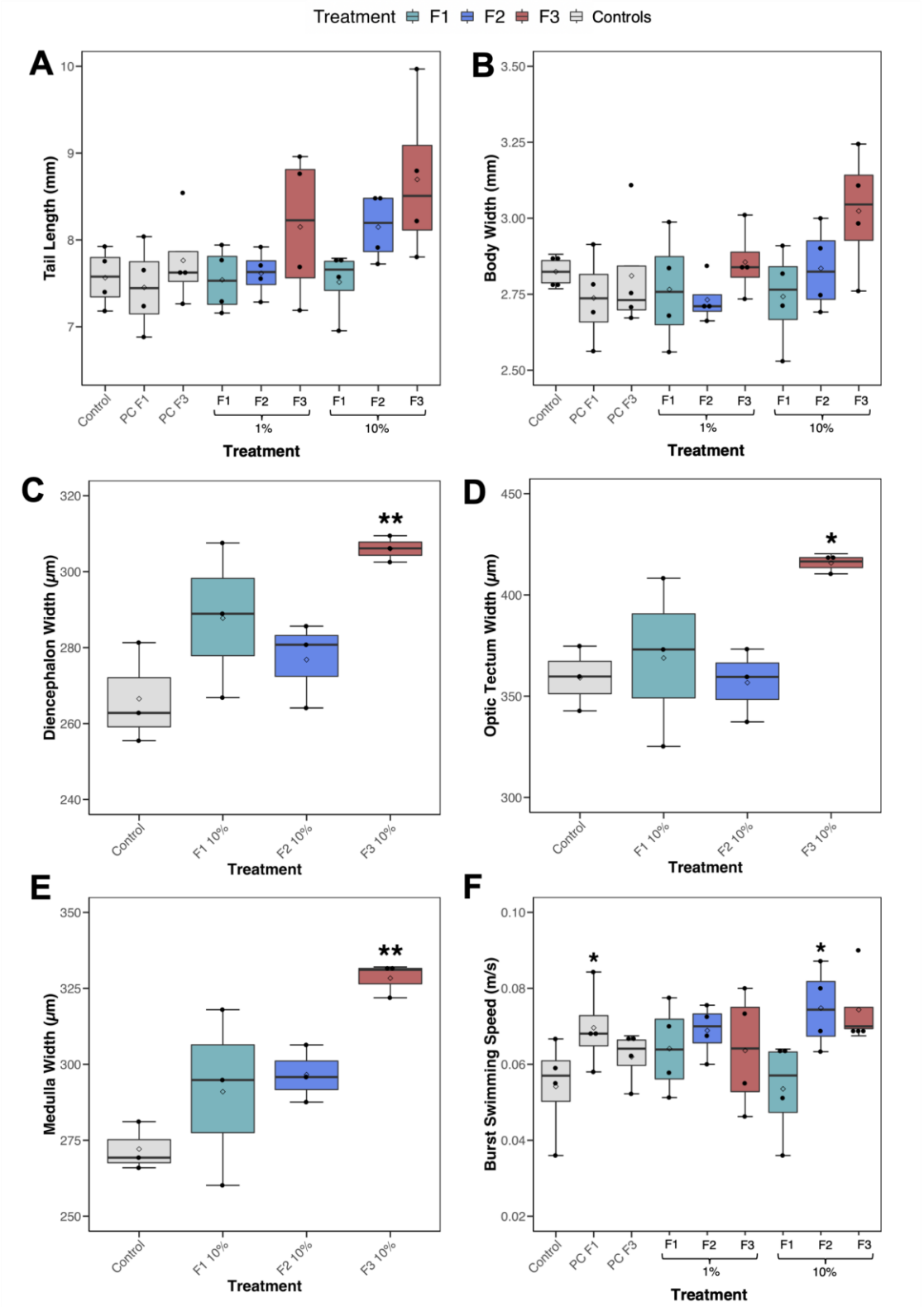

Figure S10 (A) Tail length, (B) body width, (C) diencephalon width, (D) optic tectum width, (E) medulla width and (F) burst swimming speed of tadpoles after 9-day exposure to tire-wear particle leachates.